7-6-2012 12:00 AM

The Effects of Lubrication on Pharmaceutical Granules

Garett Morin
The University of Western Ontario

Supervisor
Dr. Lauren Briens
The University of Western Ontario

Graduate Program in Biomedical Engineering
A thesis submitted in partial fulfillment of the requirements for the degree in Master of Engineering Science

THE EFFECTS OF LUBRICATION ON PHARMACEUTICAL GRANULES

(Thesis format: Integrated-Article)

by

Garett Jonathan Morin

Graduate Program in Engineering Science
Biomedical Engineering

A thesis submitted in partial fulfillment
of the requirements for the degree of
Master of Engineering Science

School of Graduate and Postdoctoral Studies
The University of Western Ontario
London, Ontario, Canada

CERTIFICATE OF EXAMINATION

Supervisor

Dr. Lauren Briens

Supervisory Committee

Dr. Elizabeth Gillies

Dr. Shahzad Barghi

Examiners

Dr. Paul Charpentier

Dr. Argyrios Margaritis

Dr. Sohrab Rohani

The thesis by

Garett Jonathan Morin

entitled:

The Effects of Lubrication on Pharmaceutical Granules

is accepted in partial fulfilment of the
requirements for the degree of
Master of Engineering Science

Date_____

_____
Chair of the Thesis Examination Board

Abstract

Spray-dried lactose was mixed with 4 different lubricants – magnesium stearate, magnesium silicate, stearic acid, and calcium stearate – in various concentrations. Flowability testing revealed that magnesium stearate improved powder flow until a threshold was reached, at which addition of lubricant had no effect. The addition of calcium stearate also improved flow; however, additional lubricant over the optimum amount further decreased flow. Full placebo granules were manufactured by both high shear and fluidized bed techniques. A granule comparison showed different growth mechanisms, surface morphology, particle size distribution, and flow characteristics for each manufacturing technique. The high shear granules demonstrated better overall flow properties. Granules made from both techniques were mixed with magnesium stearate in varying concentrations. Again, it was determined that after a threshold addition of magnesium stearate, there was little change in flowability. After lubricant addition, the flowability characteristics of both granule types were very similar.

Keywords: high shear granulation, fluidized bed granulation, lubricant, magnesium stearate, granule characteristics, flowability, powder avalanching, pharmaceutical manufacturing

Statement of Co-Authorship

Chapter 2:

The effect of lubricants on powder flowability for pharmaceutical application

Authors: Garett J. Morin, Lauren Briens

Status: To be submitted to Powder Technology

All experimental work including the production of granules and granule characterization was performed by Garett J. Morin. Data analysis was performed by Garett J. Morin. Consultation regarding experimental work and interpretation of experimental data was provided by Lauren Briens. The manuscript was written and revised by Garett J. Morin, and reviewed by Lauren Briens.

Chapter 3:

A comparison of granules produced by high shear and fluidized bed granulation techniques

Authors: Garett J. Morin, Lauren Briens

Status: To be submitted to International Journal of Pharmaceutics

All experimental work including the production of granules and granule characterization was performed by Garett J. Morin. Data analysis was performed by Garett J. Morin. Consultation regarding experimental work and interpretation of experimental data was provided by Lauren Briens. The manuscript was written and revised by Garett J. Morin, and reviewed by Lauren Briens.

Chapter 4:

The effect of magnesium stearate on high shear and fluidized bed granule flowability

Authors: Garett J. Morin, Lauren Briens

All experimental work including the production of granules and granule characterization was performed by Garett J. Morin. Data analysis was performed by Garett J. Morin. Consultation regarding experimental work and interpretation of experimental data was provided by Lauren Briens. The manuscript was written and revised by Garett J. Morin, and reviewed by Lauren Briens.

“Good. Better. Best. Never let it rest, until your good, is better.

And your better, is the best.”

- *Dr. Seuss*

Acknowledgments

I would like to acknowledge the assistance provided to me by several people. I would first like to thank my thesis advisor Dr. Lauren Briens for her guidance and encouragement throughout the duration of my studies. Without her contributions and support, the completion of this thesis would not have been possible. I would also like to thank Dr. Elizabeth Gillies and Dr. Shahzad Barghi for serving on my advisory committee.

I would like to acknowledge the Natural Sciences and Engineering Research Council of Canada (NSERC), the Ontario Graduate Scholarship Program (OGS), and the Biomedical Engineering Scholarship Program for their financial support. The University of Western Ontario Graduate Thesis Research Award Fund (GTRAF) is also acknowledged for financial contribution.

I would like to thank Heather Bloomfield of Surface Science Western for her assistance examining my granules. Assistance provided by Clayton Cook of the University Machine Services as well as Brian Dennis and Souheil Afara is also much appreciated.

I would like to thank the Biomedical Engineering faculty and staff for providing education and constant support during my studies. Finally, I would like to thank my friends, family and lab members for their constant encouragement and support.

Table of Contents

List of Figures

List of Tables

CHAPTER.1. INTRODUCTION

1.1. Downstream pharmaceutical tablet manufacturing

A pharmaceutical tablet is a solid dosage form created by compressing a formulation of powders into a desired shape. The tablet is the most widely used dosage form in modern medicine, encompassing more than 80% of the 200 most prescribed drugs in the United States (Armstrong, 2007; Niazi, 2004).

Figure 1.1 shows a common downstream pharmaceutical tablet manufacturing pathway. There are several process steps in the pathway. Each step is conducted batchwise and then tested extensively before the products can move to the next step. This extensive testing at every step helps to ensure that the final tablets are of high quality.

One of the first steps is to mix and then use wet granulation to agglomerate the majority of the excipients in the formulation with the active drug. Excipients are the components of the formulation that determine tablet properties. Common excipients include disintegrants – powder(s) ensuring correct dissolution of the tablet – and fillers – powder(s) ensuring sufficient final tablet volume. Typically, a high shear granulator is used to agglomerate, but other equipment, such as fluidized bed granulators, may be utilized. During the granulation process, a liquid binder is added to promote agglomeration of the powder into granules. Once optimal granule size is reached, the wet granules are dried, usually in a fluidized bed unit, to remove excess moisture that increases cohesivity and promotion of bacterial growth. Milling ensures that the dried

granules are within a specified size range. After milling, lubricant and/or glidant excipients are added and mixed with the granules.

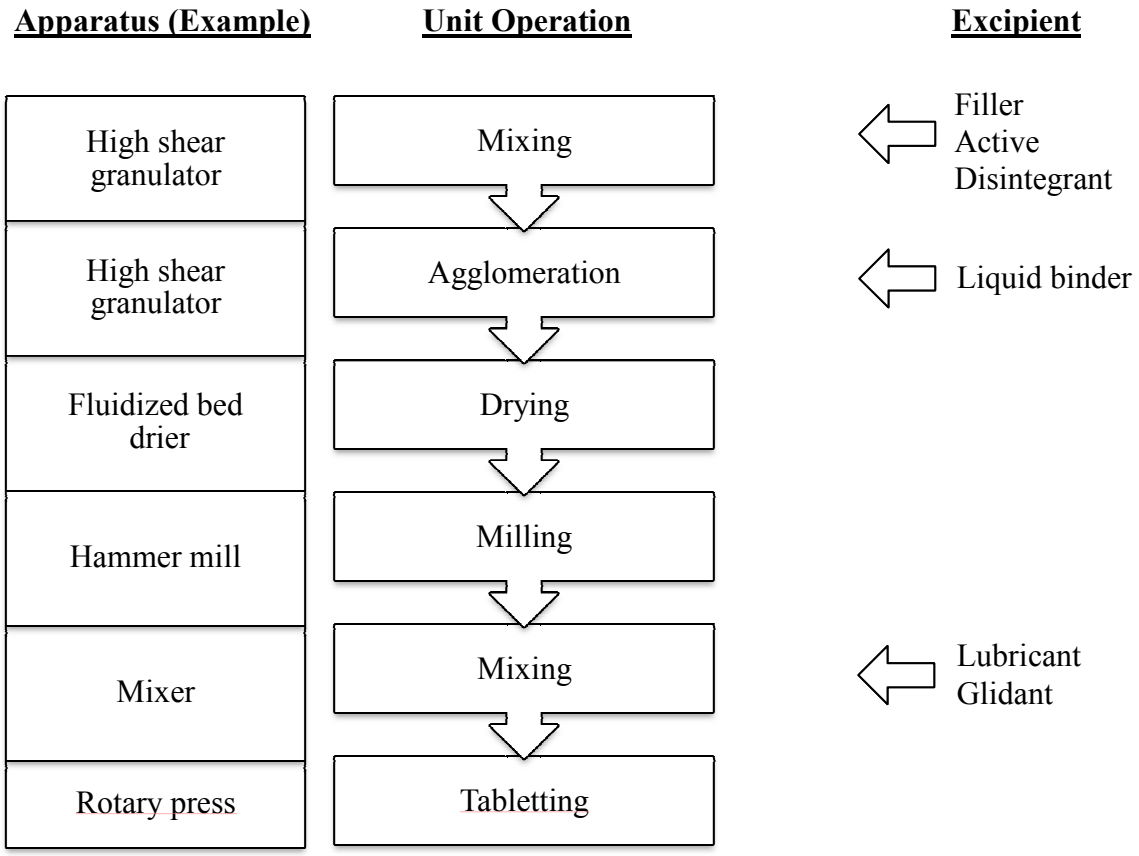

Figure 1.1: Common downstream pharmaceutical manufacturing pathway (adapted from Alderborn, 2002).

Each successive step in the manufacturing process modifies the original powder formulation to provide a final mixture that will flow easily, without segregation, into the tablet press. The final mixture flows, under the force of gravity, into the tablet press die from a hopper. An upper punch descends and enters the tablet die where the powder is compressed to form a tablet. After compression, the upper punch leaves the powder and the lower punch rises until its tip reaches the level of the top of the die, where the tablet is

thus removed (Alderborn, 2002). If the formulation does not flow into the press properly, the resulting tablets will be poor in quality and may have to be discarded.

Two major steps that most affect the tablet compression process, and ultimately the final tablet properties, are the granulation of the active and excipients and the addition of lubricant and/or glidant to the granule. A better understanding of these two processes would help process optimization, leading to improved tablet quality, reduced development time, and in due course, manufacturing cost.

1.2. Granulation

Granulation is the process whereby small powder particles are made to adhere to form larger, relatively permanent masses in which the original particles can still be distinguished (Ennis and Litster, 1997). Granulation is done for a variety of reasons, mainly to prevent segregation of the constituents of the powder, to improve flow properties, and to improve compaction characteristics. There are two main methods of granulation: wet granulation, in which a liquid is used, and dry granulation, in which no liquid is used. Over 70% of the pharmaceutical industry uses wet granulation to prepare granules for tableting (Tousey, 2002). In wet granulation, a liquid binder, often water, is added to the powder mixture to promote agglomeration. Within wet granulation, there are two main techniques: high shear granulation and fluidized bed granulation.

1.2.1. High shear granulation

High shear granulation is used extensively in pharmaceutics. High shear granulators typically consist of a stainless steel bowl with an impeller that revolves in the horizontal

plane and a chopper that rotates in either the horizontal or vertical planes. The unmixed dry powder formulation is loaded into the bowl and mixed by the main impeller for a few minutes. After the mixing time has elapsed, the liquid binder is added, typically by use of an atomizing nozzle. The chopper is used to aid in agglomeration by breaking large masses and redistributing the powder. The process is continued until granules of a satisfactory size are produced, at which point the granules are transferred to another unit for drying, commonly a fluidized bed dryer.

One of the advantages of high shear granulation is that both mixing and granulation are completed in the same piece of equipment in a matter of minutes. However, the process needs to be supervised with caution as the granulation can progress very quickly into an unusable, overmassed system. In order to avoid material waste, research continues to be conducted in order to systematically determine the appropriate stopping or end point-point of granulation by the use of on-line monitoring. Many methods have been investigated for end-point and process monitoring, including: power consumption methods (Holm et al., 1985a, 1985b; Terashita et al., 1990a/b; Laicher et al., 1997; Pepin et al., 2000a, 2000b; Watano et al., 1995; Betz et al., 2003, 2004), acoustic emission measurements (Whitaker et al., 2000; Briens et al., 2007; Daniher et al., 2008; Papp et al., 2008; Gamble et al., 2009; Hansuld et al., 2009, 2001a, 2011b), near-infared spectroscopy (Jorgensen et al., 2002; Alcala et al., 2010), raman spectroscopy (Wikstrom et al., 2005), impeller torque measurements (Parker et al., 2009; Hancock et al., 1982), image processing using a fuzzy logic control system (Watano et al., 2001), and measuring particle collision impact using vibration probes (Ohike et al., 1999; Talu et al., 2001; Briens et al., 2007; Daniher et al., 2008).

1.2.2. Fluidized bed granulation

Fluidized bed granulation is used much less extensively than high shear granulation within the pharmaceutical industry. In fluidized bed granulation, the powder particles are fluidized by air and the liquid binder is sprayed from an atomizing nozzle onto the powder bed. The fluidized air is typically heated and/or filtered. The escape of powder from the unit is prevented by exhaust filters, which are periodically agitated to reintroduce the powder to the bed. Sufficient liquid is sprayed to produce granules of satisfactory size, at which point spray is stopped but the fluidizing air stream remains engaged in order to dry the granules.

Fluidized bed granulation has many advantages over conventional wet granulation. All the granulation processes – mixing, granulation, and drying – that normally require separate pieces of equipment are performed in the same unit. This consolidation saves labour costs, transfer losses, and time. However, the equipment is initially expensive and the development and optimization of the process and product parameters requires extensive work. Similar development work for traditional processes is not as extensive. Research continues in the area of process control and online monitoring to improve the development and optimization of the process. Research utilizing experimental design has been conducted to optimize the fluidized bed process (Rambali et al., 2001a, 2001b; Meshali et al., 1983). Multiple methods of online monitoring and process control have also been studied, including near infared spectroscopy (Frake et al., 1997; Paul Findlay et al., 2005; Rantanen and Yliruusi, 1998), raman spectroscopy (Walker et al., 2009), acoustic emissions (Matero et al., 2009), and image processing using fuzzy logic control (Watano et al., 1995; Watano et al., 2001).

1.2.3. Granule formation and growth mechanisms

The formation of multi-particle agglomerates, known as granules, depends on inter-particle bonding. Granule structure, shape, and size are affected by the presence and strength of particle bonding. Five primary bonding mechanisms between particles exist: adhesion and forces in immobile liquid films between powder particles, interfacial forces in mobile liquid films within granules, solid bridge formation after solvent evaporation, solid particle attractive forces, and mechanical interlocking. Of the primary bonding mechanisms, interfacial forces play the largest role (Summers and Aulton, 2002).

Throughout liquid binder distribution during granulation, agitation provided by the impeller and chopper helps distribute binder throughout the bed. Three states of liquid distribution between particles are described by Summers and Aulton (2002): pendular, funicular, and capillary states. Particles are adhered together by lens-shaped rings of liquid at low moisture levels, called the pendular state; the surface tension forces of the liquid/air interface and hydrostatic pressure in the liquid bridges are the forces responsible for the adhesion affect. As more liquid enters the system, the liquid bridges are strengthened and less air is present in the granule structure, known as the funicular state. The capillary state is reached when all the air has been displaced from between the particles in the granule. The particles are held together by capillary suction and the liquid air interface, now only at the granule surface since all the air has been displaced from between the particles (Summers and Aulton, 2002). Increasing moisture content is crucial to reaching the capillary state, but not the sole means. Decreasing particle separation by increased agitation during the pendular state can increase granule density, thus reducing air pore volume.

The methods of particle bonding provide the basis for the traditional granule formation and growth mechanism, as described by Sastry and Fuerstenau (1973). The mechanism is divided into three main stages: nucleation, transition, and ball growth. Nucleation begins with liquid bridge formation between particles, to form a pendular state. Continued agitation increases the density of the initial agglomerates to form a capillary state and these dense agglomerates act as nuclei for granule growth. The transition stage, after initial nucleation, is the stage during which granules grow by one of two mechanisms: by single particle addition through liquid bridges forming or by the merging of nuclei. The transition stage is characterized by a particle size distribution containing a large number of small granules with a wide size range. Further granule growth occurs in the ball growth stage, producing larger, spherical granules whose size increases over time. If ball growth is continued for too long, an unusable, overmassed system will develop.

In the traditional granule formation and growth mechanism, there are three competing forces responsible for granule development: coalescence, breakage, and abrasion transfer. All three mechanisms are visualized in Figure 1.2.

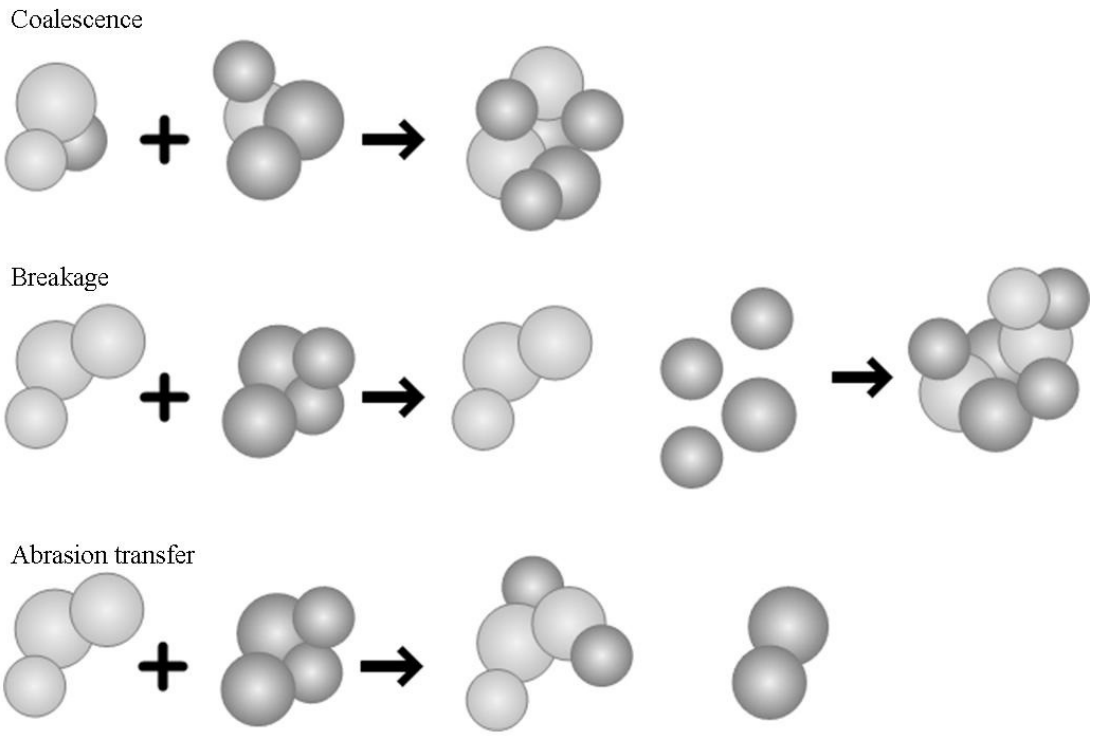

Figure 1.2: Granule growth mechanisms (adapted from Summers and Aulton, 2002).

Coalescence is typically the dominant force in granule growth and occurs when multiple granules join to form a large granule. Although contributing to growth, the other two mechanisms are responsible for the size reduction of granules during development. When granules break into fragments, these fragments adhere to other granules into which they collide. Abrasion transfer occurs from granule attrition caused by agitation of the granule bed. The abraded material adheres to other granules, leading to increased size.

The traditional granule growth and mechanism is described in a number of different competing methods. Such a picture of many competing methods is daunting and quantitative prediction of granule attributes is difficult using the traditional approach (Iveson et al., 2001). The competing mechanisms could all be considered as cases of

coalescence and/or breakage. Thus, as stated by Iveson et al (2001), it has become common to view granule growth as a combination of three rate processes described by Ennis and Litster (1997) and shown in Figure 1.3.

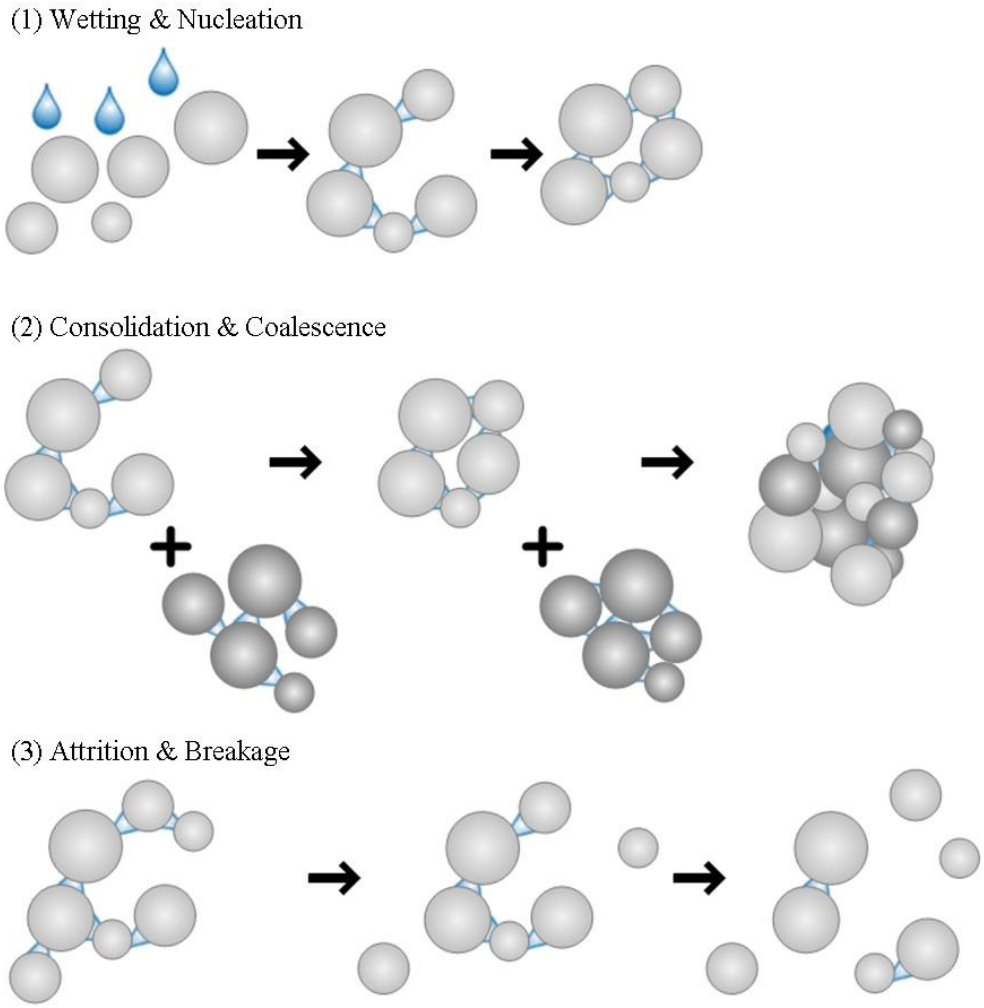

Figure 1.3: Rate processes describing granule growth (adapted from Ennis and Litster, 1997).

The advantage of the modern approach for describing granulation is that it distinguishes between granule growth and breakage. The competing mechanisms in the traditional approach are critical to the granulation process, but do not provide a means of measuring

granulation progression since they can all be considered to play both roles in growth and/or breakage (Iveson et al., 2001).

1.3. Lubrication

Lubricants are commonly added excipients to many pharmaceutical tablet formulations. Following compression, a tablet must be ejected out of the tablet press die. Lubricants reduce the friction between the tablet and the die metal surface which reduces the ejection force and helps to ensure that the tablet is completely ejected. High friction during tableting can cause a series of problems, including inadequate tablet quality from capping or even fragmentation during ejection.

There are two main mechanisms by which lubrication is achieved: fluid lubrication and boundary lubrication. In fluid lubrication, the lubrication forms a thin, continuous fluid layer between the tablet and metal dies surface. Fluid lubricants are seldom used in tablet formulations. However, liquid paraffin has been used in formulations for effervescent tablets. Lubricants utilizing the boundary lubrication mechanism are the most common (Wang et al., 2010). In boundary lubrication, the sliding surfaces are separated by a very thin film of lubricant. The nature of the tablet and die surface properties will thus affect the frictional forces present.

There are six categories of boundary lubricants commonly used for pharmaceutical tableting: (i) metallic salts of fatty acids, (ii) fatty acids, hydrocarbons and fatty alcohols, (iii) fatty acid esters. (iv) alkyl sulfates, (v) polymers, and (vi) inorganic materials (Wang et al., 2010). Magnesium stearate, a metallic salt boundary lubricant, is probably the most

commonly used lubricant for pharmaceutical tableting; it is relatively inexpensive, provides high lubrication, has a high melting point and is chemically stable (Perrault et al., 2010). Common lubricants and their classification are summarized in Table 1.1: Classification of common lubricants.

Table 1.1: Classification of common lubricants (adapted from Wang et al., 2010).

Lubricant classification	Name of lubricant
Metallic salts of fatty acids	magnesium stearate, aluminum stearate, calcium stearate, sodium stearate, zinc stearate
Fatty acids, hydrocarbons and fatty alcohols	stearic acid, decanoic, dodecanoic, docosanoic, octadecanol, eicosanoic
Fatty acid esters	sodium stearyl fumarate, sodium lauryl sulfate, magnesium lauryl sulfate, glyceryl behenate, dodecanoic triglyceride, samarium stearate, sucrose monopalmitate
Alkyl sulfates	magnesium lauryl sulfate, sodium lauryl sulfate
Polymers	PEG 4000, PEG 6000, polyoxyethylene-polyoxyproprylene copolymer, polytetrafluoroethylene
Inorganic materials	magnesium silicate, aluminum silicate

As magnesium stearate is the most commonly used boundary layer lubricant, it has been the most extensively studied. It has been hypothesized that the film formed by magnesium stearate around other excipient particles could be: (i) as a monomolecular film of magnesium stearate particles bound to the other excipients by their apolar heads, (ii) as a monoparticulate film of magnesium stearate particles covering the surface of the other excipients, and (iii) as layers of magnesium stearate particles first filling any cavities of the other excipients before forming a continuous layer (Perrault et al., 2010; Roblot-Treupel and Puisieux, 1986). The third hypothesized mechanism of first filling any cavities is the most popular. With this mechanism, magnesium stearate would

improve flow by minimizing any surface irregularities of the excipients which reduces contact points between excipients, decreasing friction forces.

1.3.1. Effect on flow

Powder flow is critical during tableting as it must flow easily and uniformly into the tablet dies to ensure tablet weight uniformity and production of tablets with consistent and reproducible properties (Fassihi and Kanfer, 1986; Tan and Newton, 1990; Sandler et al., 2010). Powder flows when gravitational forces become higher than the friction and cohesion forces that influence particle-particle interactions. Cohesive forces refer to the attraction between particles and include van der Waals' forces, capillary forces and electrostatic forces. Cohesive forces are affected by the surface properties of the particles. As boundary layer lubricants form a film around particles, these lubricants affect the cohesive forces thereby also affecting powder flow. Furthermore, friction is also affected by the surface properties of the particles. Friction acts at contact points between particles; thus, surface morphology affects friction forces. If the contact area is increased, the potential contact points are increased, thus increasing friction. Boundary layer lubricants reduce friction by reducing surface irregularities, reducing contact points between particles, and thus friction forces

The effect of lubricants on flow has been examined by numerous researchers. Liu et al. (2008) mixed ibuprofen powder with 0.5 wt% magnesium stearate for a period of 10 minutes. After mixing, the samples were dry sieved into various size cuts. A control sample with no added lubricant was also partitioned into the same size cuts for comparison. Using both the Hausner ratio and shear cell measurements to analyze the

changes in flowability, Liu et al. (2008) found that the addition of magnesium stearate improved the flow of the cohesive ibuprofen powder at all size cuts.

Danish and Parrott (1971) studied the effect on concentration of lubricant on the flow rate of granules composed of lactose. The materials studied as lubricants were glyceryl monostearate, hydrogenated castor oil, polyethylene glycol 4000, and stearic acid. The lubricants were added to 500 grams of the granules and mixed for 5 minutes in a two quart v-blender. A flowmeter was used to quantify the flow of powders through an orifice. In all cases, the addition of lubricant increased flowability of the granules. A maximum flow rate was obtained at 1 wt% stearic acid, 0.7 wt% hydrogenated castor oil, 0.5 wt% glyceryl monostearate, and 0.5 wt% polyethylene glycol 4000. In all cases, a decrease in flow rate was observed with the addition of excess lubricant.

Faqih et al. (2007) used a gravitational displacement rheometer to examine the avalanche behaviour of commonly used pharmaceutical powders mixed with various amounts of magnesium stearate (0.25-2.0 wt%). Magnesium stearate had almost no effect on free-flowing powder, while a small addition of lubricant had a significant effect of flow on the most cohesive powders.

The flow behaviour of acetaminophen and levalbuterol tartrate after being mixed with lubricants colloidal silica, talc, and magnesium stearate was examined by Pingali et al. (2009). The powders were blended with the lubricants using a 16 quart v-blender operated at 30 rpm with an intensifier bar rotating at 350 rpm. Combinations of lubricants were blended in samples ranging in concentration from 3-9 wt%. A flow index obtained from avalanche behaviour using a gravitational displacement rheometer was used to

quantify flowability. In the study of acetaminophen, all lubricants improved flow, but with different effectiveness. Colloidal silica was the most effective with magnesium stearate being slightly less effective and talc the least effective. The silica-magnesium stearate blend was by far the most effective combination. In terms of the levalbuteral tartrate, a very cohesive powder, the same trend was observed for individual lubricants as with the acetaminophen. Again, silica-magnesium stearate was the most effective pairing.

1.3.2. Effect on tablet properties

Besides reducing friction and cohesion, lubricants may cause undesirable changes in the properties of the tablet. The presence of lubricant in a powder is thought to interfere in a destructive way with the bonding between particles during compaction, thus reducing final tablet strength (Alderborn, 2002). Lubricant type, concentration, method of lubrication, and the manner of incorporating the lubricant all affect the tablet compression (Akser et al., 1975). It is generally accepted that magnesium stearate has more negative effect on the hardness and tensile strength of the tablets with more deformable materials than brittle ones (Wang et al., 2010). Jarosz et al. (1984) conducted a study using dibasic calcium phosphate as an example of a material that is susceptible to brittle fracture during compaction. Results showed that the tablet strength showed no change when magnesium stearate up to 3 wt% was present. Other lubricants, such as stearic acid and talc, showed no effect on the interparticle bonding, and thus tablet strength, of dibasic calcium phosphate dehydrate up to 8 wt%. Alternatively, when microcrystalline cellulose, an example of a plastic material, was mixed with magnesium stearate, the tablet strength was weakened significantly as the amount of added lubricant increased. Similar results were obtained when other lubricants (stearic acid, talc, and

PEG) were mixed with microcrystalline cellulose. The adverse impact of magnesium stearate on lactose and starch, excipients that also deform plastically, was also observed (Mitrevej et al., 1996).

Because many lubricants are hydrophobic, tablet disintegration and dissolution are often retarded by the addition of lubricant (Alderborn, 2002). Multiple studies (Johansson 1986, Johansson 1985a) have led to the theoretical conclusion that the deleterious effects observed are a cause of the combination of the large surface area and hydrophobicity of the lubricant. Johansson (1986b) showed that the powder form of magnesium stearate have more adverse effects on tablet hardness and disintegration than the granular form. A decrease in the magnesium stearate level from 1.7 mg to 0.85 mg in a tablet comprised of mostly calcium phosphate dibasic reduced the disintegration time from 10 to 4.5 min (Bavitz et al., 1986). Strickland et al. (1956) showed that disintegration time increased substantially more for increases of magnesium stearate than other lubricants stearic acid and stearyl alcohol. Furthermore, Levy et al. (1963) shoed the dissolution of salicylic acid was reduced significantly by the presence of 3% magnesium stearate, while the dissolution actually increased with the addition of hydrophilic sodium lauryl sulfate compared to a tablet with no lubricant.

1.4. Granule characterization

After the granulation step, multiple granule properties are commonly measured to assess the flowability of the granules for subsequent downstream processes, since one of the main objectives of granulation is to improve product flow. Tablet quality can be

influenced by a variety of granule properties. Thus, several granule properties, including size, size distribution, density, and flowability, are measured.

Several different techniques can be utilized to measure each individual property. Particle size and size distribution can be measured by sieving, microscopy, laser diffraction, dynamic light scattering, electrolytic resistivity, sedimentation, and adsorption methods (Fonner et al., 1981; Staniforth, 2002a). Microscopy, specifically scanning electron microscopy, can be used to examine the shape and morphology of the particles. Measurements such as the Hausner ratio and Carr index are used to predict powder flow and compressive properties using ratios of bulk and tapped density. Further tests to measure flowability include the static angle of repose, powder avalanche behaviour, critical orifice diameter identification, and shear cell behaviour.

1.4.1. Size and shape analysis

Particle size will influence the flowability of powder due to the phenomena of cohesion and adhesion. The effects of cohesion and adhesion occur at the surface of the particle, thus, the size of the particle determines the severity of the effects. Fine particles with high surface to mass ratios are more cohesive that coarser particles, which are influenced more by gravitational forces. Therefore, particles greater than 250 μm typically flow well; as the particle size drops below 100 μm, powders become increasingly affected by cohesion and adhesion, leading to reduced flow. Furthermore, particles similar in size, yet dissimilar in shape, can have drastically different flow properties due to the disparity in interparticle contact area. Particle shapes leading to high surface to volume ratios (ie.

nonspherical particles) are more cohesive and thus have decreased flowability. (Staniforth, 2002a)

Several different techniques can be utilized to measure particle size and size distribution. Size distribution has traditionally been measured by sieving. Sieving is executed by passing a sample of powder through a series of woven mesh trays with different square aperture diameters. The series of trays is stacked in such a manner that only particles with a critical diameter smaller than that of the square aperture can continue down through the set of sieves. The sieve set is typically mechanically agitated to induce full particle segregation. Both a size distribution and median size can be calculated using the sieving technique. Furthermore, a large range of particles sizes, from micrometers to centimeters, can be accommodated with sieves (Merkus, 2008). However, the long processing time and inability to calculate equivalent diameter for non-spherical particles are drawbacks. Moreover, sieving cannot be used with fragile particles as the mechanical agitation promotes attrition. Thus, it is imperative to determine particle strength before sieving to ensure the sieves are not being shaken so vigorously as to encourage breakage and attrition (Staniforth, 2002a, 2002b). Progress has been made to improve the efficiency of traditional sieving, including the use of ultrasound technology (Monteith, 2004) and partial vacuums (Staniforth, 2002a).

Laser light scattering can also be utilized to measure particle size and particle size distribution. A laser beam of light is directed at the particles which scatter the light in different angles. Particle size distribution are calculated by comparing a sample's scattering pattern with an appropriate optical model using a mathematical inversion

process. Traditionally, two models, the Fraunhofer Approximation and Mie theory, are used (Staniforth, 2002a). While the appropriate particle size range for testing is wide (1-3000 μm), some fragile particles can undergo breakage and attrition during dispersion due to sonication (Merkus, 2008).

Microscopy, specifically scanning electron microscopy, can confirm size estimates and provide visualizations of the shape and morphology of granules. A powder sample is prepared on a small aluminum plate and coated with gold before a high-energy beam of electrons that interacts with the particles produces signals reflecting particle appearance at a microscopic level. However, the potential for sampling preparation and error, as well as the small size of sample analyzed, may not provide an accurate depiction of the entire powder.

1.4.2. Density measurements

The bulk density of a powder is dependent on particle packing geometry and powder consolidation. A more consolidated powder is likely to be more resistant to flow (Stanifoth, 2002b). Powder packing geometry is affected by particle size and size distribution, particle shape and texture, and surface properties. Powders with a large size distribution typically result in a more closely packed cohesive powder as void spaces between coarse particles are filled with finer particles. However, powders with an overall larger median size will be less affected by adhesion and cohesion forces, increasing the porosity in packing. Arches or bridges formed by the interaction of non-isometric, highly textured, and/or irregular shaped particles cause the powder to have a larger difference between loose packing and tight packing geometries over regularly shaped particles

(Staniforth 2002a). Furthermore, the presence of electrostatic forces can add to interparticle interactions and promote closer particle packing, increasing cohesion.

Both the Hausner ratio and Carr index are used to indicate the cohesiveness of a powder using a ratio of bulk and tapped densities. The initial bulk density, otherwise known as fluff or poured bulk density, can be obtained by pouring a powder down a chute. The final tapped density is achieved by mechanically tapping the cylinder of powder until the powder is consolidated and has reached a stable, unchanging arrangement (Staniforth 2002a). The ratios used to determine both the Hausner ratio and Carr index are provided:

$$Hausner\ Ratio = \frac{tapped\ density}{bulk\ density} \tag{1-1}$$

$$Carr\ Index = \frac{tapped\ density - bulk\ density}{tapped\ density} \times 100\% \tag{1-2}$$

Both cohesivity and flow properties of powders have been numerically indicized for both the Hausner ratio and Carr index. A Hausner ratio larger than 1.4 indicates a very cohesive powder while a ratio lower than 1.25 indicates a less cohesive, free-flowing powder. Powders with Hausner ratios in the range between 1.25 and 1.4 belong to a transitional group with some cohesive properties (Abdullah and Geldart, 1999). A Carr index below 20-25% indicates good flowability (Carr, 1965).

Both the Hausner ratio and Carr index are good measures of powder cohesivity. However, the major drawback of density measurements is the effect of powder handling on results. Variations in technique used to determine both bulk and tapped densities as well as differences in powder handling make it difficult to compare to literature results.

Nonetheless, the quick processing time and inexpensive procedure costs make density measurements a good estimate of potential flow.

1.4.3. Angle of repose

The angle of repose is defined as the critical angle, or steepest angle of descent, of a slope of powder relative to the horizontal plane when powder on the slope face is on the verge of sliding. This indirect measure of flow is used to determine differences in potential powder flowability using a basis of interparticle cohesion and adhesion (Staniforth, 2002b).

There are two main angle of repose measurements: static angle of repose and dynamic angle of repose. The static angle of repose is usually measure by pouring powder from a fixed height to form a conical pile and measuring the maximum attainable slope. Although angle of repose measurements are done quickly and are useful in comparing powders, variability in sample handling and measurement techniques make the static angle of repose not always representative of flow under specific conditions (Staniforth, 2002b). Again, this measurement technique is not easily comparable to the literature, but can still serve as a good comparative measurement technique. Furthermore, static angle of repose tests are better suited for samples that consist of particles of similar size and flowability. When measuring powders that are large with wide size distributions, such as granules, obtaining meaningful results can be a challenge. A good representation of flow can be difficult to acquire when the larger, more free-flowing particles immediately slide down the slope rather than adhering to the slope angle. Therefore, the mixture must be poured as homogeneously as possible to avoid size segregation, resulting in a

misrepresentation of the static angle of repose, and ultimately flowability (Chik and Vallejo, 2005).

The dynamic angle of repose is determined by placing the material in a cylinder with at least one transparent face. The cylinder is rotated at a fixed speed and dynamic angle of repose is the maximum slope of the powder before repositioning.

1.4.4. Shear cell measurements

A shear cell is an apparatus that is designed to measure stress at different values of normal stress. In order to test the shear strength of a powder, the powder is packed into the two halves of the cell. A normal stress is then applied, usually by use of weights. A shear force is then applied using a system of cords connected from the lid of the cell, via pulley, to the origin of the normal stress. The shear stress is determined by dividing the shear force by the cross-sectional area of the powder bed. The shear force will increase as the normal stress increases. In order to determine the amount of cohesion in a powder bed, the plotted line of normal stress vs. shear stress is extrapolated back to zero shear stress. The stress due to cohesion can be a determinant of flow (Staniforth 2002a).

1.4.5. Critical orifice diameter

Another measurement of powder flow is the size of the smallest hole through which powder discharges. Powder is filled into a shallow tray to a uniform depth with uniform packing. The base of the tray is perforated with holes, which are blocked. When the holes are unblocked, the critical orifice diameter is the size of the smallest hole through which powder flows. Again, critical orifice diameter is a measure of powder cohesion (Staniforth 2002a).

1.4.6. Powder avalanche analysis

An avalanche is a drastic, sudden flow of a large mass of snow down a slope. The term used to describe a deadly natural phenomenon has been adopted to describe a similar action to measure flow properties of, but not limited to, pharmaceutical powders.

Powder avalanching to measure flowability as a dynamic testing method is originally based on the principles of the static angle of repose adapted to measure this angle dynamically. Bretz et al. (1992) first used digital imaging analysis in a rotating Lucite-sheeted rectangular box to observe avalanching behaviour of non-cohesive granular material. A tray was rotated, slowly, around a fixed axis. It was observed that large avalanches occurred with a definite periodicity while avalanches of a smaller scale showed a power-law size distribution.

Continued research in this field led to advanced powder avalanching methods using mechanized cylindrical rotating drums. The standard dynamic avalanche measurement utilizes a rotating cylindrical drum with transparent end equipped with a measurement and recording system. A powder sample is carried up the side of the rotating drum until the accumulation of powder reaches a point of instability sufficient to cause a collapse, or avalanche. The periodicity and behaviour of the avalanche is measured and recorded. Two main types of avalanche equipment have been developed: one based on measuring avalanches using visual imaging software with the other using load distribution.

1.4.6.1. Imaging analysis

Kaye et al. (1995) first researched powder avalanching in a rotating disc. By recording the successive time between avalanches, known as avalanche time, it was possible to

assess both the mixing progress as well as comparing mixture concentrations. Using the avalanche time, discrete phase-space maps, known as strange-attractor plots, were assembled to display the time scatter. Free-flowing powders produced plots with points close to the origin with a small spread, whereas cohesive powders produced plots with points further from the origin with a large spread between points. The study and equipment design by Kaye et al. (1995, 1996) led to commercialization; the AeroFlow Powder Avalanching Analyzer was made commercially available in 1996 by Amherst Process Instruments Inc (Kaye et al., 1996).

The original Aeroflow Powder Avalanching Analyzer consisted of a cylindrical disc 13 cm in diameter and 2.5 cm in width. An electric motor was used to powder the shaft to which the disc was mounted; the disc was filled with a fractional volume of powder. The shaft was rotated at a constant speed and the slow rotation caused the powder to avalanche. The avalanches were measured using light transmitted from a source to a photocell array. Analysis of the voltage signal from the array was done using chaos theory and fractal geometry (Kaye et al. 1995).

Feeley et al. (1998) used the AeroFlow Analyzer to monitor the avalanche time for two different batches of salbutamol sulphate. One sample was obtained prior to micronisation, while the other was obtained after micronisation. By observing mean avalanche time and constructor strange-attractor plots, clear differences could be observed between the two samples. Although the differences detected were not large, the ability to detect the small differences showed promise for the use of avalanche time to characterize flow properties.

The utilization of avalanche time was expanded by Lee et al. (2000). Powder flow was characterized by using a dual approach that also relied on visual observation of the avalanche behaviour. Correlations for ranking the flowability of six pharmaceutical powders were established as statistically significant in comparing the results obtained from the AeroFlow Analyzer and other standard powder characterization methods: Carr's index, critical orifice diameter, particle size, and particle shape.

Lavoie et al. (2002) determined that strange-attractor plots did not quantify a difference in the flow of material with different properties at single rotation rates. However, plotting avalanche time against inverse rotation rates between 0.25 and 2.4 rpm in an AeroFlow Analyzer revealed characteristic linear slopes. Since distinction was improved by the range of rotation rates, the flow and cohesion indices were calculated by averaging standard deviation and average avalanche time over the entire range of rotation rates. The resistance to initial movement during avalanching was indicated by the flow index, while the particle arrangement stability was designated by the cohesion index.

In contrast to using the average of avalanche time and scatter, Soh et al. (2006) found that using gradients improved flow and cohesion indices. Samples of lactose and microcrystalline cellulose were rotated in the AeroFlow Analyzer at rates between 0.25 and 1 rpm. The data used to assemble the indices reflected changes in both avalanche time and scatter over a range of rotation rates, similar to Lavoie et al. (2002). The inverse of the gradient of avalanche time was used to construct the flow index, while the gradient of scatter against rotation rate was utilized to create the cohesion index. By using the two indices concurrently, a more precise nature of the powder could be assessed as both the

flow of the mixture and cohesivity of the individual particle could be determined. Both sets of indices developed by Lavoie et al. (2002) and Soh et al. (2006) showed strong correlation with other typical measures, including Carr's index, static angle of repose, and particle size. However the indices were limited in use to particles of nearly spherical morphology.

Lindberg et al. (2004) were also able to correlate other flow measurements, including results from the Hausner ratio, powder rheometer, uniaxial tests, and Jenike tester. Varying amounts of excipients in 4 similar formulations were rotated at 0.5 rpm for 900 seconds. Avalanche time and scatter measurements and trends agreed with results from other completed tests.

Results from the AeroFlow Analyzer were also compared to the Hausner ratio, uniaxial tester, and static angle of repose by Thalberg et al. (2004). Using a rotation rate of 0.5 rpm for 900 seconds, like Lindberg et al. (2004), the flow properties of placebo mixtures of medium and micronized particles were analyzed. Mixtures with less than 5% micronized particles behaved such that increasing the proportion of fines increased avalanche time, as predicted. However, beyond a critical concentration, no quantifiable different was observed. Furthermore, it was observed that the standard deviation was higher for powders demonstrating more cohesive properties.

In addition to the originally commercialized AeroFlow Analyzer, other powder avalanching analyzers using visual analysis have been designed and used by other research groups. Quintanilla et al. (2001) investigated avalanche size in a 7.4 cm diameter drum that was 2 cm in width using digital video analysis. Glass beads (400-600 μm) and

a cohesive magnetic material (100 μm) with a polymeric coating were rotated at 0.288 degrees/sec and 0.044 degrees/sec, respectively, until 5000 avalanches were recorded. In contrast to Bretz et al. (1992), it was found that avalanche angle and time did not follow a power-law distribution. The avalanches produced by the glass beads occurred regularly, in nearly uniform size and frequency.

In succession to the AeroFlow Analyzer, the Revolution Powder Analyzer was developed by Mercury Scientific Inc. to improve upon the original design. The ability to calculate the potential energy level of the powder, the energy loss during avalanche, and several surface parameters were among the improvements made. A camera with a resolution of 648 x 488 captures up to 60 frames per second. A variety of drum sizes are available, with the standard size measuring 11cm in diameter with a width of 3.5 cm. The apparatus can be rotated between 0.1 and 200 rpm (Martiska, 2009).

Using the Revolution Powder Analyzer, Krantz et al. (2009) characterized the dynamic flow of fine coating powders from 22 to 31 μm in diameter. The avalanche angle was compared to particle size by laser diffraction, static angle of repose testing, bed expansion ratio, and powder rheometer cohesion testing. As particle size decreased, avalanche angle increased. Since the tests measured different powder properties, relationships between all the parameters were not identified. Krantz et al. (2009) showed that combining results from various tests into a single index was not favourable, unlike the many groups who defined a single flowability index (Lee et al., 2000; Lavoie et al., 2002; Soh et al., 2006). It was determined to not be favourable since the different

measurement techniques provided valuable information about the powder at different stress states.

Nalluri and Kuentz (2010) investigated flow using the Revolution Powder Analyzer. Initial testing concluded that rotation rates greater than 2.0 rpm were not able to demonstrate slight differences in powder flow. On the basis of their initial testing, a rotation rate of 1.0 rpm was selected for all further trials. Lower avalanche times and narrower scatter were attributed to free-flowing powders. For different powder mixtures, similar trends for avalanche time, avalanche power, and avalanche angle were observed. Transitions in flow were found to be best detected by avalanche time. Furthermore, it was determined that flow parameter measurements corresponding to improved overall flow displayed less variability over the duration of avalanche analysis; higher standard deviations of avalanche time for cohesive powder agreed with previous literature (Thalberg et al., 2004).

1.4.6.2. Load cell analysis

Load cell avalanche analyzers developed use a different method than those using visual analysis techniques. A load cell based avalanche monitoring apparatus used by Davies et al. (2004) consisted of a cylindrical drum 13 cm in diameter and 2.54 cm in width. The cylindrical drum rotated over a load cell that detected the change in position of the center of mass of the powder sample within the drum. The loading measurements were synced with video recordings to observe avalanche behaviour. Lactose (206 μm) and sago (a food starch) (2.4mm) were the two excipients tested. By measuring the variance in the center of mass at different rotation rates, three phases were identified: surging, slumping,

and rolling; the three identified flow regimes corresponded to other literature observations (Dury et al., 1998; Castellanos et al., 1999; Tegzes et al., 2002).

Alexander et al. (2006) developed a gravitation displacement rheometer (GDR). Samples are loaded into a cylindrical drum 14 cm in diameter and 42 cm in width. The significant width of the drum is to minimize the frictional effect produced by the sides of the drum. Two Avicel samples (60 and 90 μm), two lactose samples (50 and 100 μm), and glass bead (700 μm) were rotated at rates ranging from 5 to 30 rpm. Two different flow regimes were observed. A cracking mechanism in which the avalanches detached from the main powder bed by tensile cracking and a steady regime in which the avalanche detach tangentially were described. Initial Avicel avalanches were attributed to the cracking mechanism; however, the bed appeared to enter the steady regime following a small set of rotations. Since the size and frequency of the Avicel avalanches varied greatly, a 'dual' dynamic angle of repose was observed; the powder bed was described as having a crescent shape. The glass beads, on the other hand, showed a uniform avalanche angle and nearly uniform avalanche size and frequency. The significant differences observed for the dynamic angle of repose and avalanche size and frequency of the different materials was investigated by Quintanilla et al. (2001, 2006).

The GDR was used by Faqih et al. (2007) to characterize flowability of both mixtures and pure pharmaceutical powders, including lactose, cellulose, and magnesium stearate. The presence of the lubricant magnesium stearate did not affect flow properties of non-cohesive powders, but did significantly improve flowability for cohesive powders. Furthermore, the moisture content was determined to have an effect on the flow of

powders. As the moisture content of lactose increased, the flowability of the powder decreased, whereas the opposite was observed for cellulose. It was proven that the GDR was able to successfully detect differences in flow properties.

Powder avalanching has become a promising and increasingly popular method of characterizing powder flow properties. Of the two main techniques, using visual analysis remains the most popular. However, due to the nature of the measurements conducted, the size of the drums varies considerably. The drums used in load cell techniques are larger and wider to more accurately measure changed in the center of gravity without unwanted end friction effects. Conversely, the drums used in visual analysis are much smaller, since recording sensitivity is not an issue. Furthermore, the drums are much narrower, thus allowing the calculation of surface parameters since the change in surface profile from end to end is minimal. While each method has distinct characteristics, both techniques show promising results for quantifying powder flow.

1.5. Thesis overview

Chapter 1 provides an introduction to the thesis with a literature review of some key aspects related to granulation and tablet lubrication. There is a short overview of pharmaceutical tablet manufacturing focusing on granulation. Both high shear and fluidized bed granulation are discussed, including important studies relating to both granulation techniques. A section on granule formation and growth is given. A section on lubrication and relevant studies involving lubrication and tableting is included. In addition, a detailed review of granule characterization methods is provided.

The overall objective of the thesis research was to investigate the effect of the lubrication on pharmaceutical powder flow, specifically a placebo formulation prepared using different granulation methods. The research is summarized in three manuscripts presented in Chapters 2, 3, and 4. In Chapter 2, the focus was on the effect of lubricants on the flowability of spray dried lactose, a common pharmaceutical powder. Chapter 3 compares the granule characteristics of both high shear and fluidized bed granules. Chapter 4 compares the effect of magnesium stearate on the flow properties of the two granule types.

Chapter 5 provides an overall conclusion for the thesis research.

1.6. References

Abdullah, E., Geldart, D., 1999. The use of bulk density measurements as flowability indicators. Powder technology 102, 151-165.

Alcalà, M., Blanco, M., Bautista, M., González, J.M., 2010. On-line monitoring of a granulation process by NIR spectroscopy. Journal of pharmaceutical sciences 99, 336-345.

Alexander, A.W., Chaudhuri, B., Faqih, A.M., Muzzio, F.J., Davies, C., Tomassone, M.S., 2006. Avalanching flow of cohesive powders. Powder technology 164, 13-21.

Armstrong, N.A., 2007. Tablet manufacture. Encyclopedia of pharmaceutical technology 6, 3655.

Bavitz, J.F., Shiromani, P.K., 1986. Granulation surface area as basis for magnesium stearate concentration in tablet formulations. Drug development and industrial pharmacy 12, 2481-2492.

Betz, G., Bürgin, P.J., Leuenberger, H., 2003. Power consumption profile analysis and tensile strength measurements during moist agglomeration. International journal of pharmaceutics 252, 11-25.

Betz, G., Bürgin, P.J., Leuenberger, H., 2004. Power consumption measurement and temperature recording during granulation. International journal of pharmaceutics 272, 137-149.

Bretz, M., Cunningham, J.B., Kurczynski, P.L., Nori, F., 1992. Imaging of avalanches in granular materials. Physical review letters 69, 2431-2434.

Briens, L., Daniher, D., Tallevi, A., 2007. Monitoring high-shear granulation using sound and vibration measurements. International journal of pharmaceutics 331, 54-60.

Carr, R.L., 1965. Evaluating flow properties of solids. Chem Eng 72.

Castellanos, A., Valverde, J.M., Pérez, A.T., Ramos, A., Watson, P.K., 1999. Flow regimes in fine cohesive powders. Physical review letters 82, 1156-1159.

Chik, Z., Vallejo, L.E., 2005. Characterization of the angle of repose of binary granular materials. Canadian geotechnical journal 42, 683-692.

Daniher, D., Briens, L., Tallevi, A., 2008. End-point detection in high-shear granulation using sound and vibration signal analysis. Powder technology 181, 130-136.

Danish, F., Parrott, E., 1971. Effect of concentration and size of lubricant on flow rate of granules. Journal of pharmaceutical sciences 60, 752-754.

Davies, C.E., Williams, A., Tallon, S., Fenton, K., Brown, N., 2004. A new approach to monitoring the movement of particulate material in rotating drums. Developments in Chemical Engineering and Mineral Processing 12, 263-275.

Dawoodbhai, S., Rhodes, C.T., 1990. Pharmaceutical and cosmetic uses of talc. Drug development and industrial pharmacy 16, 2409-2429.

Dawoodbhai, T.S., Suryanarayan, E., Woodruff, C., Rhodes, C., 1991. Optimization of Tablet Formulations Containing. Drug development and industrial pharmacy 17, 1343-1371.

Dury, C.M., Ristow, G.H., Moss, J.L., Nakagawa, M., 1998. Boundary effects on the angle of repose in rotating cylinders. Physical Review E 57, 4491.

Ennis, B., 1990. Design & Optimization of Granulation Processes for Enhanced Product Performance. E&G Associates, Nashville, Tenn.

Ennis, B., Litster, J., 1997. Particle size enlargement. Perry's Chemical Engineer's Handbook, 7th edn., McGraw-Hill, New York, 20-89.

Faqih, A.M.N., Mehrotra, A., Hammond, S.V., Muzzio, F.J., 2007. Effect of moisture and magnesium stearate concentration on flow properties of cohesive granular materials. International journal of pharmaceutics 336, 338-345.

Fassihi, A., Kanfer, I., 1986. Effect of compressibility and powder flow properties on tablet weight variation. Drug development and industrial pharmacy 12, 1947-1966.

Feeley, J., York, P., Sumby, B., Dicks, H., 1998. Determination of surface properties and flow characteristics of salbutamol sulphate, before and after micronisation. International journal of pharmaceutics 172, 89-96.

Fonner, D., Anderson, N., Banker, G., 1981. Granulation and tablet characteristics. Pharmaceutical Dosage Forms: Tablets 2, 185-239.

Frake, P., Greenhalgh, D., Grierson, S., Hempenstall, J., Rudd, D., 1997. Process control and end-point determination of a fluid bed granulation by application of near infra-red spectroscopy. International journal of pharmaceutics 151, 75-80.

Gamble, J.F., Dennis, A.B., Tobyn, M., 2009. Monitoring and end-point prediction of a small scale wet granulation process using acoustic emission. Pharmaceutical development and technology 14, 299-304.

Hancock, B., York, P., Rowe, R., 1982. Characterization of wet masses using a mixer torque rheometer: 2. Mixing kinetics. International journal of pharmaceutics 83, 147-153.

Hansuld, E.M., Briens, L., McCann, J.A.B., Sayani, A., 2009. Audible acoustics in high-shear wet granulation: Application of frequency filtering. International journal of pharmaceutics 378, 37-44.

Hansuld, E.M., Briens, L., Sayani, A., McCann, J.A.B., 2011a. An investigation of the relationship between acoustic emissions and particle size. Powder technology.

Hansuld, E.M., Briens, L., Sayani, A., McCann, J.A.B., 2011b. Monitoring quality attributes for high-shear wet granulation with audible acoustic emissions. Powder technology.

Holm, P., Schaefer, T., Kristensen, H., 1985a. Granulation in high-speed mixers Part V. Power consumption and temperature changes during granulation. Powder technology 43, 213-223.

Holm, P., Schaefer, T., Kristensen, H., 1985b. Granulation in high-speed mixers Part VI. Effects of process conditions on power consumption and granule growth. Powder technology 43, 225-233.

Iveson, S.M., Litster, J.D., Hapgood, K., Ennis, B.J., 2001. Nucleation, growth and breakage phenomena in agitated wet granulation processes: a review. Powder technology 117, 3-39.

Jarosz, P.J., Parrott, E.L., 1984. Effect of lubricants on tensile strengths of tablets. Drug development and industrial pharmacy 10, 259-273.

Johansson, M., 1985a. Investigations of the mixing time dependence of the lubricating properties of granular and powdered magnesium stearate. Acta pharmaceutica suecica 22, 343.

Johansson, M., Astra Laekemedel, A., Soedertaelje, S., 1986. The effect of scaling-up of the mixing process on the lubricating effect of powdered and granular magnesium stearate. Acta Pharmaceutica Technologica 32, 39-42.

Johansson, M.E., 1985b. Influence of the granulation technique and starting material properties on the lubricating effect of granular magnesium stearate. Journal of pharmacy and pharmacology 37, 681-685.

Jørgensen, A.C., Luukkonen, P., Rantanen, J., Schæfer, T., Juppo, A.M., Yliruusi, J., 2004. Comparison of torque measurements and near-infrared spectroscopy in characterization of a wet granulation process. Journal of pharmaceutical sciences 93, 2232-2243.

Kaye, B., 1996. Sampling and characterization research: Developing two tools for powder testing. Powder and Bulk Engineering 10, 44-66.

Kaye, B.H., Gratton-Liimatainen, J., Faddis, N., 1995. Studying the avalanching behaviour of a powder in a rotating disc. Particle & particle systems characterization 12, 232-236.

Krantz, M., Zhang, H., Zhu, J., 2009. Characterization of powder flow: Static and dynamic testing. Powder technology 194, 239-245.

Laicher, A., Profitlich, T., Schwitzer, K., Ahlert, D., 1997. A modified signal analysis system for end-point control during granulation. European journal of pharmaceutical sciences 5, 7-14.

Lavoie, F., Cartilier, L., Thibert, R., 2002. New methods characterizing avalanche behavior to determine powder flow. Pharmaceutical research 19, 887-893.

Lee, Y.S.L., Poynter, R., Podczeck, F., Newton, J.M., 2000. Development of a dual approach to assess powder flow from avalanching behavior. AAPS PharmSciTech 1, 44-52.

Levy, G., Gumtow, R.H., 1963. Effect of certain tablet formulation factors on dissolution rate of the active ingredient III. Tablet lubricants. Journal of pharmaceutical sciences 52, 1139-1144.

Lindberg, N.O., Pålsson, M., Pihl, A.C., Freeman, R., Freeman, T., Zetzener, H., Enstad, G., 2004. Flowability measurements of pharmaceutical powder mixtures with poor flow using five different techniques. Drug development and industrial pharmacy 30, 785-791.

Liu, L.X., Marziano, I., Bentham, A., Litster, J.D., White, E., Howes, T., 2008. Effect of particle properties on the flowability of ibuprofen powders. International journal of pharmaceutics 362, 109-117.

Martiska, G.P., Martiska, P.L., 2009. Method for characterizing powder ina rotating cylindrical container by image analysis. Google Patents.

Matero, S., Poutiainen, S., Leskinen, J., Järvinen, K., Ketolainen, J., Reinikainen, S.P., Hakulinen, M., Lappalainen, R., Poso, A., 2009. The feasibility of using acoustic

emissions for monitoring of fluidized bed granulation. Chemometrics and Intelligent Laboratory Systems 97, 75-81.

Merkus, H.G., 2008. Particle Size Measurements: Fundamentals, Practice, Quality. Springer.

Meshali, M., El-Banna, H., El-Sabbagh, H., 1983. Use of a fractional factorial design to evaluate granulations prepared in a fluidized bed. Die Pharmazie 38, 323.

Mitrevej, A., Sinchaipanid, N., Faroongsarng, D., 1996. Spray-dried rice starch: comparative evaluation of direct compression fillers. Drug development and industrial pharmacy 22, 587-594.

Monteith, J., 2004. Improved efficiency ultrasonic sieving apparatus. EP Patent 0,996,109.

Nagel, K.M., Peck, G.E., 2003. Investigating the effects of excipients on the powder flow characteristics of theophylline anhydrous powder formulations. Drug development and industrial pharmacy 29, 277-287.

Nalluri, V.R., Kuentz, M., 2010. Flowability characterisation of drug-excipient blends using a novel powder avalanching method. European Journal of Pharmaceutics and Biopharmaceutics 74, 388-396.

Niazi, S., 2004. Handbook of Pharmaceutical Manufacturing Formulations: Compressed solid products. CRC Press.

Ohike, A., Ashihara, K., Ibuki, R., 1999. Granulation monitoring by fast Fourier transform technique. Chemical and pharmaceutical bulletin-Tokyo- 47, 1734-1739.

Ouabbas, Y., Dodds, J., Galet, L., Chamayou, A., Baron, M., 2009. Particle–particle coating in a cyclomix impact mixer. Powder technology 189, 245-252.

Papp, M.K., Pujara, C.P., Pinal, R., 2008. Monitoring of high-shear granulation using acoustic emission: predicting granule properties. Journal of Pharmaceutical Innovation 3, 113-122.

Parker, M., Rowe, R., Upjohn, N., 1990. Mixer torque rheometry: a method for quantifying the consistency of wet granulations. Pharmaceutical Technology International 2, 50-62.

Paul Findlay, W., Peck, G.R., Morris, K.R., 2005. Determination of fluidized bed granulation end point using near-infrared spectroscopy and phenomenological analysis. Journal of pharmaceutical sciences 94, 604-612.

Pepin, X., Blanchon, S., Couarraze, G., 2001a. Power consumption profiles in high-shear wet granulation. I: Liquid distribution in relation to powder and binder properties. Journal of pharmaceutical sciences 90, 322-331.

Pepin, X., Blanchon, S., Couarraze, G., 2001b. Power consumption profiles in high-shear wet granulation. II: Predicting the overwetting point from a spreading energy. Journal of pharmaceutical sciences 90, 332-339.

Perrault, M., Bertrand, F., Chaouki, J., 2010. An investigation of magnesium stearate mixing in a V-blender through gamma-ray detection. Powder technology 200, 234-245.

Perry, R.H., Green, D.W., Maloney, J.O., 1997. Perry's Chemical Engineers' Handbook. McGraw-Hill.

Pingali, K.C., Saranteas, K., Foroughi, R., Muzzio, F.J., 2009. Practical methods for improving flow properties of active pharmaceutical ingredients. Drug development and industrial pharmacy 35, 1460-1469.

Quintanilla, M., Valverde, J., Castellanos, A., 2006. The transitional behaviour of avalanches in cohesive granular materials. Journal of Statistical Mechanics: Theory and Experiment 2006, P07015.

Quintanilla, M., Valverde, J., Castellanos, A., Viturro, R., 2001. Looking for self-organized critical behavior in avalanches of slightly cohesive powders. Physical review letters 87, 194301.

Rambali, B., Baert, L., Massart, D., 2001a. Using experimental design to optimize the process parameters in fluidized bed granulation on a semi-full scale. International journal of pharmaceutics 220, 149-160.

Rambali, B., Baert, L., Thoné, D., Massart, D., 2001b. Using experimental design to optimize the process parameters in fluidized bed granulation. Drug development and industrial pharmacy 27, 47-55.

Rantanen, J., Yliruusi, J., 1998. Determination of Particle Size in a Fluidized Bed Granulator With a Near Infrared Set-up. Pharmacy and Pharmacology Communications 4, 73-75.

Roblot-Treupel, L., Puisieux, F., 1986. Distribution of magnesium stearate on the surface of lubricated particles. International journal of pharmaceutics 31, 131-136.

Sadek, H., Olsen, J., Smith, H., Onay, S., 1982. A systematic approach to glidant selection. Pharm Tech.

Sandler, N., Wilson, D., 2010. Prediction of granule packing and flow behavior based on particle size and shape analysis. Journal of pharmaceutical sciences 99, 958-968.

Sastry, K.V.S., Fuerstenau, D.W., 1973. Mechanisms of agglomerate growth in green pelletization. Powder technology 7, 97-105.

Soh, J.L.P., Liew, C.V., Heng, P.W.S., 2006. New indices to characterize powder flow based on their avalanching behavior. Pharmaceutical development and technology 11, 93-102.

Staniforth, J., 2002a. Particle-size analysis. Aulton ME. Pharmaceutics: The Science of Dosage form Design, 152-165.

Staniforth, J., 2002b. Powder flow. Aulton ME. Pharmaceutics: The Science of Dosage form Design, 197-210.

Strickland Jr, W., Nelson, E., Busse, L., Higuchi, T., 1956. The physics of tablet compression IX. Fundamental aspects of tablet lubrication. Journal of the American Pharmaceutical Association 45, 51-55.

Summers, M., Aulton, M., 2002. Granulation. Aulton ME. Pharmaceutics The Science of Dosage Form Design.

Talu, I., Tardos, G.I., Ruud van Ommen, J., 2001. Use of stress fluctuations to monitor wet granulation of powders. Powder technology 117, 149-162.

Tan, S., Newton, J., 1990. Powder flowability as an indication of capsule filling performance. International journal of pharmaceutics 61, 145-155.

Tegzes, P., Vicsek, T., Schiffer, P., 2002. Avalanche dynamics in wet granular materials. Physical review letters 89, 94301.

Terashita, K., Kato, M., Ohike, A., Miyanami, K., 1990a. Analysis of end-point with powxer consumption in high speed mixer. Chemical and pharmaceutical bulletin 38, 1977-1982.

Terashita, K., Watano, S., Niyanami, K., 1990b. Determination of end-point by frequency analysis of power consumption in agitation granulation. Chemical and pharmaceutical bulletin 38, 3120-3123.

Thalberg, K., Lindholm, D., Axelsson, A., 2004. Comparison of different flowability tests for powders for inhalation. Powder technology 146, 206-213.

Tousey, M.D., 2002. The granulation process 101: Basic technologies for tablet making. Pharmaceutical technology, 8-13.

Walker, G., Bell, S., Greene, K., Jones, D., Andrews, G., 2009. Characterisation of fluidised bed granulation processes using in-situ Raman spectroscopy. Chemical Engineering Science 64, 91-98.

Wang, D.P., Yang, M.C., Wong, C.Y., 1997. Formulation development of oral controlled-release pellets of diclofenac sodium. Drug development and industrial pharmacy 23, 1013-1017.

Wang, J., Wen, H., Desai, D., 2010. Lubrication in tablet formulations. European Journal of Pharmaceutics and Biopharmaceutics 75, 1-15.

Watano, S., Miyanami, K., 1995. Image processing for on-line monitoring of granule size distribution and shape in fluidized bed granulation. Powder technology 83, 55-60.

Watano, S., Numa, T., Miyanami, K., Osako, Y., 2001. A fuzzy control system of high shear granulation using image processing. Powder technology 115, 124-130.

Watano, S., Tanaka, T., Miyanami, K., 1995. A method for process monitoring and determination of operational end-point by frequency analysis of power consumption in agitation granulation. Advanced Powder Technology 6, 91-102.

Whitaker, M., Baker, G.R., Westrup, J., Goulding, P.A., Rudd, D.R., Belchamber, R.M., Collins, M.P., 2000. Application of acoustic emission to the monitoring and end point determination of a high shear granulation process. International journal of pharmaceutics 205, 79-91.

Wikström, H., Marsac, P.J., Taylor, L.S., 2005. In-line monitoring of hydrate formation during wet granulation using Raman spectroscopy. Journal of pharmaceutical sciences 94, 209-219.

Yang, J., Sliva, A., Banerjee, A., Dave, R.N., Pfeffer, R., 2005. Dry particle coating for improving the flowability of cohesive powders. Powder technology 158, 21-33.

CHAPTER.2. THE EFFECT OF LUBRICANTS ON POWDER FLOWABILITY FOR PHARMACEUTICAL APPLICATION

Garett J. Morin and Lauren Briens

Biomedical Engineering, Western University, London, CANADA

2.1. Introduction

Almost 80% of pharmaceuticals are sold in tablet form. Tablets are commonly manufactured through a series of batch steps that modify and mix excipient powders together with the active drug and then compress the final powder mixture into a tablet form. The success of many of the manufacturing steps relies on the flowability of the powders. Poor powder flow results in tablets that are not uniform in content and weight and therefore must be discarded as inadequate, unsuitable, and possibly unsafe for distribution to patients.

Lubricants are commonly added excipients to many pharmaceutical tablet formulations. Following compression, a tablet must be ejected out of the tablet press die. Lubricants reduce the friction between the tablet and the die metal surface, which reduces the ejection force and helps to ensure that the tablet is completely ejected with no visible surface imperfections.

There are two ways in which lubricants reduce friction: a liquid lubricant can form a thin, continuous fluid layer between the tablet and the metal die surface or lubricant particles

can form a boundary layer on the formulation particles or metal die surfaces. Boundary lubricants are more commonly used over fluid lubricants (Wang et al., 2010). There are six types of commonly used boundary lubricants for pharmaceutical tableting: (i) metallic salts of fatty acids, (ii) fatty acids, hydrocarbons and fatty alcohols, (iii) fatty acid esters. (iv) alkyl sulfates, (v) polymers, and (vi) inorganic materials (Wang et al., 2010).

Magnesium stearate, a metallic salt boundary lubricant, is probably the most commonly used lubricant for pharmaceutical tableting; it is relatively inexpensive, provides high lubrication, has a high melting point, and is chemically stable (Perrault et al., 2010). Calcium stearate is another metallic salt boundary lubricant that can replace magnesium stearate in a formulation (Wang et al., 2010). Metallic salt lubricants are typically added to formulations in the range of 0.25 to 1.0 wt% (Wang et al., 2010). Stearic acid is the most commonly used fatty acid boundary lubricant. In general, fatty acids are more effective die lubricants than the corresponding alcohols, and the alcohols are better than the corresponding hydrocarbons (Alderborn, 2002). Stearic acid is typically added at levels of approximately 2.5 wt% (Wang et al., 2010). Hydrous magnesium silicate or talc is an inorganic boundary lubricant. It is useful when other lubricants cannot be used due to chemical instabilities (Wang et al., 2010). Magnesium silicate was the most widely used lubricant in the past. Magnesium silicate is typically added in the range of 1.0 to 10.0 wt% when being used as a tablet glidant and/or lubricant ((Dawoodbhai and Rhodes, 1990; Dawoodbhai et al., 1991; Wang et al., 1997).

Powder flow is critical during tableting as it must flow easily and uniformly into the tablet dies to ensure tablet weight uniformity and production of tablets with consistent

and reproducible properties (Fassihi and Kanfer, 1986; Tan and Newton, 1990; Sandler and Wilson, 2010). Powder flows when gravitational forces become higher than the friction and cohesion forces that influence particle-particle interactions. Friction acts at contact points between particles to oppose their relative motion. Particle shape and surface morphology affect contact and therefore can increase friction if contact area is increased. Cohesive forces refer to the attraction between particles and include van der Waals' forces, capillary forces and electrostatic forces. Cohesive forces are affected by the surface properties of the particles. As boundary layer lubricants form a film around particles, these lubricants affect the friction and cohesive forces, thereby also affecting powder flow.

The role of glidant is to improve the flowability of the power. Traditionally, magnesium silicate has been used as a glidant in concentration of approximately 1-2 wt% (Alderborn, 2002). While the main role of a lubricant is to ensure that tablet formation and ejection can occur in a low friction environment, some lubricants can also promote powder flow. Dawoodbhai and Rhodes (1990) reviewed the effects of magnesium stearate and magnesium silicate in both traditional glidant and lubricant roles. It was determined that magnesium silicate demonstrated better properties for improving flow, while magnesium stearate was a better choice as a traditional lubricant. Although lubricants can provide some improvement in flow, the addition of a glidant is often still needed to improve the overall mixture flowability.

As magnesium stearate is the most commonly used boundary layer lubricant, it has been the most extensively studied. It has been hypothesized that the film formed by

magnesium stearate around other excipient particles could be: (i) as a monomolecular film of magnesium stearate particles bound to the other excipients by their apolar heads, (ii) as a monoparticulate film of magnesium stearate particles covering the surface of the other excipients, and (iii) as layers of magnesium stearate particles first filling any cavities of the other excipients before forming a continuous layer (Perrault et al., 2010; Roblot-Treupel and Puisieux, 1986). The third hypothesized mechanism of first filling any cavities is the most popular. With this mechanism, magnesium stearate would improve flow by minimizing any surface irregularities of the excipients, which reduces contact points between excipients, decreasing friction and cohesive forces.

The amount of lubricant particles required to form a monolayer around another excipient particle can be calculated. Assuming that the lubricant and the excipient particles are monosized and spherical and that the particles do not deform, then the weight percentage of lubricant particles for 100% monolayer coverage is (Yang et al., 2005):

$$W\% = \frac{N(d_{lubricant})^3 \rho_{lubricant}}{(d_{lubricant})^3 \rho_{excipient} + N(d_{lubricant})^3 \rho_{lubricant}} \times 100\% \quad (2\text{-}1)$$

with the number of lubricant particles per excipient given by:

$$N = \frac{(d_{excipient} + d_{lubricant})^2}{(d_{lubricant})^2} \quad (2\text{-}2)$$

Using equations (2-1) and (2-2), Ouabbas et al. (2009) found that 15% would be required for magnesium stearate with d_{50} of 4.6 μm to form a layer around silica gel particles with

a d50 of 55 μm. Sadek et al. (1982) proposed that the minimum amount of lubricant required to form a complete film over excipient particles would be:

$$Minimum\% = 6 \times \frac{d_{lubricant}\rho_{lubricant}}{d_{excipient}\rho_{bulk}} \times 100\% \quad (2\text{-}3)$$

They further developed equations that then incorporated the geometric packing of the lubricant around the excipient:

$$Lubricant\ \% = \ f^2 \times 6 \times \frac{d_{lubricant}\rho_{lubricant}}{d_{excipient}\rho_{bulk}} \times 100\% \quad (2\text{-}4)$$

where f is the packing factor and usually ranges from 0.5 to 0.75.

Many methods have been developed to measure the flow properties of powders. These methods commonly include the static angle of repose, Carr's compressibility index, Hausner ratio and shear cell testing. Avalanche testing is an emerging powder flowability measurement method. The avalanche testing equipment consists of a rotating drum and measurement system. As the drum rotates, the powder sample is carried up the side of the drum until the weight of the powder causes it to collapse or avalanche. Properties of this powder avalanche are then measured and analyzed to indicate powder flowability. The original equipment was developed by Brian Kaye and commercialized as the Aero-Flow Automated Powder Flowability Analyzer in the 1990s. The Aero-Flow system detected avalanches in a transparent drum by measuring light transmitted from a source to a photocell array. The voltage signal from the photocell array was then analyzed using chaos theory. The Mercury Scientific Revolution Analyzer improved

upon the Aero-Flow system by including an advanced camera and imaging system and more analysis of the images (Nalluri and Kuentz, 2010). A group at Rutgers University has developed a gravitational displacement rheometer (GDR) which consists of a rotating drum mounted on a hinged table connected to a load cell that measures the change in moment of inertia as the powder avalanches within the drum (Faqih et al., 2007). The drum of the GDR is transparent for visual observations rather than advanced avalanche image analysis. Lim et al (2003) also developed avalanche testing equipment, but measurements were based on positron emission particle tracking of the movement of a tracer particle in powder within the rotating drum.

The effect of lubricants on flowability has been examined by several researchers. Using the Hausner ratio and shear cell measurements, Liu et al. (2008) found that the addition of 0.5 wt% of magnesium stearate improved the flowability of cohesive ibuprofen. Faqih et al. (2007) examined the avalanche behavior of commonly used pharmaceutical powders mixed with varying amounts of magnesium stearate. The effect of magnesium stearate on the flowability varied with the powder; there was almost no effect on the already free flowing Fast-Flo lactose but a significant effect on the very cohesive regular lactose. Pingali et al. (2009) examined the flow behavior of acetaminophen, didesmethylesibutramine tartarate and levalbuterol tartrate after mixing with lubricants colloidal silica, talc and magnesium stearate. A flow index obtained from avalanche behaviour showed that the flowability increased with the addition of the lubricants.

Besides reducing friction, lubricants may cause undesirable changes in the properties of the tablet. Lubricant type, concentration, method of lubrication, and the manner of

incorporating the lubricant all affect the tablet compression (Akser et al., 1975). It is generally accepted that magnesium stearate has a more negative effect on the hardness and tensile strength of the tablets with more deformable materials than brittle ones (Wang et al., 2010). When microcrystalline cellulose, an example of plastic materials, was mixed with magnesium stearate, the tablet strength was weakened significantly as the amount of added lubricant increased. Similar results were obtained when other lubricants—such as stearic acid, talc, and PEG—were mixed with microcrystalline cellulose (Jarosz et al., 1984). The adverse impact of magnesium stearate on other commonly used plactically deformable excipients—such as lactose and starch—were also observed (Mitrevej et al., 1996). Because many lubricants are hydrophobic, tablet disintegration and dissolution are often retarded by the addition of lubricant (Alderborn, 2002). Multiple studies (Johansson 1986a/b, Johansson 1985) have led to the theoretical conclusion that the deleterious effects observed are a cause of the combination of the large surface area and hydrophobicity of the lubricant. Strickland et al. (1956) showed that disintegration time increased substantially more for increases of magnesium stearate than other lubricants stearic acid and stearyl alcohol. Furthermore, Levy et al. (1963) shoed the dissolution of salicylic acid was reduced significantly by the presence of 3% magnesium stearate.

The objective of this work is to evaluate the impact of lubricants on the flowability of pharmaceutical powders to determine critical values that optimally balances the positive impact on flowability with the negative impact on tablet properties.

2.2. Materials and methods

2.2.1. Excipients

Spray dried lactose (Flowlac 100, Meggle) was used as the starting material. Four lubricants – magnesium stearate (Alfa Aesar), magnesium silicate (Alfa Aesar), calcium stearate (Alfa Aesar), and stearic acid (triple pressed, J.T. Baker) – were blended with the spray dried lactose at weight percentages indicated in Table 2.1.

2.2.2. Mixing process

The powders were blended using a Patterson Kelly V blender with a stainless steel 4-quart V shell for 15 minutes at a rotation speed of 25 rpm. Each trial size was 0.4 kg, thereby filling the shell to about 15% of the volume.

Table 2.1: Summary of tested mixtures of lubricants and spray dried lactose.

wt% lubricant	Magnesium stearate	Calcium stearate	Magnesium silicate	Stearic acid
0.00	✓	✓	✓	✓
0.25	✓			
0.50	✓	✓	✓	✓
0.75	✓		✓	
1.00	✓	✓	✓	✓
1.25	✓		✓	
1.50	✓	✓	✓	✓
1.75	✓		✓	
2.00	✓	✓	✓	✓
2.50	✓			
3.00	✓	✓	✓	✓
4.00	✓	✓	✓	✓
5.00	✓	✓	✓	✓

2.2.3. Mixture analysis

2.2.3.1. Particle size

Particle size distributions and estimates of the specific surface area of the spray dried lactose and lubricants were measured using a Malvern Mastersizer 2000.

2.2.3.2. Shape and morphology

Scanning electron microscope (SEM) images of the spray dried lactose, lubricants, and samples of the mixtures were taken using a Hitachi S-4500 field emission SEM. The powders were mounted on a plate and coated with gold before examination. The images allowed the shape and morphology of the powders to be examined and allowed visualization of the interaction of the lubricants with the spray dried lactose.

2.2.3.3. Flowability

2.2.3.3.1. Density

The bulk and tapped densities of the mixtures were measured using 100 ml samples. For the bulk density measurements, the powder flowed down a vibrating chute into a 100 ml cylinder and the mass of the powder sample within the cylinder was then measured:

$$bulk\ density\ \left(\frac{g}{ml}\right) = \frac{mass\ of\ sample}{100\ mL} \tag{2-5}$$

The sample within the cylinder was then vibrated/tapped and the resulting volume was measured to determine the tapped density:

$$tapped\ density\ \left(\frac{g}{mL}\right) = \frac{mass\ of\ sample}{tapped\ density\ volume\ (mL)} \tag{2-6}$$

Duplicate density measurements were performed. The bulk and tapped density measurements then allowed the Hausner ratio and Carr index to be calculated:

$$Hausner\ Ratio = \frac{tapped\ density}{bulk\ density} \quad (2\text{-}7)$$

$$Carr\ Index = \frac{tapped\ density - bulk\ density}{tapped\ density} \times 100\% \quad (2\text{-}8)$$

2.2.3.3.2. Static angle of repose

Static angle of repose measurements were performed using a Powder Research Ltd. Angle of Repose Device. Samples of about 60 ml flowed down a vibrating chute and through a funnel to form a pile below on a calibrated level platform to allow the angle of repose to be determined. Samples were measured in triplicate.

2.2.3.3.3. Avalanche behaviour

Various indicators of flowability were investigated using a Mercury Scientific Revolution Powder Analyzer. A sample size of 118 cm^3 was loaded into a drum with a diameter of 11 cm and width of 3.5 cm. This drum was rotated at 0.3 rpm until 128 avalanches had occurred; an avalanche was defined as being a rearrangement of at least 0.65 vol% of the sample in the drum. Optical measurements with a resolution of 648 x 488 at 60 frames per second monitored the powder surface as the sample was rotated and software calculated the flowability indicators. Samples were measured in triplicate.

The two main indicators of flowability analyzed were avalanche time and dynamic density. Avalanche time is determined as the average amount of time between successive avalanches during drum rotation. The Mercury Scientific Revolution Powder Analyzer

also measured the dynamic density of powders through the known sample weight and the measured volume of the powder as it tumbled within the drum.

$$dynamic\ density = \frac{mass\ of\ sample}{volume\ of\ moving\ sample\ (mL)} \quad (2\text{-}9)$$

2.3. Results

2.3.1. Size and size distribution

The size distributions of the spray dried lactose and the lubricants are given in Figure 2.1 and Figure 2.2, respectively, while Table 2.2 summarizes the sizes and estimated densities. The magnesium silicate, magnesium stearate and calcium stearate were all smaller than the spray dried lactose. Stearic acid was the largest tested lubricant: some of its larger particles were similar in diameter to the spray dried lactose.

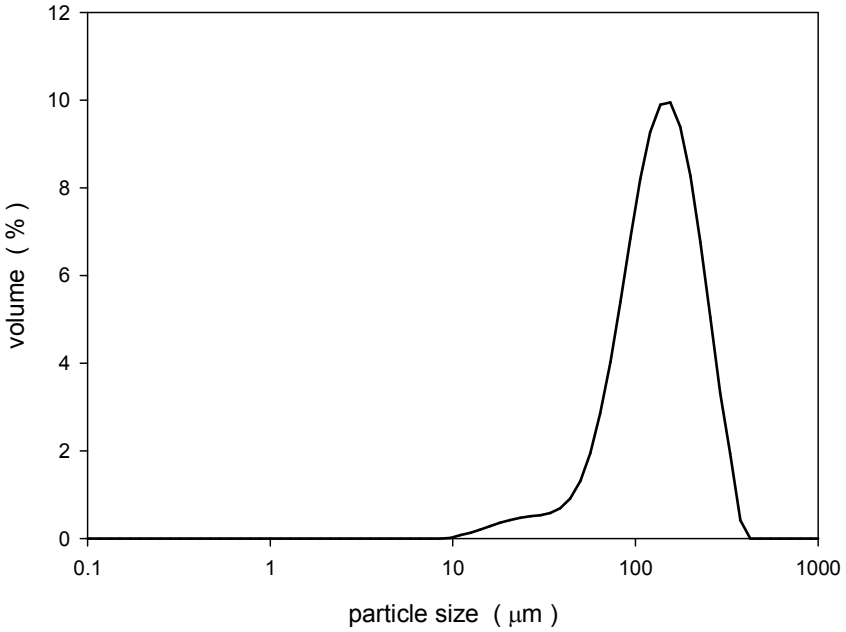

Figure 2.1: Size distribution of spray dried lactose.

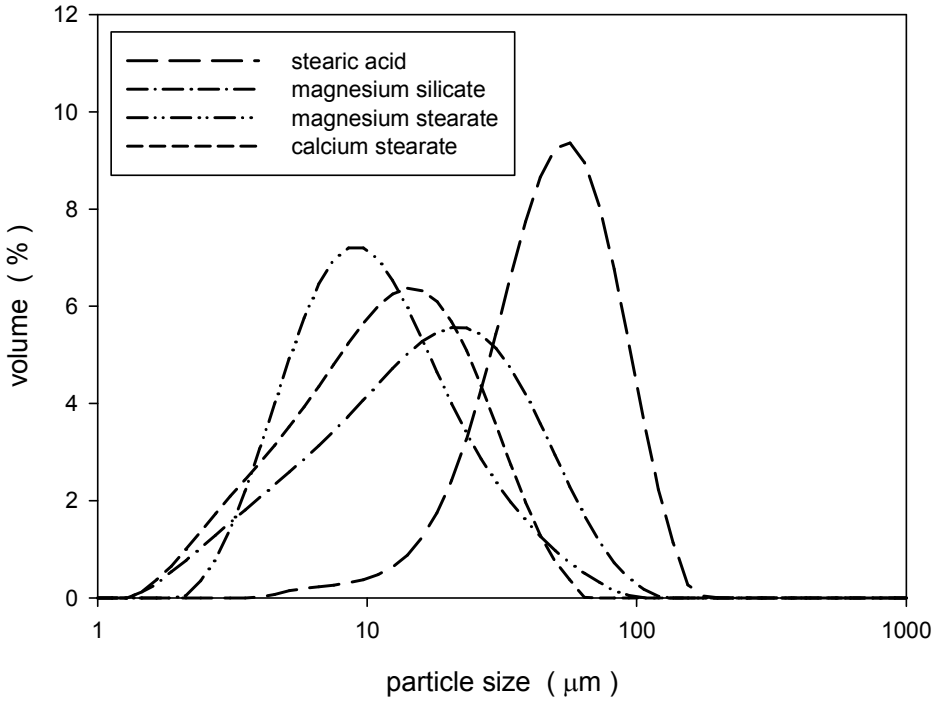

Figure 2.2: Size distributions of four lubricants studied.

Table 2.2: Summary of particle sizes and estimated densities.

powder	d_{10} (μm)	d_{50} (μm)	d_{90} (μm)	d_{psm} (μm)	specific surface area (m^2/g)	true density (g/cm^3)
spray dried lactose	64.81	136.65	244.58	104.51	0.06	1.55
magnesium stearate	4.57	10.22	28.10	8.69	0.69	1.09
calcium stearate	3.80	11.88	28.87	8.26	0.73	1.08
magnesium silicate	4.39	16.64	45.67	10.24	0.59	2.80
stearic acid	22.86	50.05	93.02	39.14	0.15	0.85

2.3.2. Visual observations

Figure 2.3 shows scanning electron images of the spray dried lactose and the lubricants. The spray dried lactose particles were approximately spherical with a slightly textured surface. The magnesium stearate, magnesium silicate and calcium stearate particles were all irregular flakes with a high surface area to volume ratio. In contrast, the stearic acid particles were almost spherical with a smooth surface morphology.

Figure 2.4, Figure 2.5, Figure 2.6, and Figure 2.7 show scanning electron images of samples of the mixtures of the spray dried lactose with the lubricants. The magnesium stearate flakes appeared to first fill any cavities on the surface of the lactose particles. A continuous layer of magnesium stearate was not formed. Instead, at high concentrations, the magnesium stearate remained unattached to the lactose particles and began to form self-agglomerates. Calcium stearate flakes attached to the surface of the lactose particles and at higher concentrations continues to layer around the lactose. Magnesium silicate first filled any surface cavities, but then continued to layer around the spray dried lactose particles and also formed self-agglomerates. Regardless of concentration, most stearic acid particles remained unattached to the lactose.

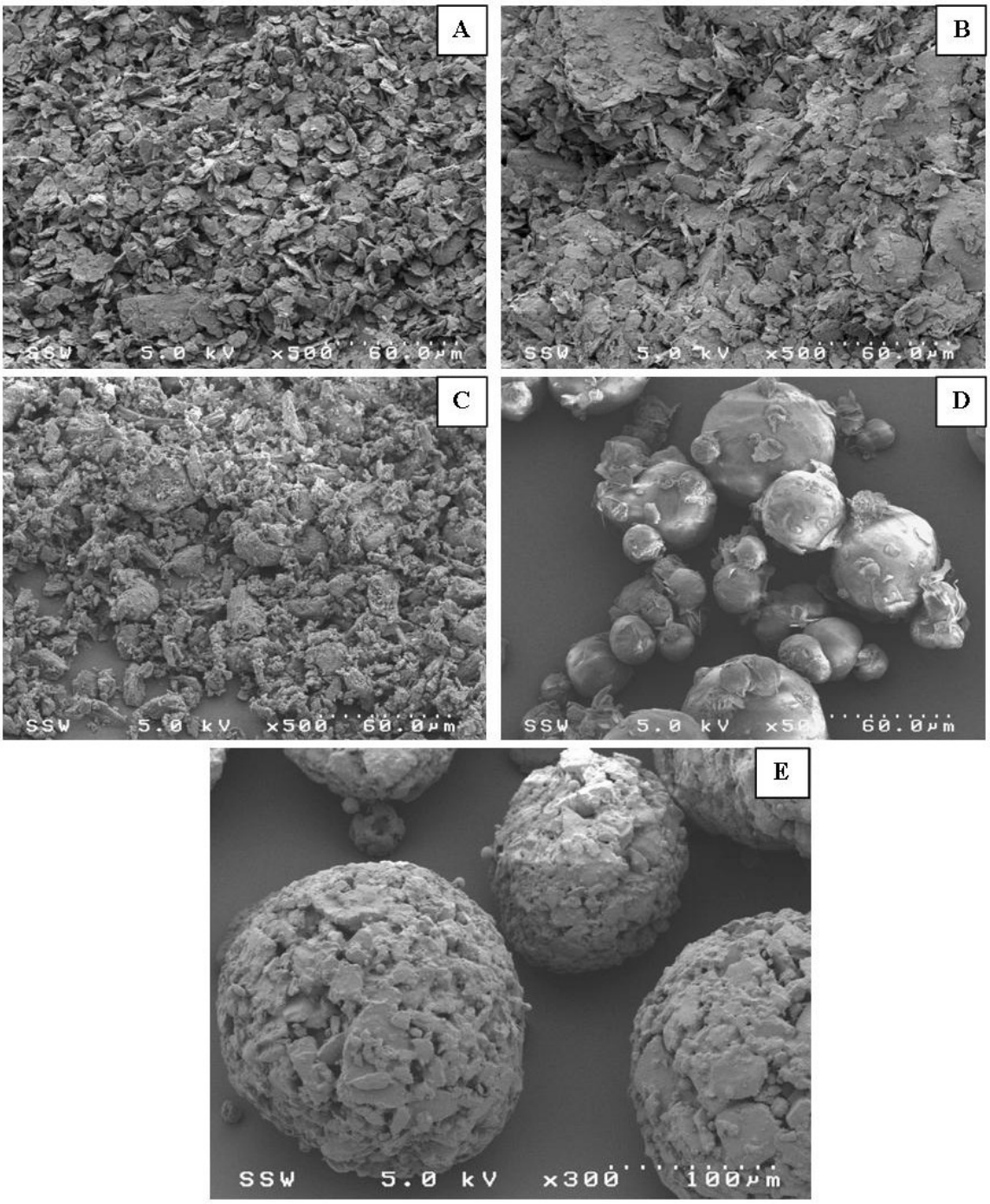

Figure 2.3: SEM images of raw components (A-magnesium stearate, B-magnesium silicate, C-calcium stearate, D-stearic acid, E-spray dried lactose).

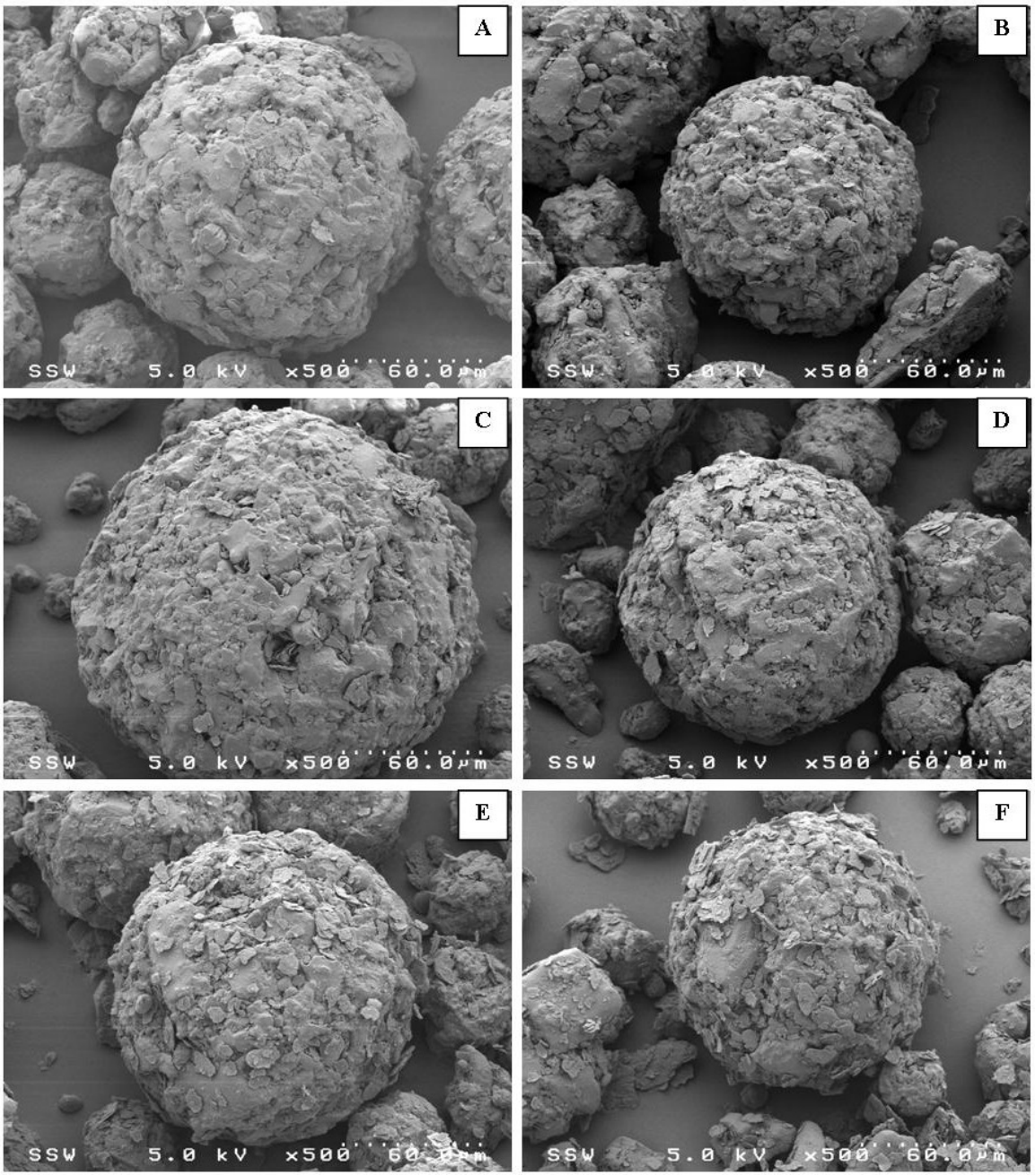

Figure 2.4: SEM images magnesium stearate and spray dried lactose mixtures (A-0.5 wt%, B-1.0 wt%, C-1.5 wt%, D-2.0 wt%, E-3.0 wt%, F-5.0 wt%).

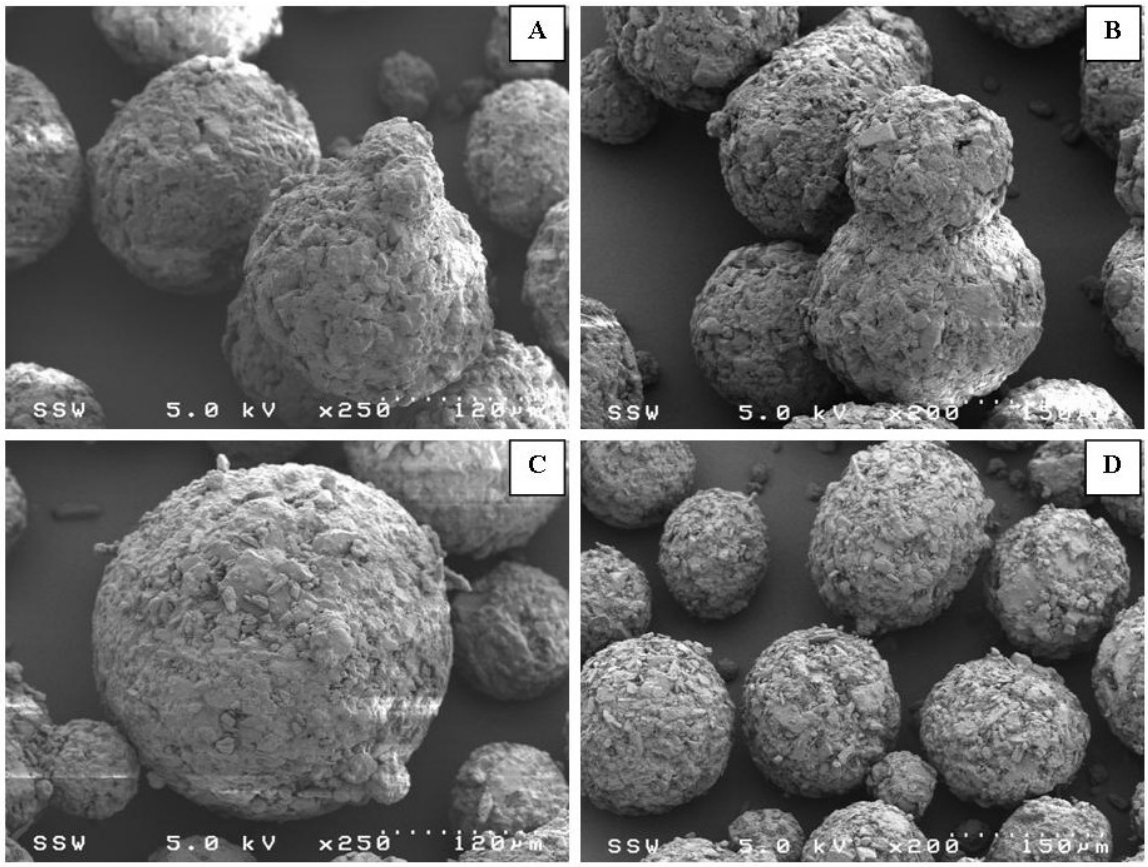

Figure 2.5: SEM images calcium stearate and spray dried lactose mixtures (A-0.5 wt%, B-1.5 wt%, C-2.0 wt%, D-3.0 wt%).

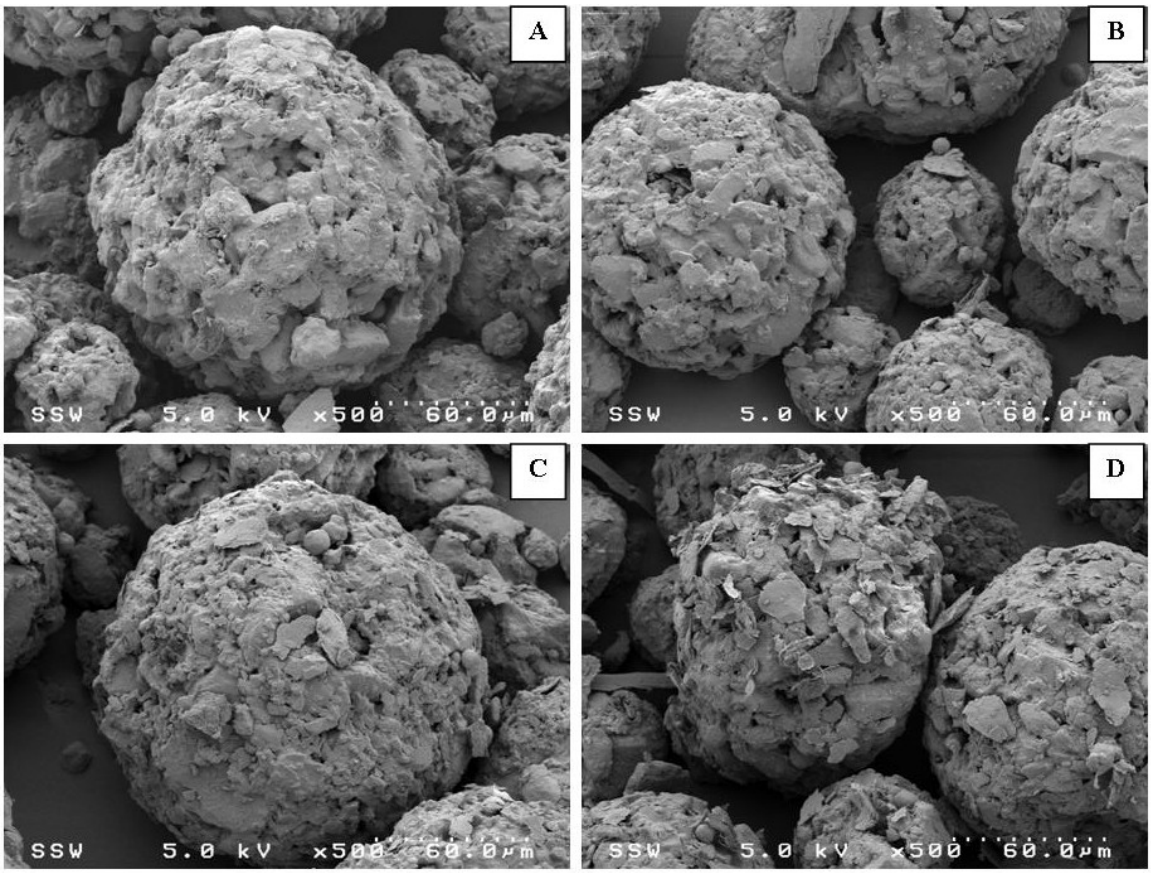

Figure 2.6: SEM images magnesium silicate and spray dried lactose mixtures (A-0.5 wt%, B-1.5 wt%, C-3.0 wt%, D-5.0 wt%).

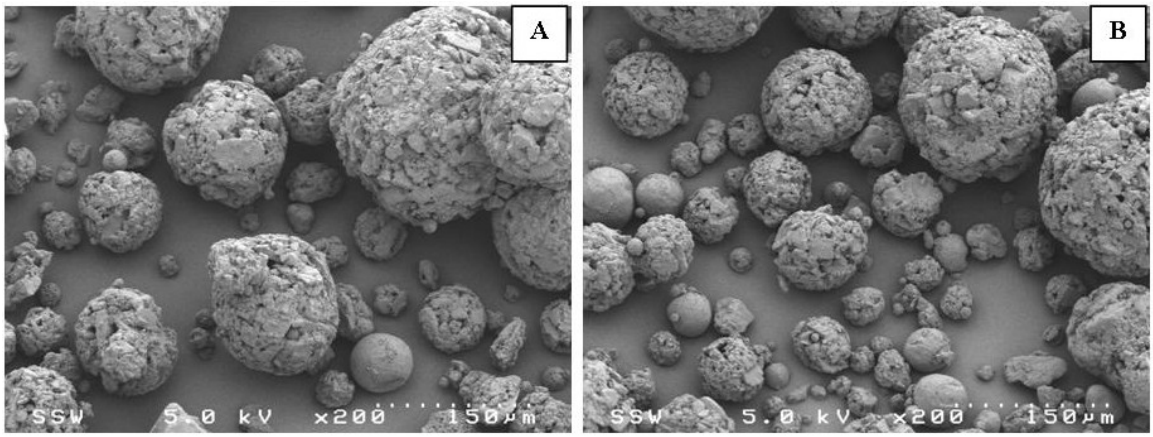

Figure 2.7: SEM images of stearic acid and spray dried lactose mixtures (A-1.0 wt%, B-3.0 wt%).

2.3.3. Flowability

2.3.3.1. Static angle of repose

Figure 2.8 shows the measured static angle of repose for the various lubricant mixtures. Spray dried lactose showed good flowability with a static angle of repose of about 32^{o}. The addition of the lubricants decreased the static angle of repose indicating an improvement in flowability. The flowability, however, did not continuously improve as more lubricant was added to the mixtures. For magnesium stearate, magnesium silicate and stearic acid, the flowability improved up to 1-2 wt% of lubricant but then further lubricant additions up to 5 wt% had no significant impact on the flow. Calcium stearate mixtures showed a different profile for the static angle of repose: the angle decreased significantly to 27^{o} at 0.5 wt% calcium stearate but then increased to 29.5^{o} at 3 wt% with further additions having no significant effect on the flow.

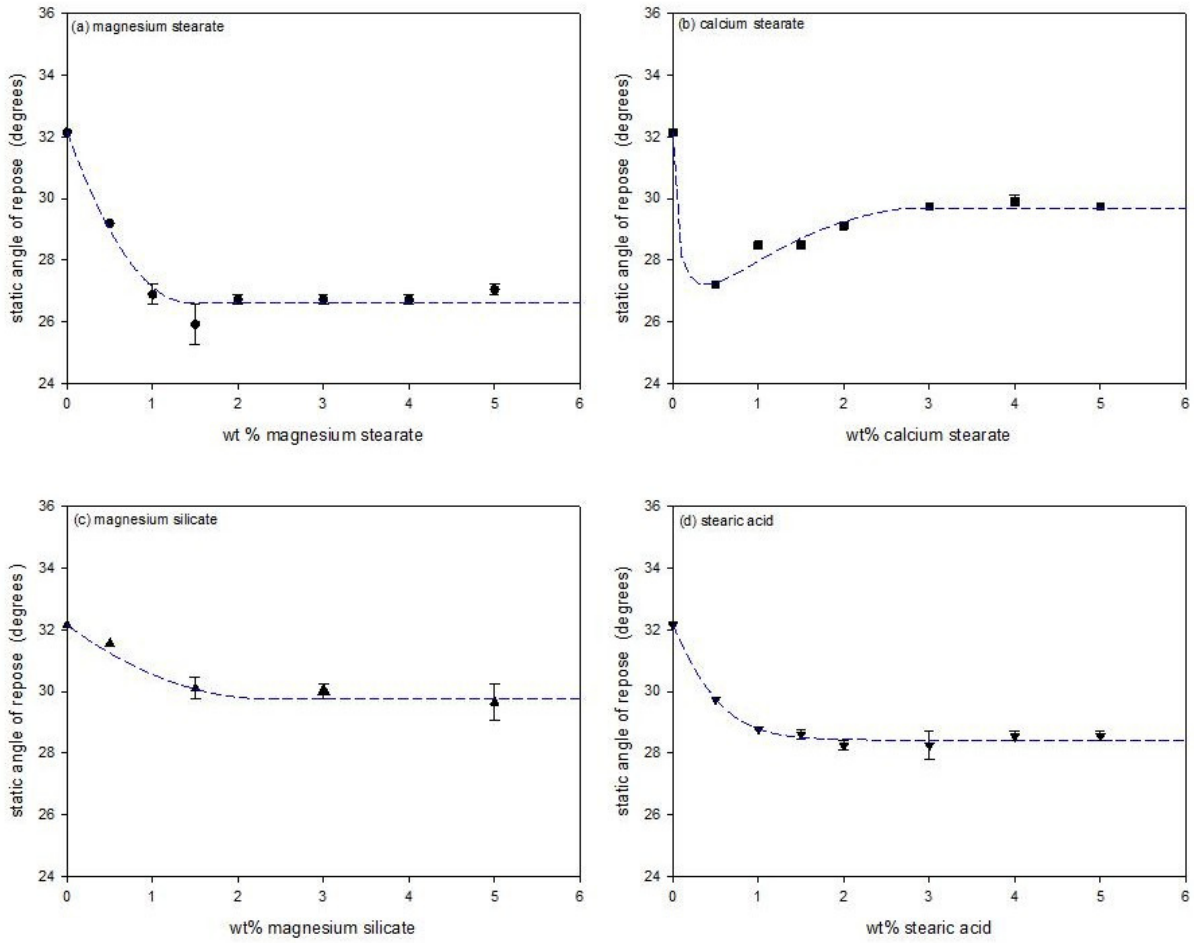

Figure 2.8: Static angles of repose for the mixtures.

2.3.3.2. Density measurements

The Hausner ratio is determined from the tapped and bulk densities. Figure 2.9 shows a Hausner ratio for spray dried lactose of 1.19 which indicates a free flowing powder. Clear trends with increasing lubricant addition were difficult to determine for magnesium silicate and stearic acid. The profiles, however, for magnesium stearate and calcium stearate were similar to those obtained with the static angle of repose (Figure 2.8). The Hausner ratio indicated that the magnesium stearate provided the largest improvement in flowability, but additions larger than 1-2 wt% provided no further improvement.

The Carr index also uses the bulk and tapped densities in indicating flowability. A Carr index below 20-25% indicates good flowability (Carr, 1965). Profiles of the lubricant mixtures for the Carr index were similar to those of the Hausner ratio with magnesium stearate providing the largest improvement in flowability.

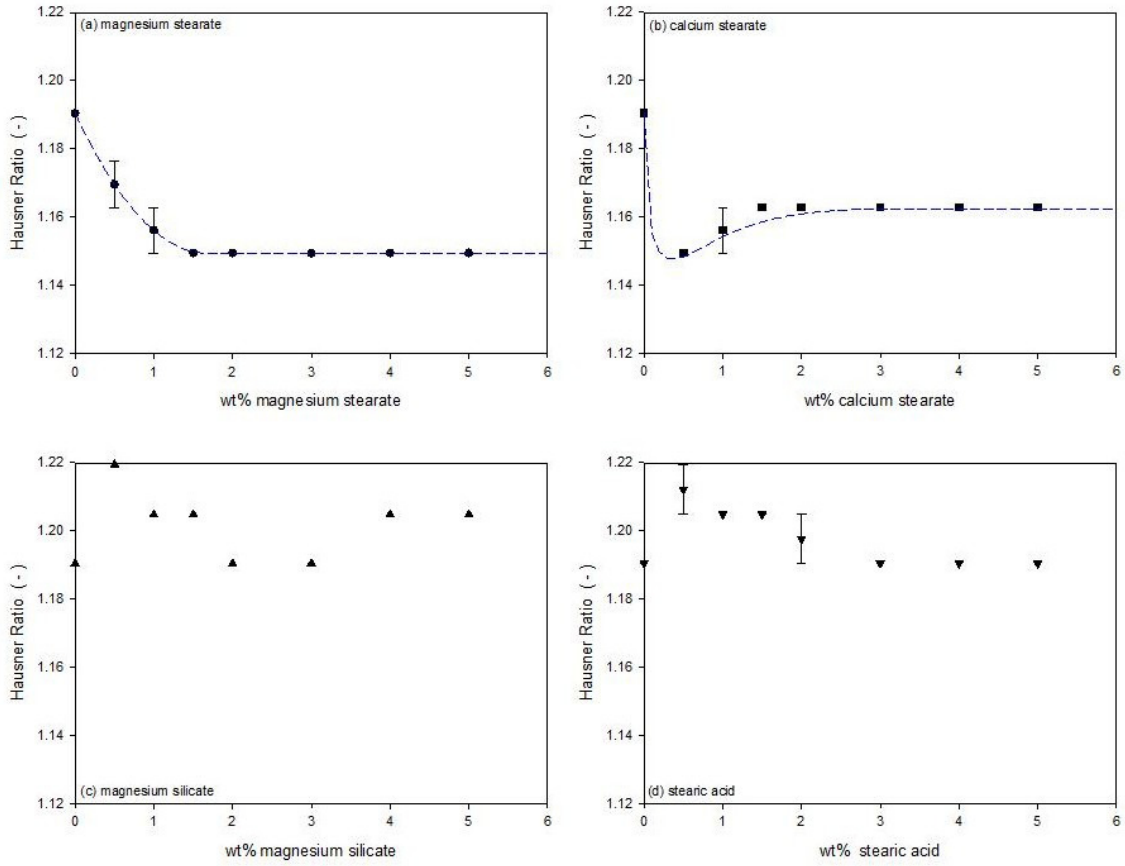

Figure 2.9: Hausner ratios for the mixtures.

2.3.3.3. Avalanche time

The avalanche time is a flowability indicator measured by the Mercury Scientific revolution Powder Analyzer. Figure 2.10 shows that the avalanche time decreased with the introduction of the lubricants. The avalanche time for the mixture with magnesium

stearate and magnesium silicate decreased to an avalanche time near 3 s by 2 – 3 wt% of the lubricant. Calcium stearate decreased the avalanche time to a low value of 2.5 s at a concentration of only 1 wt%, but the addition of more lubricant then increased the avalanche time. The addition of stearic acid to the spray dried lactose initially slightly decreased the avalanche time. Larger amounts of stearic acid, however, showed no significant changes in the avalanche time.

2.3.3.4. Dynamic density

The dynamic density shown in Figure 2.11 was also measured by the Mercury Scientific Revolution Powder Analyzer. The addition of magnesium stearate increased the dynamic density from about 0.63 to a maximum of 0.69 g/ml near 2 wt% addition of magnesium stearate. Further addition of magnesium stearate decreased the dynamic density slightly. Calcium stearate provided a large increase to a density near 0.83 g/ml. There were, however, no significant changes in the dynamic density with the additions of magnesium silicate or stearic acid.

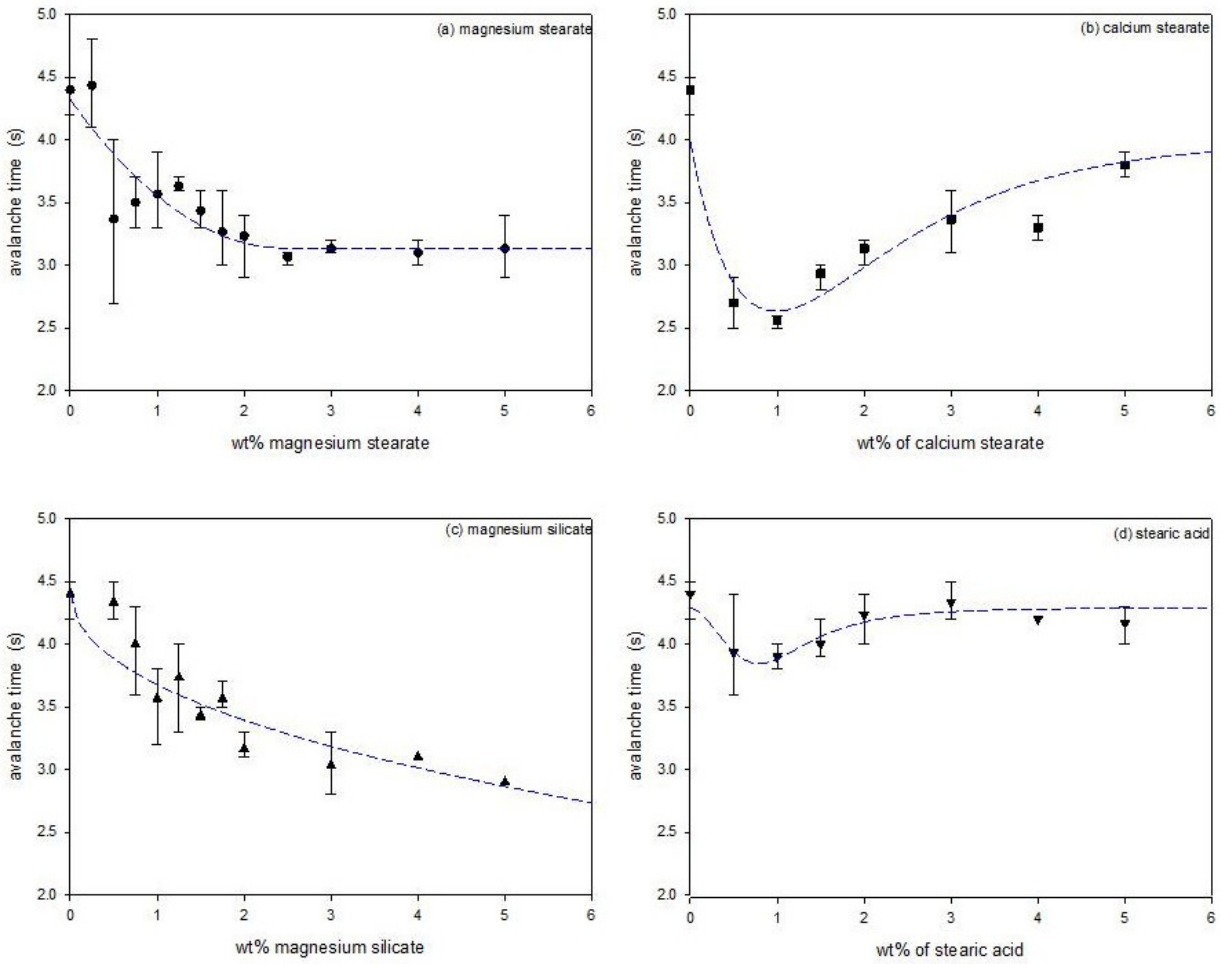

Figure 2.10: Avalanche time for the mixtures.

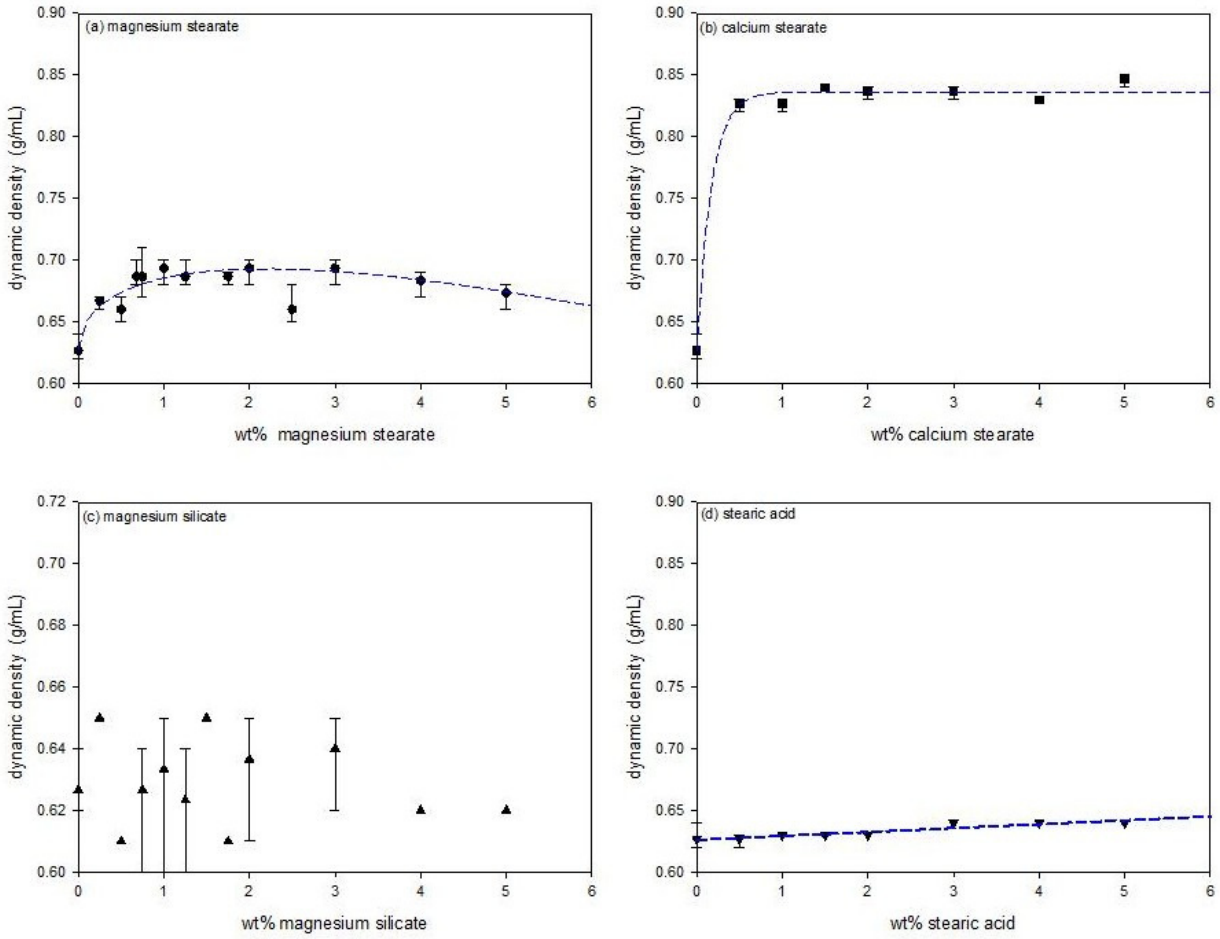

Figure 2.11: Dynamic densities for the mixtures.

2.4. Discussion

The scanning electron micrographs in Figure 2.4 showed that the magnesium stearate flakes first filled the surface cavities of the spray dried lactose. At levels above 1.5 – 2 wt%, the magnesium stearate no longer attached to the spray dried lactose. Instead, the flakes began to form self-agglomerates. This critical point of 1.5 – 2 wt% was observed as a transition point in all the flowability measurements. The static angle of repose decreased from 32^0 to 27^0 by 1.5 wt% (Figure 2.8a). According to the flowability relationships summarized by Nagel and Peck (2003), this indicated that the addition of

the magnesium stearate improved the flow from good to excellent. The magnesium stearate decreased the Hausner ratio from 1.19 to 1.15 by 1.5 wt% (Figure 2.9a). This range of the Hausner ratio indicated a free flowing powder (Abdullah and Geldart, 1999). The Hausner ratio does not provide enough resolution to detect small changes in flowablity. Finally, the avalanche time decreased from 4.4 s to 3.1 s by 2 wt% magnesium stearate addition indicating an increase in the flowability (Figure 2.10a).

The magnesium stearate filled the surface cavities of the spray dried lactose. This selective adhesion to the surface improved the flowability of the powder by improving the surface morphology of the lactose particles. The particles became more spherical with a smoother surface morphology, which reduced the frictional forces by reducing contact points, thus improving flow (Perrault et al., 2010; Roblot-Treupel and Puiseux, 1986).

The selective adhesion of magnesium stearate to the surface cavities is also supported by the dynamic density measurements (Figure 2.11a). The dynamic density increased from 0.63 g/ml to 0.69 g/ml at 2 wt%, but further additions of magnesium stearate then reduced the density to 0.67 g/ml. Filling the surface cavities of the lactose with the magnesium stearate increased the weight of each lactose particle without adding any bulk volume. The agglomerates of magnesium stearate that began to form after 2 wt%, then began to change the bulk volume of the powder mixture which decreased the dynamic density.

Although calcium stearate is also a metallic salt boundary lubricant and similar to magnesium stearate, its behaviour and effects when added to the spray dried lactose were

very different. The scanning electron micrographs (Figure 2.5) indicated that the calcium stearate did not preferentially fill the surface cavities of the lactose particles after approximately 1 wt%. At higher levels, the calcium stearate continued to attach to the surface of the spray dried lactose particles without the formation of a significant amount of self-agglomerates. As the addition of calcium stearate continued, the surface morphology of the lactose particles began to change: the adhered calcium stearate formed an irregular surface. This change in the surface irregularity increased the contact points which increased frictional forces. The larger frictional forces decreased flowability and this was shown in the flowablity measurements: the static angle of repose decreased from 32^0 to 27^0 by 0.5 wt% addition of calcium stearate, but further additions increased the angle to 30^0 (Figure 2.8b), the Hausner ratio decreased to 1.15 by 0.5 wt% but then increased with further additions to 1.16 (Figure 2.9b), and the avalanche time decreased to 2.6 s by 1 wt%, but then increased to beyond 3.8 s with further additions (Figure 2.10b).

The layering of calcium stearate on the spray dried lactose particles is reflected in the increased dynamic density (Figure 2.11b). The dynamic density increased from 0.63 g/ml to 0.85 g/ml with the addition of calcium stearate. The adhered calcium stearate increased the weight of the lactose particles without significantly increasing the volume; the small flakes only formed a thin layer on the lactose surface.

Magnesium silicate flakes appeared to first partially fill in the surface cavities of the spray dried lactose (Figure 2.6). However, above 2 wt%, magnesium silicate both continued to adhere to the surface of the lactose and also form self-agglomerates. The

initial preferential filling of the surface cavities improved flowability by increasing the sphericity of the lactose and smoothing the surface. This was reflected in the static angle of repose which decreased slightly from 32^0 to 30^0 (Figure 2.8c) and in the decrease in avalanche times (Figure 2.9c). Improvements in the flowability beyond 2 wt% were only detected through the avalanche times which continued to decrease to just below 3 s. Coating of the lactose surface would form an irregular surface increasing contact points and friction thereby decreasing flowability. However, with a high density of 2.8 g/cm^3 and larger median size near 17 μm, the self-agglomerates of magnesium silicate should exhibit reasonable flowability potential. The effect on flowability by additions of magnesium silicate beyond 2 wt% were complicated and therefore not detected by all flowability measurements. Changes in the dynamic density (Figure 2.11c) were difficult to detect with the varying interactions between the magnesium silicate and the spray dried lactose.

Given its large size and spherical shape (Figure 2.2 and Figure 2.3), stearic acid did not fill in any surface cavities of the spray dried lactose. Stearic acid did not adhere to the surface of the lactose (Figure 2.7). As shown by the static angle of repose (Figure 2.8d) and the avalanche time (Figure 2.10d), stearic acid slightly improved the flowability for additions less than about 1 wt%. The smooth and almost spherical stearic acid particles acted as spacers between the lactose particles. This reduced the cohesive forces between the lactose particles and also reduced frictional forces as there were fewer stearic acid – lactose contact points than lactose-lactose contact points.

The interactions between the lubricant and the spray dried lactose varied with the lubricant and the amount of added lubricant. With the smallest median size, the magnesium stearate easily filled the cavities on the surface of the lactose particles. This small size also corresponds to strong van der Waals forces (Dawoodbhai and Rhodes, 1990; Li et. al., 1994) which promoted the self-agglomeration of the magnesium stearate flakes which did not immediately adhere to the lactose. The small changes in the size, size distribution and the composition between the stearates and the magnesium silicate significantly affected the interaction with the lactose and the effect on flowability.

Considering all the flowability measurements, it can be concluded that magnesium stearate and calcium stearate increased the flowability to about the same level. Calcium stearate achieved this reduction by about 1 wt% addition while magnesium stearate required closer to 2 wt% addition. The smaller addition of calcium stearate should minimize any possible negative effects on tablet properties. However, the reduction in flowability provided by the calcium stearate was only achieved over a small range. Therefore, the addition of calcium stearate would need to be carefully controlled and uniform mixing ensured as small changes in the addition along with incomplete mixing would result in irregular flow into the tablet press. A reduction in flowability provided by the magnesium stearate was achieved for additions larger than about 2 wt%. Although a higher addition might impact tablet properties, it is easier to uniformly mix larger amounts and small changes would have a limited effect on the flowability.

Studies have been conducted showing that mixing time affects lubricating properties of magnesium stearate (Kikuta and Kitamori, 1994; Bossert and Stains, 1980). During the

initial stages of mixing, magnesium stearate adheres to the other particles. As mixing continues, some magnesium stearate can detach by delamination or deaggregation. Therefore over time, the magnesium stearate continues to be distributed throughout the powder which negatively affects tablet properties: further increases in disintegration times and decreases in mechanical strength. For all the trials, the mixing was conducted using a V blender at 25 rpm for 15 minutes. This corresponded to 375 revolutions. During the avalanche measurements, the samples were tumbled. However, as an avalanche occurred approximately every 4 s, each avalanche measurement of 128 avalanches would have only tumbled the sample for a further 3 revolutions and therefore the avalanche measurements did not contribute significantly towards any further mixing of the lubricant with the spray dried lactose.

Perrault et al. (2010) investigated magnesium stearate mixing and expressed concerns, that in many cases, magnesium stearate may not be homogeneously mixed given the low amount usually added to a formulation combined with its cohesiveness. The variablility in avalanche times at low lubricant additions, particularly for magnesium stearate, was shown in Figure 2.10a. The avalanche measurements are dynamic and were conducted in triplicate with each measurement an average of 128 avalanches. Small changes in the magnesium stearate distribution in the sample were therefore detected resulting in the high variability of the avalanche times.

Yang et al. (2005) and Sadek et al. (1982) developed equations to determine the amount of lubricant or glidant required to form a monolayer around excipient particles. These however assumed monosize, spherical and non-deforming particles both for the additive

and the excipient. As shown in the particle size distributions (Figure 2.2) and the scanning electron images (Figure 2.3), these assumptions are not realistic. Using median sizes and a packing factor of 0.5, both equations estimate that 20% magnesium stearate would be required to form a monolayer around the spray dried lactose. Magnesium stearate shows significant improvement in flowability and lubricating effects by 2 wt%. This provides some validation that magnesium stearate does not provide these effects by forming a monolayer, but by selectively filling surface cavities of the excipient.

2.5. Conclusions

Four frequently used lubricants (magnesium stearate, magnesium silicate, stearic acid and calcium stearate) were mixed, in varying amounts, with spray dried lactose, a common excipient used in the pharmaceutical industry. The results indicated differences in the lubrication mechanism between lubricants, subsequently affecting powder flow. Both magnesium stearate and magnesium silicate preferentially filled the voids and cavities on the spray dried lactose before forming self agglomerates. Since the observed mechanism was similar, flowability trends were similar for both lubricants, with magnesium stearate being more effective at improving powder flow. Calcium stearate did not seem to preferentially fill surface voids, and thus showed a different flowability effect. After an initial improvement in flow, excess calcium stearate decreased overall flow, since the excess lubricant increased surface irregularities on the spray dried lactose. Stearic acid produced little effect on flowability, with only a minor improvement. As flowability is critical for tablet formation, the conclusions of this study highlight the importance of including flowability measurements in lubricant selection.

2.6. Acknowledgements

The authors would like to acknowledge the Natural Sciences and Engineering Research Council of Canada (NSERC) and the Ontario Graduate Scholarship (OGS) for their financial support. The University of Western Ontario Graduate Thesis Research Award Fund (GTRAF) is also acknowledged for financial contribution.

2.7. References

Abdullah, E., Geldart, D., 1999. The use of bulk density measurements as flowability indicators. Powder technology 102, 151-165.

Alderborn, G., 2002. Tablets and compaction. Aulton ME. Pharmaceutics The Science of Dosage Form Design.

Asker, A., Saied, K., Abdel-Khalek, M., 1975. Investigation of some materials as dry binders for direct compression in tablet manufacture. Part 5: Effects of lubricants and flow conditions. Die Pharmazie 30, 378.

Bossert, J., Stains, A., 1980. Effect of mixing on the lubrication of crystalline lactose by magnesium stearate. Drug development and industrial pharmacy 6, 573-589.

Carr, R.L., 1965. Evaluating flow properties of solids. Chem Eng 72.

Dawoodbhai, S., Rhodes, C.T., 1990. Pharmaceutical and cosmetic uses of talc. Drug development and industrial pharmacy 16, 2409-2429.

Dawoodbhai, T.S., Suryanarayan, E., Woodruff, C., Rhodes, C., 1991. Optimization of Tablet Formulations Containing. Drug development and industrial pharmacy 17, 1343-1371.

Faqih, A.M.N., Mehrotra, A., Hammond, S.V., Muzzio, F.J., 2007. Effect of moisture and magnesium stearate concentration on flow properties of cohesive granular materials. International journal of pharmaceutics 336, 338-345.

Fassihi, A., Kanfer, I., 1986. Effect of compressibility and powder flow properties on tablet weight variation. Drug development and industrial pharmacy 12, 1947-1966.

Jarosz, P.J., Parrott, E.L., 1984. Effect of lubricants on tensile strengths of tablets. Drug development and industrial pharmacy 10, 259-273.

Johansson, M., 1985a. Investigations of the mixing time dependence of the lubricating properties of granular and powdered magnesium stearate. Acta pharmaceutica suecica 22, 343.

Johansson, M., Astra Laekemedel, A., Soedertaelje, S., 1986. The effect of scaling-up of the mixing process on the lubricating effect of powdered and granular magnesium stearate. Acta Pharmaceutica Technologica 32, 39-42.

Johansson, M.E., 1985b. Influence of the granulation technique and starting material properties on the lubricating effect of granular magnesium stearate. Journal of pharmacy and pharmacology 37, 681-685.

Kikuta, J.I., Kitamori, N., 1994. Effect of mixing time on the lubricating properties of magnesium stearate and the final characteristics of the compressed tablets. Drug development and industrial pharmacy 20, 343-355.

Levy, G., Gumtow, R.H., 1963. Effect of certain tablet formulation factors on dissolution rate of the active ingredient III. Tablet lubricants. Journal of pharmaceutical sciences 52, 1139-1144.

Li, Q., Rudolph, V., Weigl, B., Earl, A., 2004. Interparticle van der Waals force in powder flowability and compactibility. International journal of pharmaceutics 280, 77-93.

Lim, S.Y., Davidson, J., Forster, R., Parker, D., Scott, D., Seville, J., 2003. Avalanching of granular material in a horizontal slowly rotating cylinder: PEPT studies. Powder technology 138, 25-30.

Liu, L.X., Marziano, I., Bentham, A., Litster, J.D., White, E., Howes, T., 2008. Effect of particle properties on the flowability of ibuprofen powders. International journal of pharmaceutics 362, 109-117.

Mitrevej, A., Sinchaipanid, N., Faroongsarng, D., 1996. Spray-dried rice starch: comparative evaluation of direct compression fillers. Drug development and industrial pharmacy 22, 587-594.

Nagel, K.M., Peck, G.E., 2003. Investigating the effects of excipients on the powder flow characteristics of theophylline anhydrous powder formulations. Drug development and industrial pharmacy 29, 277-287.

Nalluri, V.R., Kuentz, M., 2010. Flowability characterisation of drug-excipient blends using a novel powder avalanching method. European Journal of Pharmaceutics and Biopharmaceutics 74, 388-396.

Ouabbas, Y., Dodds, J., Galet, L., Chamayou, A., Baron, M., 2009. Particle–particle coating in a cyclomix impact mixer. Powder technology 189, 245-252.

Perrault, M., Bertrand, F., Chaouki, J., 2010. An investigation of magnesium stearate mixing in a V-blender through gamma-ray detection. Powder technology 200, 234-245.

Pingali, K.C., Saranteas, K., Foroughi, R., Muzzio, F.J., 2009. Practical methods for improving flow properties of active pharmaceutical ingredients. Drug development and industrial pharmacy 35, 1460-1469.

Roblot-Treupel, L., Puisieux, F., 1986. Distribution of magnesium stearate on the surface of lubricated particles. International journal of pharmaceutics 31, 131-136.

Sadek, H., Olsen, J., Smith, H., Onay, S., 1982. A systematic approach to glidant selection. Pharm Tech.

Sandler, N., Wilson, D., 2010. Prediction of granule packing and flow behavior based on particle size and shape analysis. Journal of pharmaceutical sciences 99, 958-968.

Strickland Jr, W., Nelson, E., Busse, L., Higuchi, T., 1956. The physics of tablet compression IX. Fundamental aspects of tablet lubrication. Journal of the American Pharmaceutical Association 45, 51-55.

Tan, S., Newton, J., 1990. Powder flowability as an indication of capsule filling performance. International journal of pharmaceutics 61, 145-155.

Wang, D.P., Yang, M.C., Wong, C.Y., 1997. Formulation development of oral controlled-release pellets of diclofenac sodium. Drug development and industrial pharmacy 23, 1013-1017.

Wang, J., Wen, H., Desai, D., 2010. Lubrication in tablet formulations. European Journal of Pharmaceutics and Biopharmaceutics 75, 1-15.

Yang, J., Sliva, A., Banerjee, A., Dave, R.N., Pfeffer, R., 2005. Dry particle coating for improving the flowability of cohesive powders. Powder technology 158, 21-33.

CHAPTER.3. A COMPARISON OF GRANULES PRODUCED BY HIGH SHEAR AND FLUIDIZED BED GRANULATION TECHNIQUES

Garett J. Morin and Lauren Briens

Biomedical Engineering, Western University, London, Canada

3.1. Introduction

Perry's *Chemical Engineer's Handbook* defines the granulation process as "any process whereby small particles are gathered into larger, permanent masses in which the original particles can still be identified." (Ennis and Litster, 1997) In wet granulation, a process widely used in the pharmaceutical industry to agglomerate the active ingredient(s) and any excipients, a liquid binder is sprayed onto the particles as they are agitated, particularly in a high shear mixer or fluidized bed. The particles are agglomerated, with the help of the liquid binder, by a combination of capillary and viscous forces until more permanent bonds are formed by drying. Granulation in the pharmaceutical industry is done primarily to prevent segregation of the constituents of the powder mixture, to increase flowability of the mixture, and to improve the compaction characteristics of the mixture.

Fluidized bed and high shear granulation differ both on the technical mode of solid agitation and fundamentally on the mode of granule growth. In fluid bed granulation, the

powder bed is maintained in a fluidized state by a flow of air injected upwards through a distributor plate at the base of the granulator. Escape of the granulation material is prevented by exhaust filters, which can be periodically agitated to reintroduce material into the bed. The liquid binder is typically sprayed, opposite to the air flow, through a nozzle positioned over the bed of particles. The granules result from the adhesion of solid particles to the liquid droplets that hit the bed (Faure et al., 2001). The flow of fluidizing air creates continuous partial drying throughout the granulation process. Sufficient liquid is sprayed to produce granules of the required size, at which point the spray is ceased and the granules are dried in the fluidizing airstream. Fluidized bed granulators have many advantages over high shear mixing. All the granulation processes, including drying, which usually require separate pieces, of equipment, are all performed within the same apparatus. This consolidation saves labour cost, transfer losses, and time. Furthermore, once the conditions affecting the granulation have been optimized, the process can be fully automated. However, the equipment is initially expensive and the optimization of the process and product parameters requires extensive developmental work during initial formulation, scale-up, and production. Similar developmental work for high shear processes is not as extensive.

In high shear granulation, the unmixed dry powders are placed in a mixing bowl containing a main impeller, which revolves on a horizontal plane, and an auxiliary chopper, which rotates either in the vertical or horizontal plane. The dry powders are mixed by the rotating impeller before the liquid binder is sprayed over the top of the bed of powder. Agitation is maintained throughout the process by the rotating impeller. As

the liquid droplets disperse throughout the powder, they form the first nuclei of granules. The shear applied by the impeller prevents the development of large agglomerates. Granulation is continued until specified granule properties are obtained. The granules are then typically transferred to another piece of equipment for drying, such as a fluid bed dryer. An advantage of the high shear granulation process is that mixing, massing, and granulation are all performed within a few minutes in the same piece of equipment. However, the process needs to be controlled with care as the can progress rapidly so that the change from an optimum granule to an overmassed system can occur very quickly. The high shear process is also sensitive to variations in raw materials (Faure et al., 1999).

Both high shear and fluidized bed granulation processes exhibit the four key rate processes that contribute to granulation, as originally described by Ennis (1990): wetting and nucleation, coalescence, consolidation, and attrition. Although these rate mechanisms can occur simultaneously in all processes, certain mechanisms may dominate and be more pronounced within each technique. For instance, fluidized bed granulators are strongly influenced by the wetting and nucleation process, whereas the mechanical re-dispersion of binding liquid by the impeller and chopper diminish the wetting contributions to granule size in high shear operations. Consequently, granule consolidation is far more pronounced in high shear mixing than fluidized bed granulation.

Although there is much information known about each of the individual processes of high shear granulation and fluidized bed granulation, there is little literature documenting the observed physical differences in the final granules. Flore et al. (2007) presented a

comparison of a variety of granulation mechanisms, including those of fluidized bed and high shear mechanisms, using a polymeric powder. Flore et al. used an Eirich R02 batch-wise laboratory scale mixer operated at 1500 rpm to conduct high shear granulations. Fluidized bed granulations were conducted in a conical laboratory scale fluidized bed. It was found that granules in the appropriate size range, 0.3-1mm, could be prepared with both methods. The high shear process resulted in a strong caking of the wet product in the mixing vessel. Furthermore, the different granulation methods produced differing granule morphologies. The fluidized bed process produced porous particles with a fluffy, fractal appearance. The high shear particles were not quite spherical, but more round than fluidized bed particles. In a dissolution measurement, it was determined that both dissolved at similar rates, with the fluidized bed granules dissolving slightly faster. Lastly, in comparing the bulk densities of the products, the high shear granules had a much higher bulk density (400-500 g/cm^3) compared to that of the fluidized bed granules (250-290 g/cm^3).

Agnese et al. (2010) also presented a comparison of high shear and fluidized bed processes, using an aqueous solution of a variety of PVP grades and PVA-PEG graft copolymer. It was determined that much higher concentrated binder solutions were needed in high shear granulation to perform the process properly. Moreover, it was found that the high shear granules were more solidified as a result of higher mechanical stress applied during the process, whereas the fluidized bed granules finished with a high porosity and less spherical particle shape. Moreover, despite the fact that the agglomerates from the high shear process were found to be much mechanically stronger,

the tablets pressed based on fluidized bed agglomerates yielded higher tensile strengths. In terms of the particles size distribution, coarser agglomerates with fewer fines could be produced using high shear granulation, whereas the particle size distribution was much more homogeneous using a fluidized bed process.

A comparison of low shear, high shear and fluidized bed processes on the effect of granule and tablet properties was also done by Hausman (2004). The high shear granulation was performed in a Diosna VAC20 unit with an impeller speed of 150 rpm and a chopper speed of 3000 rpm, while fluidized bed granulation were performed in a Glatt GPCG-5 unit utilizing top-spray. The formulation consisted of an active, lactose monohydrate, povidone, and microcrystalline cellulose. Before tablet compaction, additional microcrystalline cellulose and crospovidone, as well as magnesium stearate, were blended into the mixture. Drying was done in the unit in which the granulation was completed. It was determined that the particles size distribution of granules done by high shear granulation was tighter than that of granules done by fluidized bed granulation, while the granules produced by fluidized bed granulation had a high mean diameter. Furthermore, both the bulk and tapped densities of the fluidized bed granules were lower than those composed by high shear methods. The final tablet made of fluidized bed granules had a larger relative standard deviation in terms of final tablet weight than those compressed form high shear granules. Also, the fluidized bed granules produced harder tablets, but again with a larger relative standard deviation.

N'Dri-Stempfer et al. (2003) compared tablets and granules made from both high shear and fluidized bed granulation techniques. They used a formulation of microcrystalline cellulose, talc, and pthalocyanin, a blue organic pigment. High shear granulations were completed in a Diosna P1/6 high shear mixer at a speed of 200 rpm for both the impeller and chopper blades. Fluidized bed granulation was completed in a GEA Strea 1 unit. The granules produced by high shear mixing had a much larger mean particle diameter. Also, the granules from the high shear mixer also demonstrated a much wider size distribution. The fluidized bed particles were determined to have intermediate-type properties, that is, in terms of compressibility and flow as described by the Carr index and Hausner ratio. However, under compression tests, it was found that the granules from the high shear mixer to be slightly more compressible than their behaviour would indicate, whereas the fluidized bed particles were found to be less compressive than their behaviour would indicate and gave the least dense compact.

A comparison of both granulation techniques was also done by Gao et al. (2001) in studying a poorly water soluble, low density, micronized drug. A micronized drug substance was granulation with a aqueous solution of a cellulose-based binder. Fluid bed granulation was done in a Niro MP-1, varying inlet temperature, inlet air flow, binder spray rate, and atomizing air pressure. The high shear granulation were completed in a Gral 10L unit, using an experimentally optimized process with drying done in a Glatt WSG-3 fluid bed dryer. In studying the granule size distribution, it was determined that the atomizing air pressure and spray rate of the binder solution were the most important process variables in fluid bed granulation. It was concluded that the inlet air flow rate had

little effect on the granule size. The bulk densities recorded for the fluidized bed granules were significantly smaller than the particles prepared by the high shear technique, as was the mean particle diameter itself. The high shear process produced granules with better flow properties, as described by Carr's Index, than the fluidized bed method. The fluidized bed granules did demonstrate a higher compressibility. The difference in granule compressibility was attributed to granule porosity as visualized in images taken by scanning electron microscope (SEM). Granules manufactured by high shear granulation were more spherical and denser with fewer fines, a direct result of the mechanism of granulation in a high shear environment. The images from the SEM showed that the fluidized bed granules were more loosely agglomerated, more irregular in shape, and appeared to be more porous.

Research presented in the literature comparing high shear and fluidized bed granulation processes focuses on the comparison of final tablet properties, and less on the comparison of granulation mechanisms and the granule properties themselves. Reported variations in granule properties may be attributed to formulations or the variance of granulation process parameters. Moreover, the effect of the granulation technique on flowability as described by dynamic flowability measurements has yet to be reported. The objective of this research was therefore to examine the effect of the granulation technique on the granulation mechanism and physical properties of the granules specifically utilizing dynamic flowability measurements utilizing a placebo formulation.

3.2. Materials and methods

3.2.1. Product formulation

A placebo formulation consisting of 50 wt% (dry basis) lactose monohydrate (Merck, d_{psm} of 113 μm), 45 wt% microcrystalline cellulose (Alfa Aesar, d_{psm} of 77 μm), 4 wt% hydroxypropyl methylcellulose (Alfa Aesar, d_{psm} of 48 μm) and 1 wt% croscarmellose sodium (Alfa Aesar, d_{psm} of 139 μm) was used for all the trials.

3.2.2. High shear granulation

All high shear granulations were performed in a Fielder PMA1 (GEA Pharma Systems, UK) high shear granulator shown schematically in Figure 3.1. The impeller and chopper were operated without binder addition for the first 2 minutes of each trial to mix the dry powder. A dry mass of 1.5 kg was used for each trial. The impeller and chopper speeds were constant for all trials at 700 rpm and 1000 rpm, respectively. These parameters were previously identified as providing a large fraction of optimal granules (Logan and Briens, 2012).

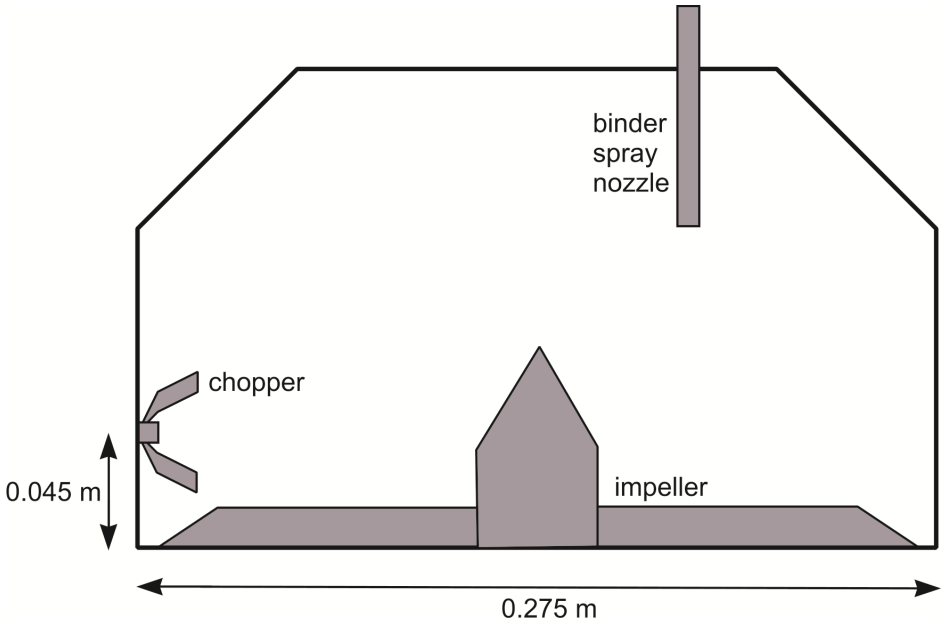

Figure 3.1: Schematic of vertical high shear granulator used in experiments.

At 2 minutes, binder addition was started with distilled water at 24^{o}C as the liquid binder. The water was sprayed at a rate of approximately 46 ml/minute into the granulator using a nozzle left-of-centre. Binder spraying continued for the entire specified wetting time for a trial. An optimal endpoint of ten minutes, corresponding to a granule moisture content of about 31 wt%, was previously identified (Logan and Briens, 2012). Trials, therefore, were conducted for different time intervals up to ten minutes wetting to examine the progress of granulation.

Granules from each trial were spread out in a thin layer onto trays and oven dried at 24^{o}C and a relative humidity of 2 to 3% for more than 24 hours to ensure a granule moisture content of less than 2 wt%. The dried granules were then immediately analyzed for various characteristics.

3.2.3. Fluidized bed Granulation

All fluidized bed granulations were performed in a top-spray conical fluidized bed shown schematically in Figure 3.2: Schematic of fluid bed granulator. A dry mass of 1.0 kg was used for each trial. The fluidizing air velocity was constant for each trial at 0.95 or 1.35 m/s.

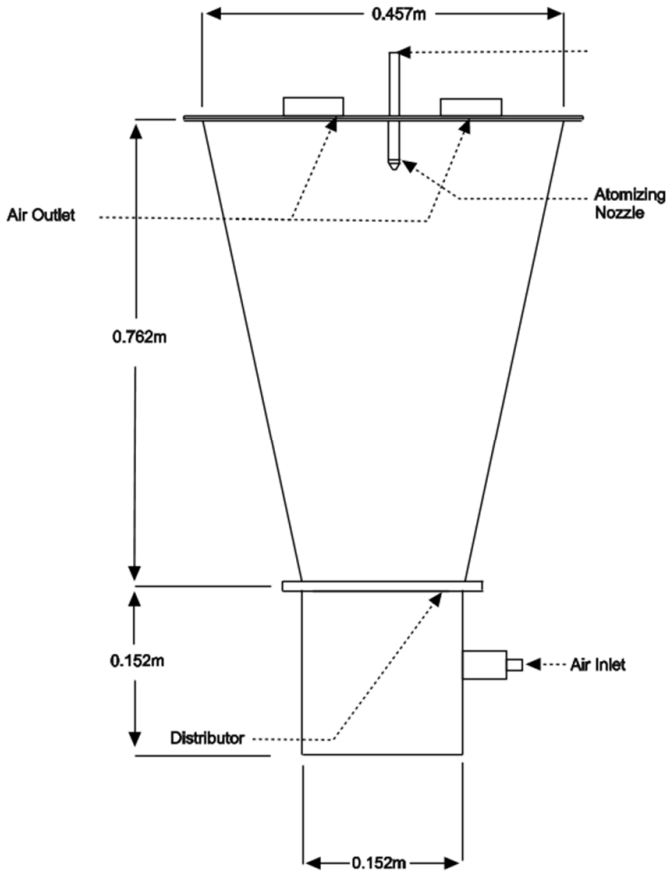

Figure 3.2: Schematic of fluid bed granulator.

The bed was first fluidized for five minutes to mix the dry powder. Binder addition was then started with distilled water at 24^{o}C as the liquid binder. The water was sprayed at a rate of approximately 52 ml/minute at an atomization pressure of 0.7 bar into the

granulator using a centered top-spray nozzle. The spraying continued for the entire specified wetting time for a trial. At a fluidizing air velocity of 0.95 m/s, trials at time intervals up to 11 minutes or 37 wt% moisture content were conducted. At 1.35 m/s fluidizing air velocity, trials continued until 13 minutes wetting time. The extra drying from the higher air flow, however, only resulted in a maximum granule moisture content of 31 wt%.

Granules from each trial were spread out in a thin layer onto trays and oven dried at 24 ^{o}C and a relative humidity of 2 to 3% for more than 24 hours to ensure a granule moisture content of less than 2 wt%. The dried granules were then immediately analyzed for various characteristics.

3.2.4. Granule analysis

3.2.4.1. Moisture content

Granule moisture content was determined through loss-on drying at 105 ^{o}C using a MettlerToledo HG63 halogen moisture analyzer. Duplicate samples of 5.00 g were analyzed.

3.2.4.2. Size

Particle size analysis was performed through sieving using a Retsch AS200 vibratory sieve shaker. For the analysis, 18 mesh cuts using standard sized stainless steel sieves ranging from 38 to 3350 μm were used.

3.2.4.3. Shape and morphology

Scanning electron microscope (SEM) images of the granules were taken using a Hitachi S4500 field emission SEM. The granules were mounted on a plate and coated with gold before examination. The images allowed the composition, shape and morphology of the granules to be examined and also for approximate comparison of size measurements from the sieving.

3.2.4.4. Flowability

3.2.4.4.1. Density

The bulk and tapped density of the particulates was measured using 100 ml samples. For the bulk density measurements, the powder flowed down a vibrating chute into a 100 ml cylinder and the mass of the powder sample within the cylinder was then measured:

$$bulk\ density\ \left(\frac{g}{ml}\right) = \frac{mass\ of\ sample}{100\ mL} \tag{3-1}$$

The sample within the cylinder was then vibrated/tapped and the resulting volume was measured to determine the tapped density:

$$tapped\ density\ \left(\frac{g}{mL}\right) = \frac{mass\ of\ sample}{tapped\ density\ volume\ (mL)} \tag{3-2}$$

Duplicate density measurements were performed. The bulk and tapped density measurements then allowed the Hausner ratio and Carr index to be calculated:

$$Hausner\ Ratio = \frac{tapped\ density}{bulk\ density} \tag{3-3}$$

$$Carr\ Index = \frac{tapped\ density - bulk\ density}{tapped\ density} \times 100\% \tag{3-4}$$

3.2.4.4.2. Static angle of repose

Static angle of repose measurements were performed using a Powder Research Ltd. Angle of Repose Device. Samples of approximately 60 ml flowed down a vibrating chute and then through a funnel to form a pile below on a calibrated level platform to allow the angle of repose to be easily determined. Samples were measured in triplicate.

3.2.4.4.3. Avalanche behaviour

Various indicators of flowability were investigated using a Mercury Scientific Revolution Powder Analyzer. A sample size of 118 cm^3 was loaded into a drum with a diameter of 11 cm and width of 3.5 cm. This drum was rotated at 0.3 rpm until 128 avalanches had occurred, with an avalanche defined as being a rearrangement of at least 0.65 vol% of the sample in the drum. The analyzer uses an optical technique with a resolution of 648 x 488 at 60 frames per second to monitor the behaviour of the powder surface as the sample is rotated. Samples were measured in triplicate.

3.3. Results

3.3.1. Visual observations

Figure 3.3 shows scanning electron micrograph images of the individual components of the formulation. Lactose monohydrate particles are large, angular, almost rectangular, and have a smooth surface morphology while microcrystalline cellulose particles are irregular fibres. Crosscarmellose sodium particles are only present at 1 wt% in the formulation, which made it difficult to detect in any agglomerates. Hydroxypropyl

methylcellulose, also irregular fibres, comprised only 4 wt% of the formulation and, since it is water soluble, it dissolved into the water binder and did not appear in images of any agglomerates.

Optimum granules were defined to have a diameter between 150 and 600 μm, be approximately spherical in shape and incorporate all components of the formulation. To focus on granule properties, scanning electron images from each trial were taken from samples sieved to include only particles sized between 150 and 600 μm.

Figure 3.4 and Figure 3.5 show scanning electron images of the 150 to 600 μm samples from the fluidized bed granulation trials. In contrast to the high shear results, nuclei from the fluidized bed granulations appeared to be loose agglomerates of lactose monohydrate coated by microcrystalline cellulose fibres. As the granulation proceeded, granules grew in size, but remained very porous and non-spherical.

Figure 3.6 shows scanning electron images of the 150 to 600 μm samples from the high shear granulation trials. The granulation nuclei appeared to be primarily microcrystalline cellulose. After approximately 7-8 minutes, when the granule moisture content reached approximately 20%, lactose monohydrate began to be incorporated into the nuclei. Further granulation created larger, denser, and more spherical granules.

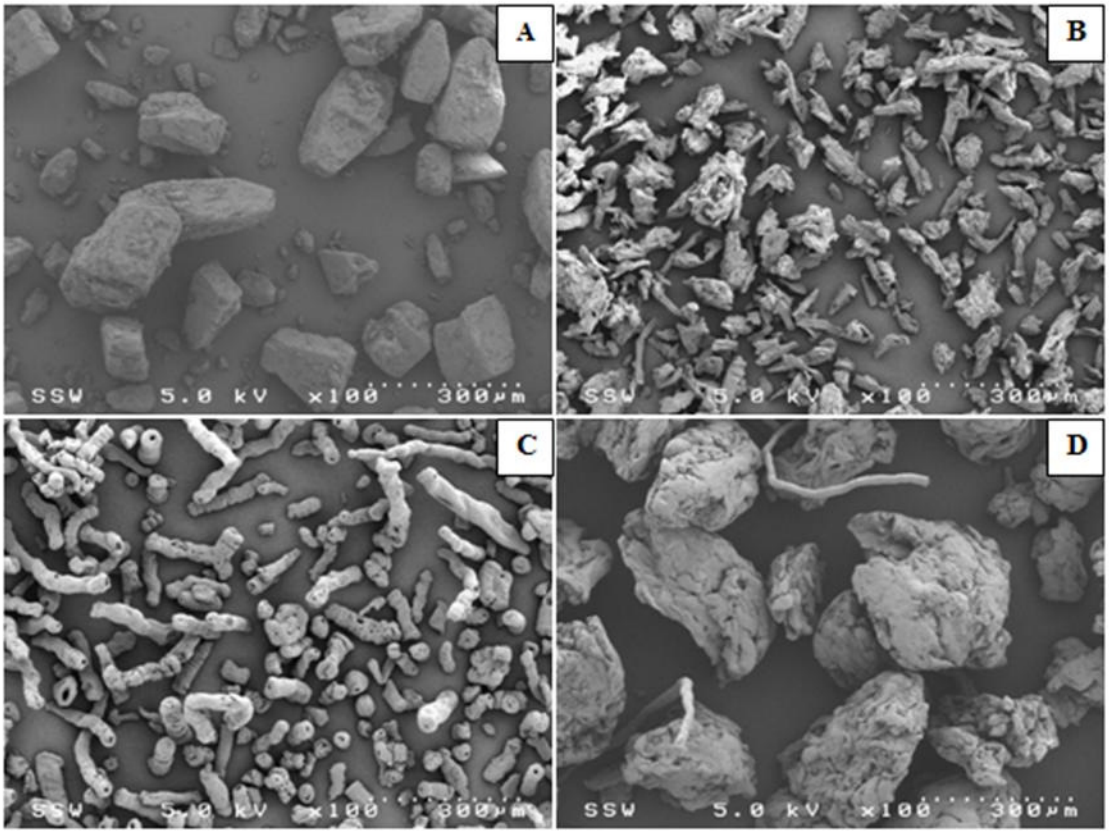

Figure 3.3: SEM images of raw components (A-lactose monohydrate, B-microcrystalline cellulose, C-hydroxypropyl methyl cellulose, D-croscarmellose sodium).

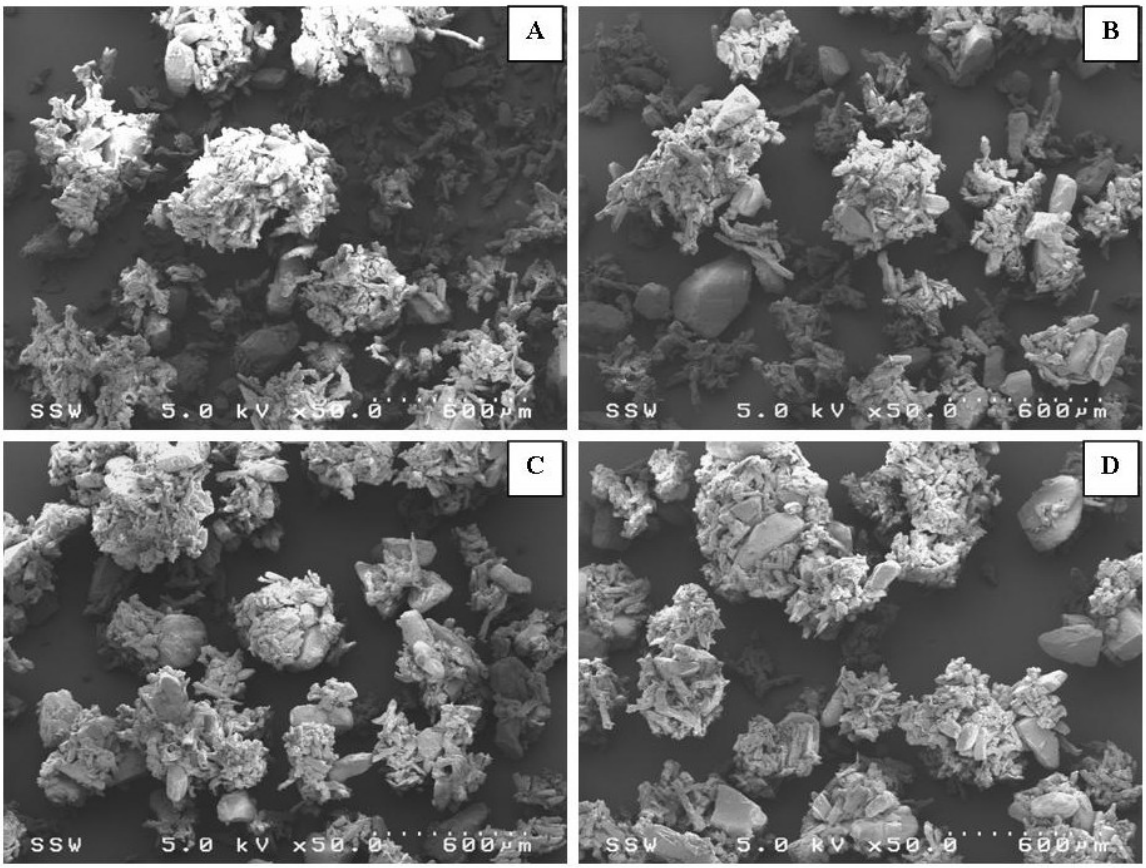

Figure 3.4: Scanning electron micrographs of samples from fluidized bed granulation at 0.95 m/s (A- 11.51%, B-19.90%, C-29.91%, D-36.59% (moisture wt%)).

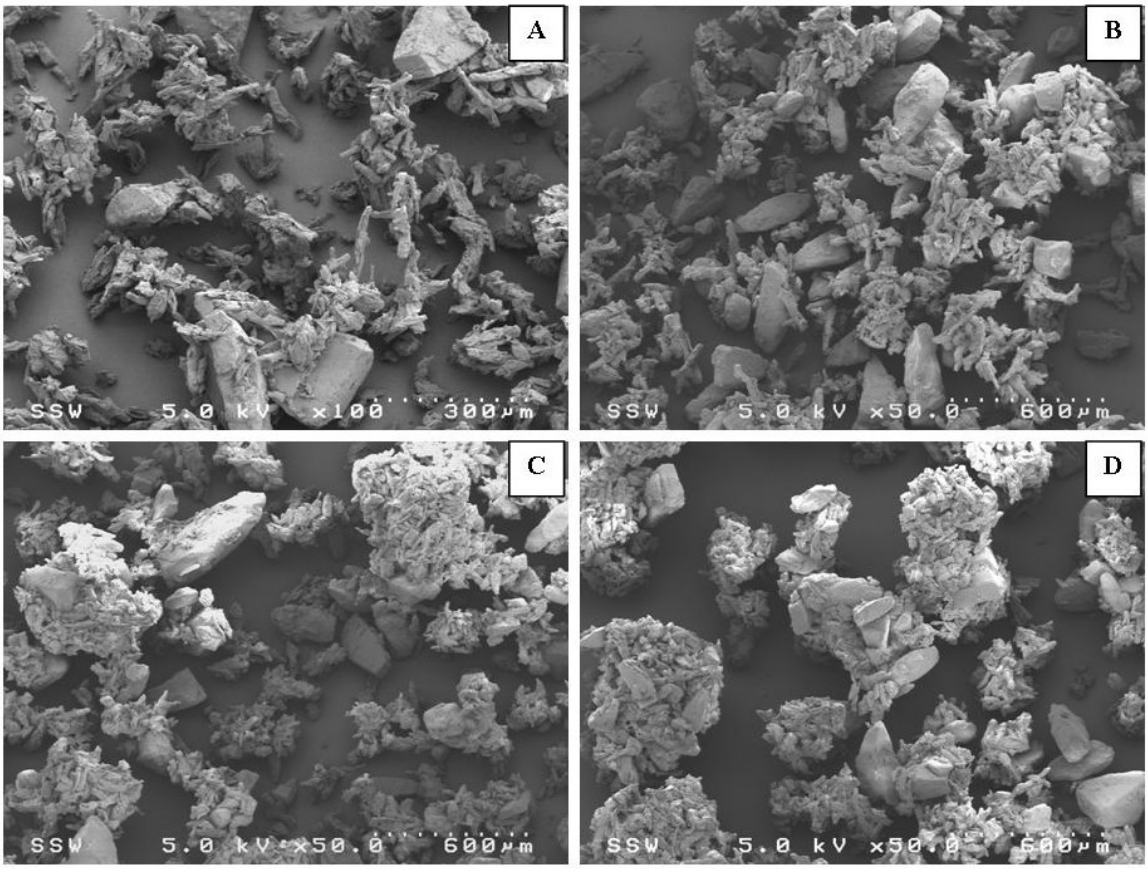

Figure 3.5: Scanning electron micrographs of samples from fluidized bed granulation at 1.35 m/s (A- 11.96%, B-16.76%, C-20.65%, D-26.76% (moisture wt%)).

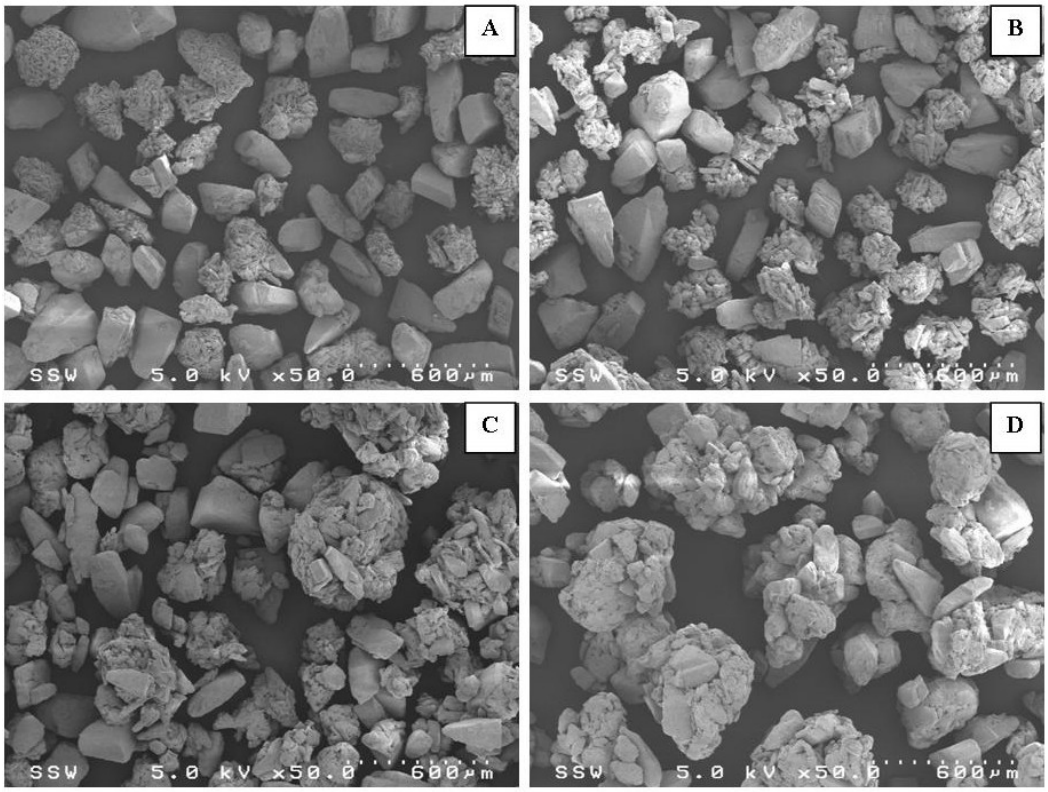

Figure 3.6: Scanning electron micrographs of samples from high shear granulations at 700 rpm (A-19.94%, B-25.97%, C-30.21%, D-33.24% (moisture wt%)).

3.3.2. Particle size and size distribution

To compare results from the different trials, the properties are presented using granule moisture content as a basis. Figure 3.7 shows that the mean diameter varied with granulation type and fluidizing velocity. For the high shear granulation, significant growth did not occur until a critical moisture content of about 20 wt%. Fluidized bed granulation at 0.95 m/s also showed only minimal increases in the mean diameter until 20 wt%. In contrast, size increases were steady, but only reached a maximum of about 225 μm at 25 wt% moisture content for fluidized bed granulation at 1.35 m/s.

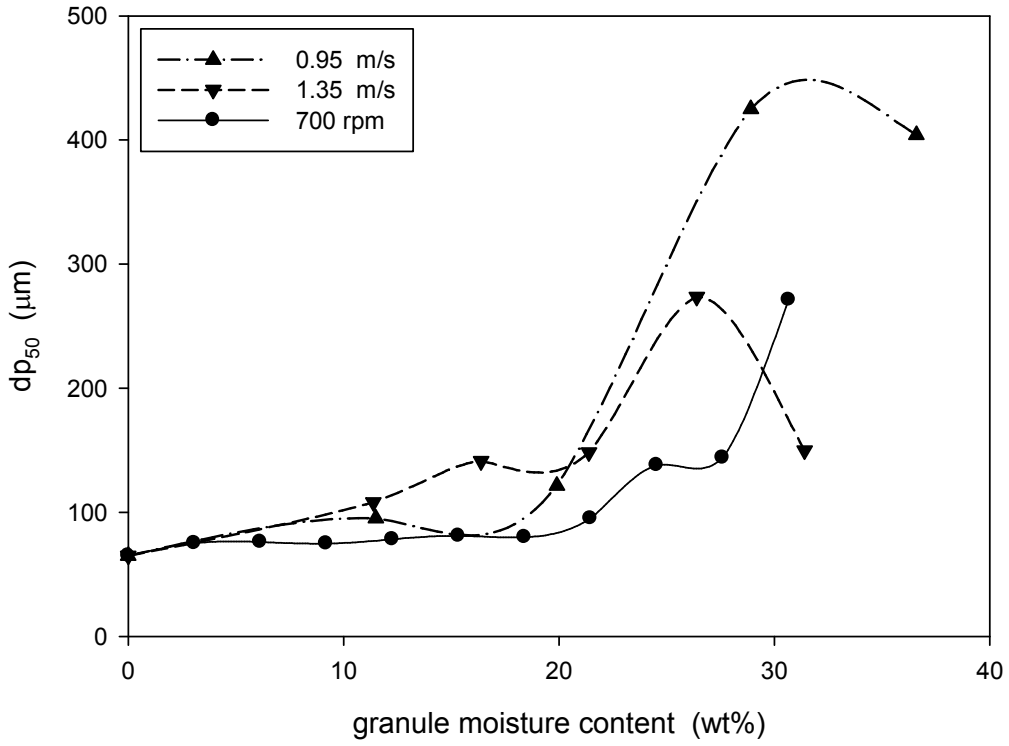

Figure 3.7: Dp_{50} for the granulation trials.

The size distributions shown in Figure 3.8 also show differences between the types of granulation. For the high shear granulation, minimal growth was observed until a moisture content of 20 wt%. More continuous growth was observed for the fluidized bed granulations, especially at a fluidization velocity of 1.35 m/s. The most favourable distribution of the maximum amount of optimum granules with minimal fines and oversized agglomerates was achieved with fluidized bed granulation at 1.35 m/s. The lower fluidization velocity produced too many oversized agglomerates while the high shear granulation started to rapidly overgranulate near a moisture content of 30 wt%.

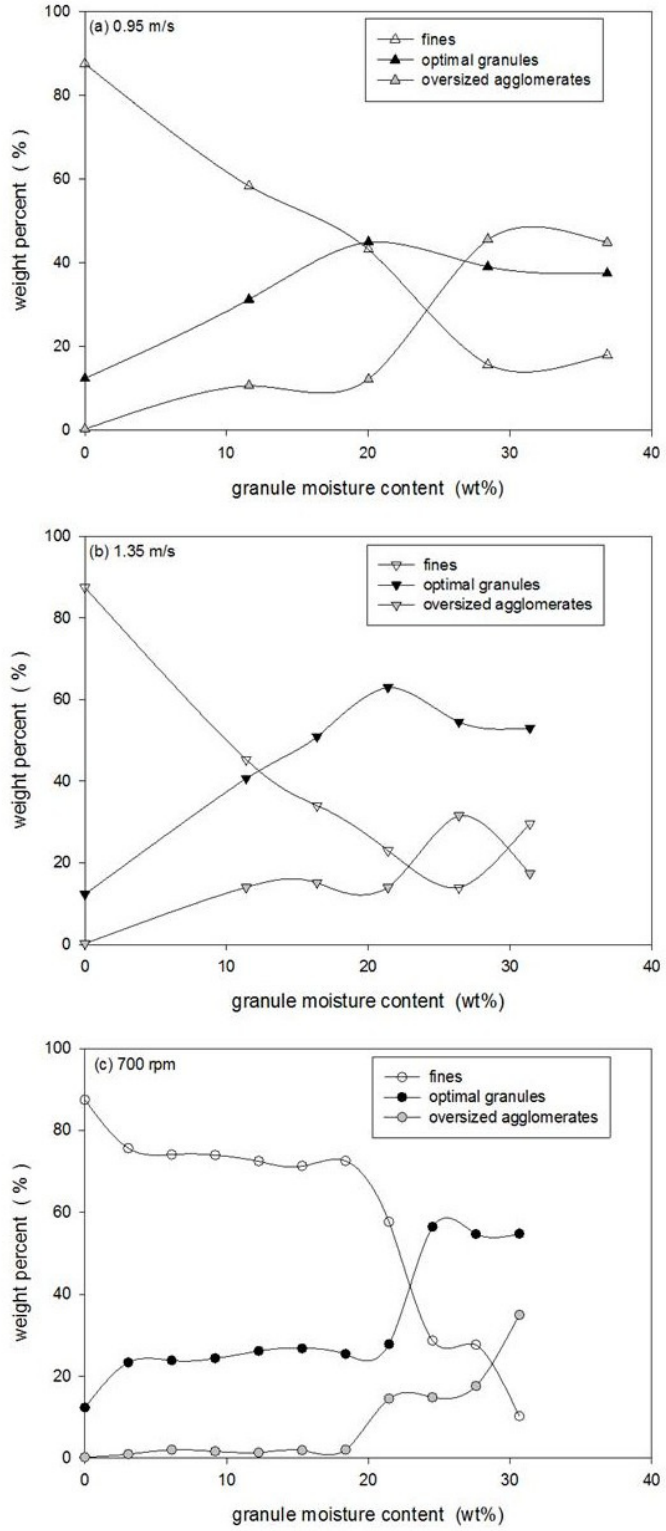

Figure 3.8: Size distributions for the granulation trials.

As particle sizes affects flowability and tabletability, the differential size distributions at granule moisture contents near 20 wt% and then just below 30 wt% are compared in Figure 3.9. The size distributions were all narrow at the lower moisture content, but at the higher moisture content the fluidized bed granulations created a wider size distribution with more large agglomerates than the high shear granulation.

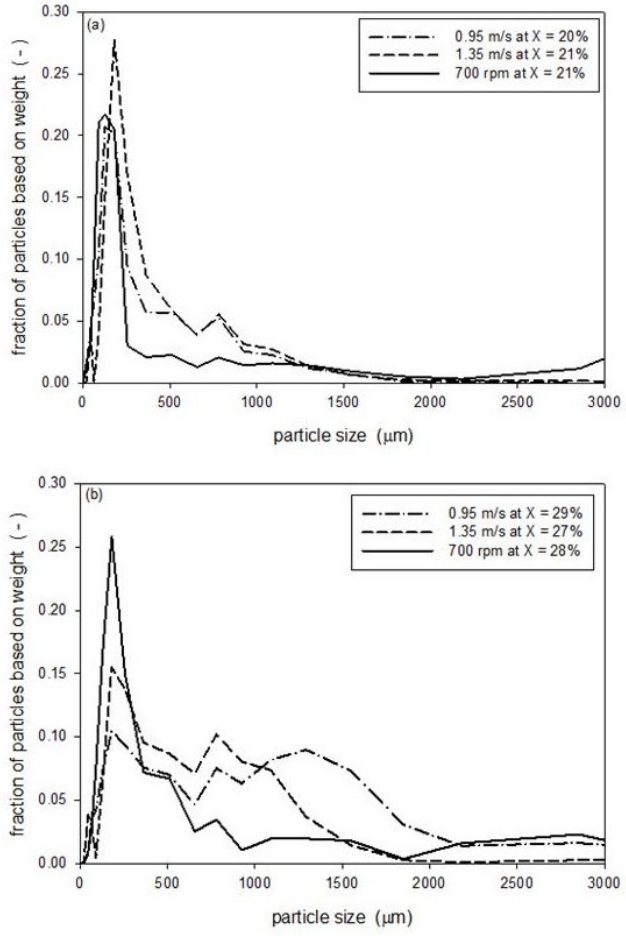

Figure 3.9: Differential size distributions for the granulations.

3.3.3. Flowability and tabletability

The Carr index and the Hausner ratio showed similar profiles. As shown in Figure 3.10 for the Carr index, the high shear granulation achieved the lowest index. Similar values were obtained for the fluidized bed granulation at 0.95 m/s. For the fluidized bed granulation at 1.35 m/s, however, the Carr index only decreased to about 20.

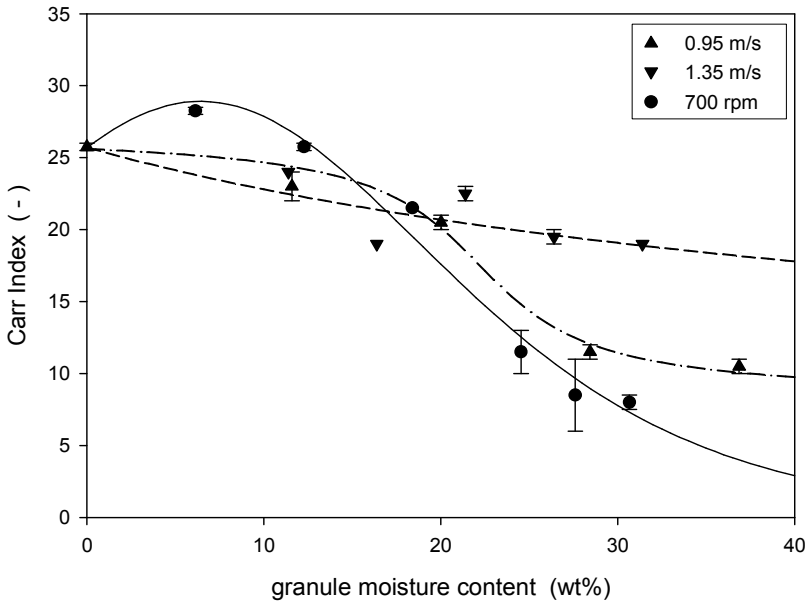

Figure 3.10: Carr index for the granulation trials.

The static angle of repose, shown in Figure 3.11, showed that the ungranulated formulation was very cohesive and would have exhibited poor flowability. The static angle of repose for the high shear granulation initially did not change, but then decreased to just below 30 degrees indicating excellent flowability potential. No significant differences were obtained for the two fluidized bed granulations. The static angle of repose decreased quickly with the addition of the liquid binder and decreased to below 30

degrees indicating excellent flowability potential as well. Minimal differences in granule flow were observed using the static angle of repose measurement technique.

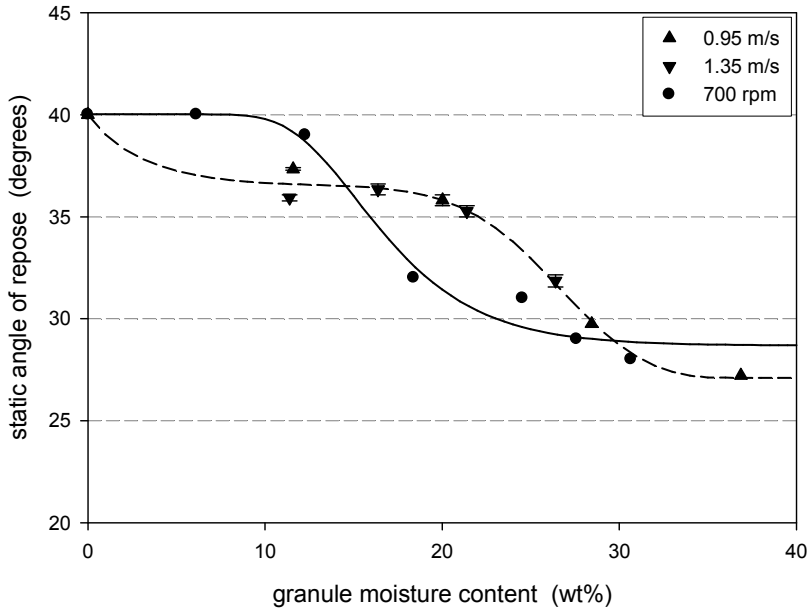

Figure 3.11: Static angle of repose measurements for the granulation trials.

Figure 3.12 shows, through the avalanche curvature, differences in the fluidized bed granulations and the high shear granulation during the process. Near the end point, however, there were no significant differences between the granulations with all values near -0.2. Also from the avalanching behaviour, the surface fractal shown in Figure 3.13 indicates differences between the two types of granulation; the surface fractal increased to a maximum of about 7 for the high shear granulation, but increased to a higher value of 10 for the fluidized bed granulations.

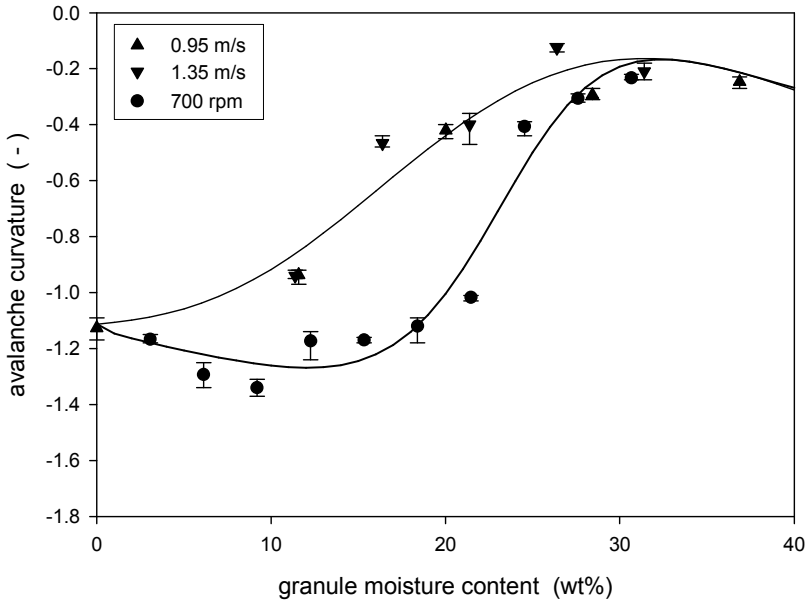

Figure 3.12: Avalanche curvature for the granulation trials.

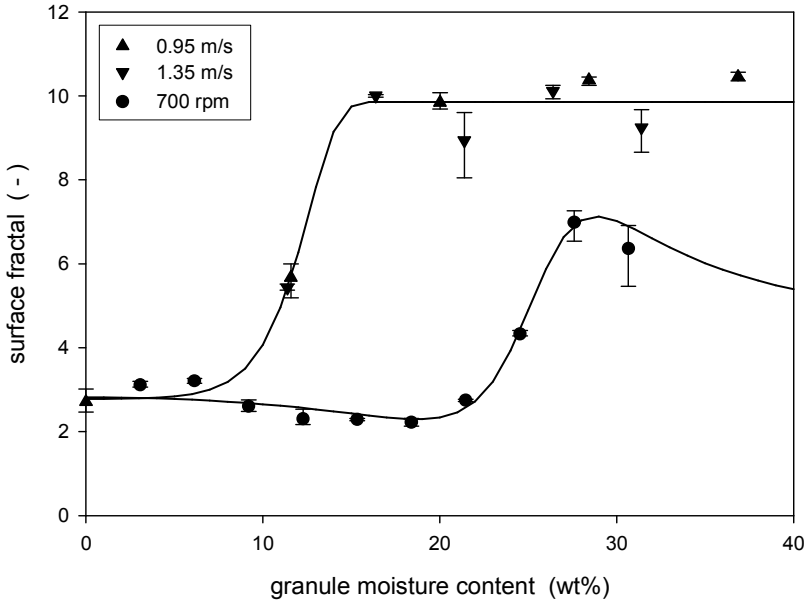

Figure 3.13: Surface fractal measurements for the granulation trials.

Figure 3.14 shows that the density of granules formed from high shear granulation was higher at 0.57 g/ml than granules with a density of only 0.3 g/ml created from the fluidized bed granulation.

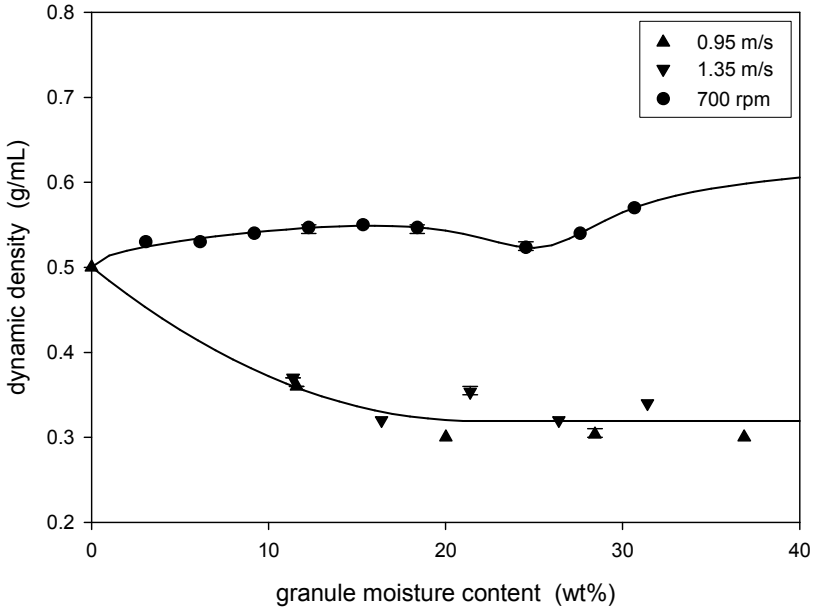

Figure 3.14: Dynamic densities for the granulation trials.

3.4. Discussion

The scanning electron images of the samples taken from the granulations (Figure 3.4, Figure 3.5, and Figure 3.6) indicated that the formation of granule nuclei was different for the high shear and fluidized bed granulations. For the high shear granulation, nuclei contained only microcrystalline cellulose. The powders were mixed for 2 minutes before liquid binder addition. During this dry mixing stage, the powders segregated: larger lactose particles were forced towards the sides and the bottom of the bowl while the microcrystalline cellulose fibres segregated to the middle of the bowl and near the top of

the powder bed. As a result, primarily microcrystalline cellulose fibres were initially exposed to the binder spray. These hygroscopic fibres easily absorbed the binder and formed nuclei (Alkhatib and Briens, 2011). For the fluidized bed granulations, the nuclei consisted primarily of lactose monohydrate particles with a few attached microcrystalline cellulose fibres. Fluidization of the dry powders was difficult: lactose monohydrate requires high air velocities as it is a large particle, but the smaller microcrystalline cellulose also does not fluidize easily due to the fibre shape of the particles. The initial fluidization of the powders therefore did not promote segregation of the microcrystalline cellulose to the top of the bed to be overexposed to the liquid binder spray. Liquid binder was absorbed by the microcrystalline cellulose, but also coated the surface of the lactose monohydrate particles. Collisions between a wetted lactose monohydrate and microcrystalline cellulose resulted in nuclei that included both particles. Differences in the formation of granule nuclei from high shear and fluidized bed granulations have not been reported in the literature.

The scanning electron images combined with the particle size analysis indicated that the granule growth mechanism was different for the two types of granulation (Figure 3.4, Figure 3.5, Figure 3.6, Figure 3.7, and Figure 3.8). For the high shear granulation, granule formation followed the induction growth mechanism: growth remained minimal until a moisture content of about 20 wt% and then increased rapidly. At this critical moisture content of 20 wt%, densification forced the water in the microcrystalline cellulose nuclei to the surface of these agglomerates making the surface more adhesive. Subsequent collisions with lactose monohydrate particles allowed the formation of liquid

bridges resulting in granules with microcrystalline cellulose and lactose monohydrate. Further collisions incorporated more lactose monohydrate into the granules and then granule consolidation and coalescence promoted further growth. The high shear forces from the impeller promoted the formation of spherical granules with low porosity. For the fluidized bed granulations, granule formation followed a slow but steady growth mechanism. Granule growth occurred through coalescence of nuclei and smaller granules as the binder continued to be sprayed onto the bed. As only low shear forces are present in the fluidized bed, the granules were irregularly shaped and highly porous. At larger granule sizes, this structure becomes particularly susceptible to attrition as shown by the decrease in agglomerates and increase in fines near the end of the granulation (Figure 3.8). The differences in the granule shape and porosity were consistent with the reported literature (Flore et al., 2007; Agnese et al., 2010; Gao et al., 2002; N'Dri-Strempfer et al., 2003).

The differences in porosity of the granules were reflected in the dynamic densities shown in Figure 3.14. High shear granules increased the density of the formulation from 0.5 g/ml to about 0.57 g/ml while the granules from the fluidized bed had very low densities of about 0.3 g/ml. These densities were comparable to the bulk densities obtained by Gao et al. (2002): 0.32 to 0.42 g/ml from the fluidized bed granulation versus 0.59 g/ml from the high shear granulation. They attributed the density differences to granule size, size distribution, shape, and porosity. Density is a critical parameter for tableting. For the same tablet die, a low density could result in a tablet with a weight below an acceptable level and the tablet must then be discarded.

Comparing the size distributions from the granulations was difficult as the different growth mechanisms meant that the progress varied with the type of granulation. Comparison using granule moisture content as a basis (Figure 3.9) showed that, at lower moisture levels, the size distributions for all the granulations were narrow. Differences between the granulations were larger at a higher moisture level just below 30%: the size distribution for the high shear granulation remained narrow while the distribution widened to include larger sizes for the fluidized bed granulations. At even higher moisture levels, it would be expected that the size distribution of the high shear granulation would widen as the formation of oversized agglomerates occurred while the distribution for the fluidized bed granulations would not change significantly as any larger agglomerates would be minimized through breakage and attrition.

In the literature, the size distribution results have varied. Hausman (2004) showed a wider distribution for fluidized bed compared to high shear granulations while others (Agnese et al., 2010; Murakami et al., 2001; Stahl, 2004) have reported the reverse with large agglomerates from the high shear granulation contributing to its wide size distribution. Different procedures were used for the granulations including liquid binder spray rate and processing time. The stopping point for each process therefore may have occurred at different stages in the granulation contributing to the differences in the size distribution results.

The flow properties of the granulations manufactured by the two methods are important to compare and assess the appropriateness of each to produce a tablet with specified

properties. Granule size and size distribution, shape and density are critical factors affecting flowability. Each flowability measurement is affected by these factors differently and therefore many measurements must be examined to provide a complete assessment of flowability.

The Carr index indicates both compressability and flowability. A Carr index below 15% indicates low compressibility but good flow properties while a value above 25% indicates a very compressible powder with very poor flow (N'Dri-Stempfer et al., 2003). As expected, Figure 3.10 shows the lowest Carr index of 8 obtained by the high shear granulation reflecting the dense and spherical granules. The high density of the granules limit further compressibility while the density and shape combined contribute to improved flowability. The Carr index of granules obtained from the fluidized bed granulations ranged from 10 to about 20 as the fluidizing velocity was increased from 0.95 m/s to 1.35 m/s. The higher Carr index for the fluid bed granulations reflects the porous granules which would be compressible. These lighter density and non-spherical granules, however, would have some flow difficulties. The range in the Carr index for the fluidized bed granulation trials reflects the differences in the size distributions with larger granules, which would exhibit better flow properties, obtained for the trials at the lower fluidization velocity (Figure 3.7, Figure 3.8, and Figure 3.9). Gao et al. (2002) reported similar Carr index values: 13 for granules from high shear granulation and 15 – 26 for granules from fluidized bed granulation with the different process parameters affecting the values.

The static angle of repose values are shown in Figure 3.11. The static angle of repose decreased for both types of granulations due to the increase in particles sizes from forming granules. The static angle of repose decreased to approximately 28^{o} for the high shear granulation and decreased to 27^{o} for the fluidized bed granulations indicating that the flowability was excellent for both the fluidized bed granules and high shear granules. The static angle of repose, although a common indicator of flowability, is sensitive to procedural and measurement error. Figure 3.11 indicates that stopping these granulations just above a moisture content of 20 wt% would result in angle of repose values for both within the fair flowability range, while increasing the moisture content to over 30% would result in both granules exhibiting excellent flowability. Little difference in flow was observed between the granules using the static angle of repose technique.

The avalanche curvature, shown in Figure 3.12, indicates the curvature of the powder surface just before an avalanche. A linear surface would have a curvature equal to zero. A concave surface, which would form with a cohesive powder that would accumulate at the drum perimeter before avalanching, would have a negative curvature. The avalanche curvature therefore shows that the formulation was initially very cohesive and that granulation improved the flowability. The improvement occurred at a lower moisture content for the fluidized bed granulation reflecting the earlier granule growth compared to the high shear granulation. Near the end of the granulations, the avalanche curvature indicated similar flowability potential for both types of granulations.

The surface fractal, shown in Figure 3.13, indicates the roughness of the powder surface

as it avalanches. A fractal value close to one indicates a smooth and even surface. This affects tablet die filling as the powder must flow well and then become evenly distributed within the die. The surface fractal values are closest to one at the beginning of the granulation. Although flowability is poor at this low moisture content and the sample powder surface is concave, the fractal value is low and the actual surface is smooth due to the still small size of the particles. As the granulation progresses, the surface fractal increased reflecting the formation of the granules and the disruption of the smooth surface by these larger particles. The surface fractal of the fluidized bed granulations reached a very high value of 10 while the high shear granulations only reached a value of 7. This variation reflected the larger particles sizes obtained with the fluidized bed granulations.

3.5. Conclusions

A lactose based placebo formulation was granulated using both high shear and fluidized bed methods. The results indicated differences in the formation and then subsequent growth of the granules from the two methods. Differences in the granule nuclei formation result from particle segregation within the high shear granulator compared to flow patterns within the fluidized bed which provide different exposure to the liquid binder spray. The differences in granule nuclei combined with flow and shear levels led to induction growth for the high shear granulation, but steady state growth for the fluidized bed.

Although the composition of the granules was the same for both types of granulations,

the properties of the granules were different, leading to variations in flowability. No one parameter can quantify the difference in flowability between high shear bed fluidized bed granules. Each parameter measures a different property of the granules, contributing to the overall flowability of the mixture. Although no one parameter wholly represents flowability, an examination of all the parameters leads to the conclusion that the high shear granules present better flow properties than those granules produced by the fluidized bed technique. Although high shear granules show better overall flow properties, higher tablet quality is not altogether represented by increased flow. Other mixture properties contribute to compressibility, dissolution, and durability, properties affecting tablet quality.

3.6. Acknowledgements

The authors would like to acknowledge the support of the Natural Sciences and Engineering Research Council of Canada (NSERC) as well as the Ontario Graduate Scholarship (OGS) for their financial support. The University of Western Ontario Graduate Thesis Research Award Fund (GTRAF) is also acknowledged for financial contribution.

3.7. References

Agnese, T., Cech, T., Geiselhart, V., Wagner, E., Comparing the Wet Granulation Properties of PVA-PEG Graft Copolymer and different PVP Grades in Fluid Bed Granulation Processes applying different Inlet Air Temperatures.

Alkhatib, A., Briens, L., 2011. Influence of initial mixing on granule properties, International Granulation Workshop, Lausanne, Switzerland.

Briens, L., Logan, R., 2011. The Effect of the Chopper on Granules from Wet High-Shear Granulation Using a PMA-1 Granulator. AAPS PharmSciTech, 1-8.

Ennis, B., 1990. Design & Optimization of Granulation Processes for Enhanced Product Performance. E&G Associates, Nashville, Tenn.

Ennis, B., Litster, J., 1997. Particle size enlargement. Perry's Chemical Engineer's Handbook, 7th edn., McGraw-Hill, New York, 20-89.

Faure, A., Grimsey, I.M., Rowe, R.C., York, P., Cliff, M.J., 1999. Process control in a high shear mixer-granulator using wet mass consistency: The effect of formulation variables. Journal of pharmaceutical sciences 88, 191-195.

Faure, A., York, P., Rowe, R., 2001. Process control and scale-up of pharmaceutical wet granulation processes: a review. European Journal of Pharmaceutics and Biopharmaceutics 52, 269-277.

Flore, K., Schoenherr, M., Feise, H., 2009. Aspects of granulation in the chemical industry. Powder technology 189, 327-331.

Gao, J.Z.H., Jain, A., Motheram, R., Gray, D., Hussain, M., 2002. Fluid bed granulation of a poorly water soluble, low density, micronized drug: comparison with high shear granulation. International journal of pharmaceutics 237, 1-14.

Hausman, D.S., 2004. Comparison of low shear, high shear, and fluid bed granulation during low dose tablet process development. Drug development and industrial pharmacy 30, 259-266.

Logan, R., Briens, L., 2012. Investigation of the effect of impeller speed on granules formed using a PMA-1 high shear granulator. Drug development and industrial pharmacy, 1-11.

Murakami, H., Yoneyama, T., Nakajima, K., Kobayashi, M., 2001. Correlation between loose density and compactibility of granules prepared by various granulation methods. International journal of pharmaceutics 216, 159-164.

N'Dri-Stempfer, B., Oulahna, D., Eterradossi, O., Benhassaine, A., Dodds, J., 2003. Binder granulation and compaction of coloured powders. Powder technology 130, 247-252.

Stahl, H., 2004. Granulation Techniques. Pharmaceutical technology europe.

CHAPTER.4. THE EFFECT OF MAGNESIUM STEARATE ON HIGH SHEAR AND FLUIDIZED BED GRANULE FLOWABILITY

Garett J. Morin and Lauren Briens

Biomedical Engineering, Western University, London, Canada

4.1. Introduction

A pharmaceutical tablet is a solid dosage form created by compressing a formulation of powders into a desired shape. The tablet is by far the most widely used dosage form in modern medicine, encompassing more than 80% of the 200 most prescribed drugs in the United States (Armstrong, 2006; Niazi, 2004). Tablets are commonly manufactured in a series of batch steps, including granulation, that modify and mix powder excipients with the active pharmaceutical ingredient before the final mixture is compressed into tablet form.

Lubricants are commonly added to the final granulated mixture prior to the tablet compression process. Lubricants reduce the friction between the tablet and the die metal surface which reduces the ejection force required to eject the tablet from the press to ensure the tablet remains intact and undamaged.

Powder flow is critical during tableting as powder must flow easily and uniformly into the tablet dies to ensure tablet weight uniformity and production of tablets with consistent

and reproducible properties (Fassihi and Kanfer, 1986; Tan and Newton, 1990; Sandler and Wilson, 2010). Poor powder flow results in tablets that are not uniform in content and weight; therefore, the tablets must be discarded as inadequate, unsuitable, and possibly unsafe for use. Powder flows when gravitational forces become higher than the friction and cohesion forces that influence particle-particle interactions. Friction forces act at contact points between particles to oppose their relative motion. Particle shape and surface morphology affect contact and therefore increase friction if contact area is increased. Cohesive forces refer to the attraction between particles and include van der Waals' forces, capillary forces and electrostatic forces. Cohesive forces are affected by the surface properties and size of the particles. Lubricants can affect both friction and cohesive forces, thereby affecting granule flow.

As magnesium stearate is a very effective and very commonly used lubricant, it has been the most extensively studied. It has been observed that the main lubrication mechanism consists of layers of magnesium stearate particles first filling any cavities of the other excipients before forming a continuous layer (Morin and Briens, 2012; Perrault et al., 2010; Roblot-Treupel and Puisieux, 1986). By this mechanism, magnesium stearate improves flow by minimizing any surface irregularities, reducing contact points between excipients, thus reducing friction forces.

Many methods have been developed to measure the flow properties of powders. Traditional methods commonly include the static angle of repose, Carr's compressibility index, Haunser ratio, and shear cell testing. Powder avalanche behaviour analysis is an

emerging powder flowability measurement method. The avalanche testing equipment consists of a rotating drum and imaging analysis system. As the drum rotates, the powder sample is carried up the side of the drum until the weight of the powder causes it to collapse or avalanche. Properties of this powder avalanche are then measured and analyzed to indicate powder flowability. The Mercury Scientific Revolution Analyzer improved upon the original Aero-Flow Analyzer, commercialised and developed by Brian Kaye, by including an advanced camera and imaging system to allow more advanced analysis of the images (Nalluri and Kuentz, 2010).

The effect of lubricants on flowability has been examined by several researchers. Using the Hausner ratio and shear cell measurements, Liu et al. (2008) found that the addition of 0.5 wt% of magnesium stearate improved the flowability of cohesive ibuprofen. Faqih et al. (2007) examined the avalanche behavior of commonly used pharmaceutical powders mixed with varying amounts of magnesium stearate. The effect of magnesium stearate on the flowability varied with the powder: there was almost no effect on the already free flowing Fast-Flo lactose but a significant effect on the very cohesive regular lactose. Pingali et al. (2009) examined the flow behavior of acetaminophen, didesmethylesibutramine tartarate and levalbuterol tartrate after mixing with lubricants colloidal silica, talc and magnesium stearate. A flow index obtained from avalanche behaviour showed that the flowability increased with the addition of the lubricants. Morin and Briens (2012) found that the addition of magnesium stearate to spray-dried lactose significantly improved flowability, but there were no increases in the flow after a critical amount of 2 wt% had been reached.

Besides reducing friction, lubricants may cause undesirable changes in the properties of the tablet. Lubricant type, amount and the method of incorporating the lubricant into the formulation all affect the tablet compression (Asker et al., 1975). It is generally accepted that magnesium stearate has deleterious effects on the hardness and tensile strength of the tablets. Many researchers have found that the addition of magnesium stearate significantly weakens tablet strength (Wang et al., 2010; Jarosz et al., 1984; Mitrevej et al., 1996). Because many lubricants are hydrophobic, tablet disintegration and dissolution are often retarded by the addition of lubricant (Alderborn, 2002). Multiple studies have led to the conclusion that the addition of magnesium stearate increases dissolution and disintegration time (Levy et al., 1963; Strickland et al., 1956), caused by a combination of the large surface area and hydrophobic properties of the lubricant (Johansson 1986a/b, Johansson 1985).

The objective of this work is to evaluate the impact of magnesium stearate on the flowability of placebo granules made through both high shear and fluidized bed processes.

4.2. Materials and methods

4.2.1. Product formulation

A placebo formulation consisting of 50 wt% (dry basis) lactose monohydrate (Merck, d_{psm} of 113 μm), 45 wt% microcrystalline cellulose (Alfa Aesar, d_{psm} of 77 μm), 4 wt% hydroxypropyl methylcellulose (Alfa Aesar, d_{psm} of 48 μm) and 1 wt% croscarmellose sodium (Alfa Aesar, d_{psm} of 139 μm) was used for all the trials.

4.2.2. High shear granulator operation

All high shear granulations were performed in a Fielder PMA1 (GEA Pharma Systems, UK), seen in Figure 4.1. The impeller and chopper were operated without binder addition for the first 2 minutes of each trial to mix the dry powder. The chopper speed was constant at 1000 rpm. The impeller speed was constant at 700 rpm (corresponding tip speed of 10.0 m/s).

At 2 minutes, binder addition was started. Distilled water was added as a liquid binder at 24℃. The binder was sprayed at a rate of approximately 46 ml/minute into the granulator for a wetting time 10 minutes. The operating parameters for the high shear granulations were previously determined by Logan and Briens (2012).

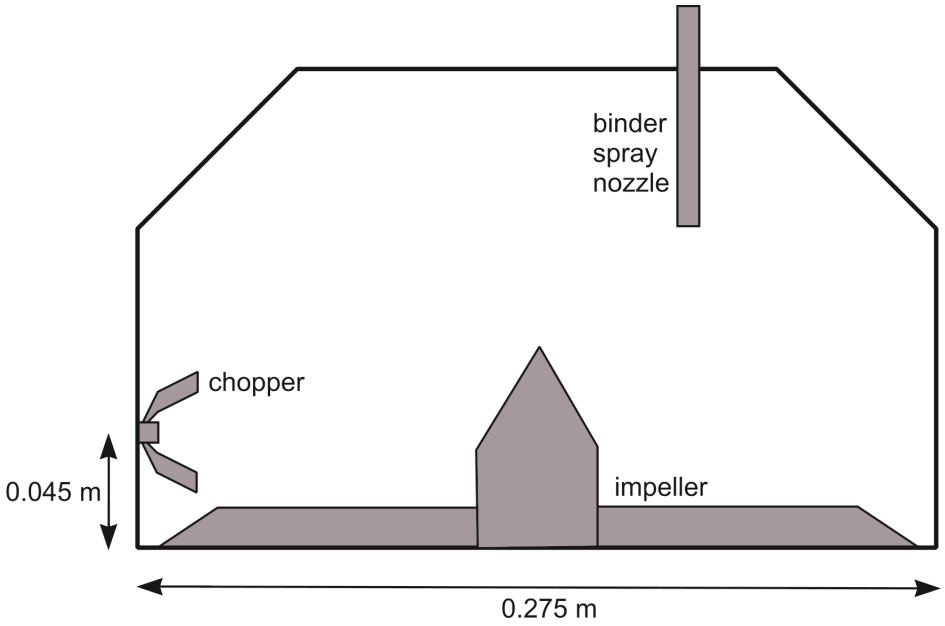

Figure 4.1: Schematic of vertical high shear granulator used in experiments.

Granules were spread into a thin layer on trays and oven dried at 24 ^{o}C and a relative humidity of 2 to 3% for more than 24 hours to ensure a granule moisture content of less than 2 wt%. Dried granules were sieved to include only those between 150 and 600 μm.

4.2.3. Fluidized bed granulator operation

All fluidized bed granulations were performed in a top-spray conical fluidized bed shown schematically in Figure 4.2. The fluidizing air velocity was constant for each trial at 1.35 m/s. The bed was first fluidized for 5 minutes to mix the dry powders. After 5 minutes, binder addition was started. Distilled water was added as a liquid binder at 24℃. The water was sprayed at a rate of approximately 52 ml/minute at am atomization pressure of 0.7 bar into the granulator using a centered top-spray nozzle. The spraying continued for

the entire wetting time of 11 minutes.

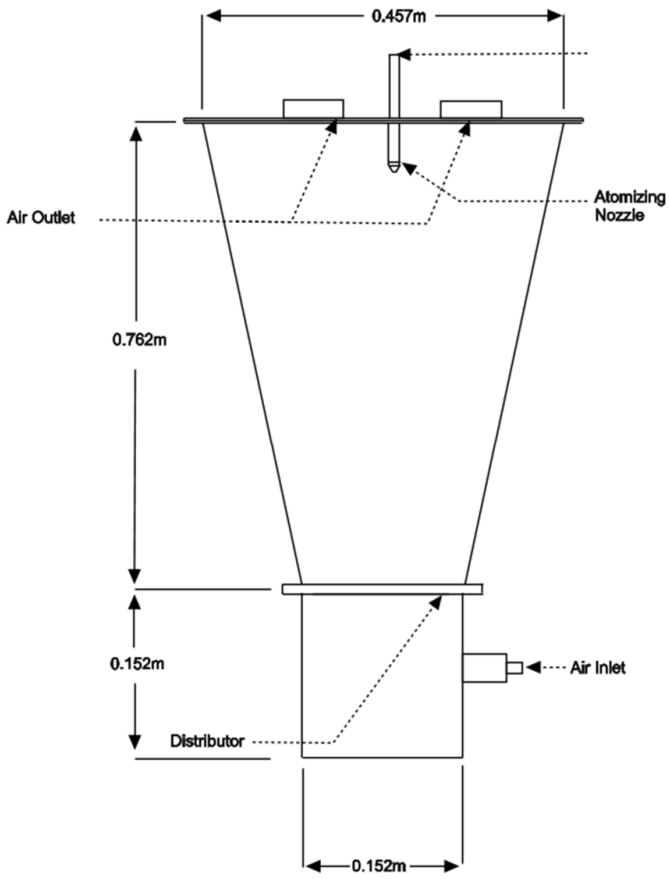

Figure 4.2: Schematic of fluidized bed granulator used in experiments.

Granules from each trial were spread into a thin layer on trays and oven dried at 24 ^{o}C and a relative humidity of 2 to 3% for more than 24 hours to ensure a granule moisture content of less than 2 wt%. Dried granules were sieved to include only those between 150 and 600 μm.

4.2.3.1. Mixing

Magnesium stearate was blended with each granule type in concentrations from 1-5 wt%. The granules and lubricant were blended using a Patterson Kelly V-blender with a stainless steel 4-quart shell for 15 minutes at a rotation speed of 25 rpm. Each trial size was 0.4 kg, thereby filling the shell to about 20% of the volume.

4.2.4. Mixture analysis

4.2.4.1. Particle size and size distribution

Particle size distributions and estimates of the specific surface area of the lubricant were measured using a Malvern Mastersizer 2000. Particle size analysis of the granules was performed through sieving using a Retsch AS200 vibratory sieve shaker, with steel sieves from W.S. Tyler.

4.2.4.2. Shape and morphology

Scanning electron microscope (SEM) images of the magnesium stearate, granules and the mixtures were taken using a Hitachi S4500 field emission SEM. The samples were mounted on a plate and coated with gold before examination. The images allowed the composition, shape and morphology of the granule and lubricant mixtures to be examined.

4.2.4.3. Flowability

4.2.4.3.1. Density

The bulk and tapped densities of the mixtures were measured using 100 ml samples. For the bulk density measurements, the powder flowed down a vibrating chute into a 100 ml cylinder and the mass of the powder sample within the cylinder was then measured:

$$bulk\ density\ \left(\frac{g}{ml}\right) = \frac{mass\ of\ sample}{100\ mL} \tag{4-1}$$

The sample within the cylinder was then vibrated/tapped and the resulting volume was measured to determine the tapped density:

$$tapped\ density\ \left(\frac{g}{mL}\right) = \frac{mass\ of\ sample}{tapped\ density\ volume\ (mL)} \tag{4-2}$$

Duplicate density measurements were performed. The bulk and tapped density measurements then allowed the Hausner ratio and Carr index to be calculated:

$$Hausner\ Ratio = \frac{tapped\ density}{bulk\ density} \tag{4-3}$$

$$Carr\ Index = \frac{tapped\ density - bulk\ density}{tapped\ density} \times 100\% \tag{4-4}$$

4.2.4.3.2. Static angle of repose

Static angle of repose measurements were performed using a Powder Research Ltd. Angle of Repose Device. Samples of approximately 60 ml flowed down a vibrating chute

and then through a funnel to form a pile below on a calibrated level platform to allow the angle of repose to be easily determined. Samples were measured in triplicate.

4.2.4.3.3. Avalanche behaviour

Various indicators of flowability were investigated using a Mercury Scientific Revolution Powder Analyzer. A sample size of 118 cm^3 was loaded into a drum with a diameter of 11 cm and width of 3.5 cm. This drum was rotated at 0.3 rpm until 128 avalanches had occurred, with an avalanche defined as being a rearrangement of at least 0.65 vol% of the sample in the drum. The analyzer uses an optical technique with a resolution of 648 x 488 at 60 frames per second to monitor the behaviour of the powder surface as the sample is rotated. Samples were measured in triplicate.

4.3. Results

4.3.1. Size and size distribution

Granules from the high shear and the fluidized bed processes were sieved to only include those between 150 and 600 μm. The size distribution of the magnesium stearate is shown in Figure 4.3 and a summary is given as Table 4.1: Summary of size and surface area of magnesium stearate. The magnesium stearate was much smaller in size than both granules.

Table 4.1: Summary of size and surface area of magnesium stearate.

d_{10} (μm)	4.57
d_{50} (μm)	10.22
d_{90} (μm)	28.10
d_{psm} (μm)	8.69
specific surface area (m^2/g)	0.69

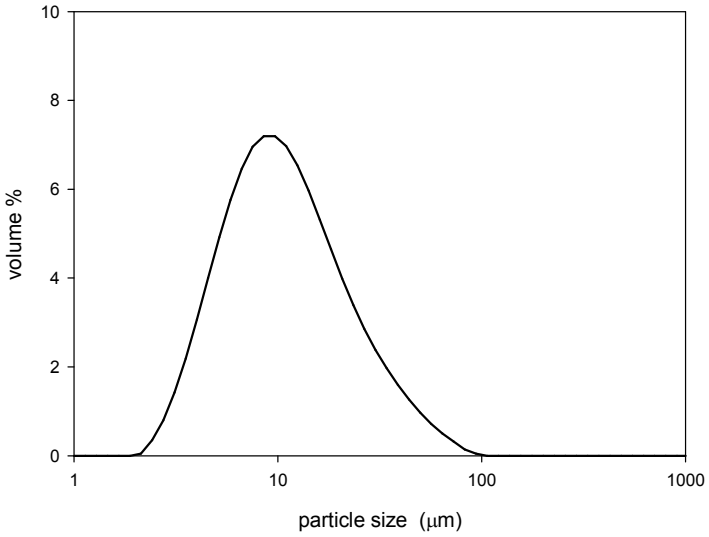

Figure 4.3: Size distribution of magnesium stearate.

4.3.2. Visual observations

Figure 4.4 shows scanning electron images of the high shear granules, fluidized bed granules, and magnesium stearate. The magnesium stearate particles were all irregular flakes with a high surface area to volume ratio. The fluidized bed process produced granules more irregular in shape than the semi-spherical granules produced by high shear granulation. Furthermore, the surface morphology of the fluidized bed granules was also more irregular with larger cavities and voids than the high shear granules.

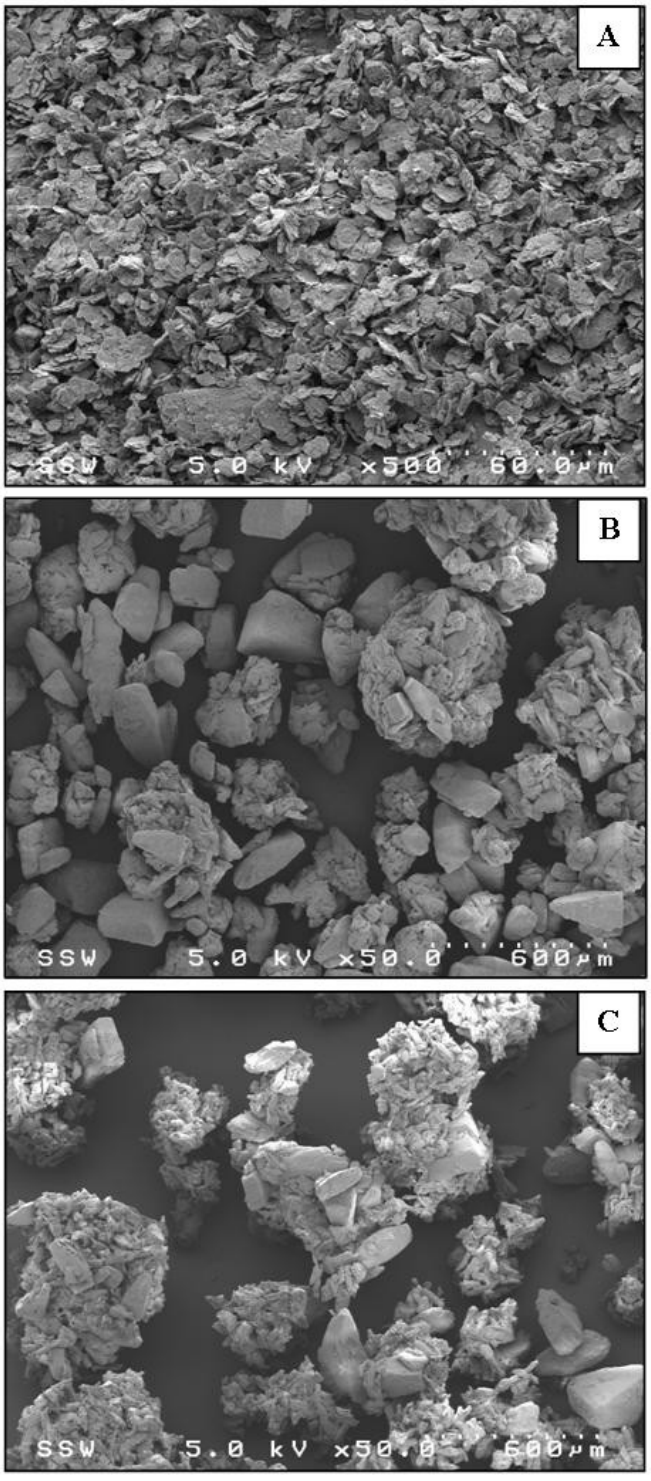

Figure 4.4: Scanning electron micrographs of mixture components (A-magnesium stearate, B-high shear granules, C-fluidized bed granules).

Figure 4.5 shows scanning electron images of samples of the mixtures of the high shear granules with magnesium stearate. The magnesium stearate flakes first filled in any surface cavities of the granules. A continuous layer of magnesium stearate was not formed. Instead, at high concentrations, the magnesium stearate remained mostly unattached to the granules and began to form self-agglomerates.

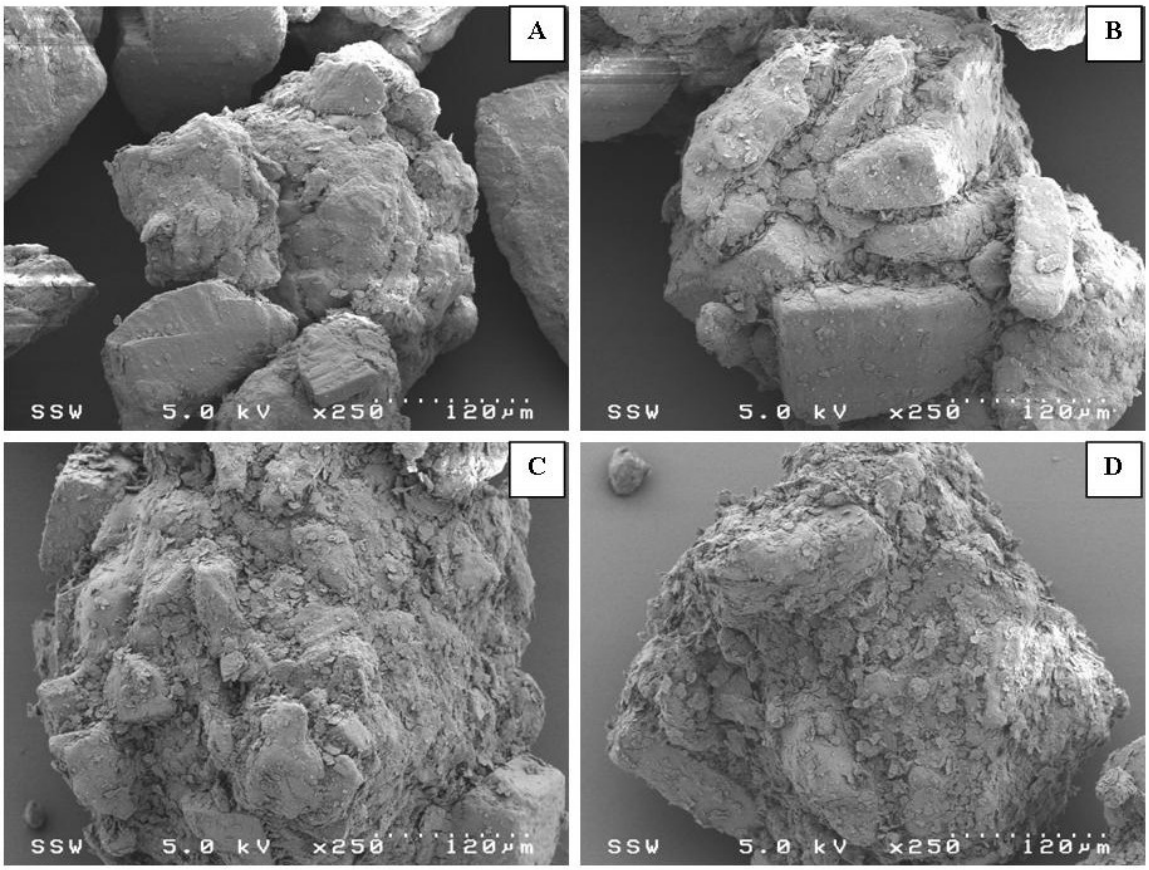

Figure 4.5: Scanning electron micrographs of high shear granules mixed with magnesium stearate (A- 1%, B- 2%, C-3%, D-5%).

Figure 4.6 shows scanning electron images of samples of the mixtures of the fluidized bed granules with magnesium stearate. The magnesium stearate flakes again first filled in any surface cavities of the granules. As with the high shear granules, a continuous layer of magnesium stearate was not formed. Instead, at high concentrations, the magnesium stearate began to form self agglomerates.

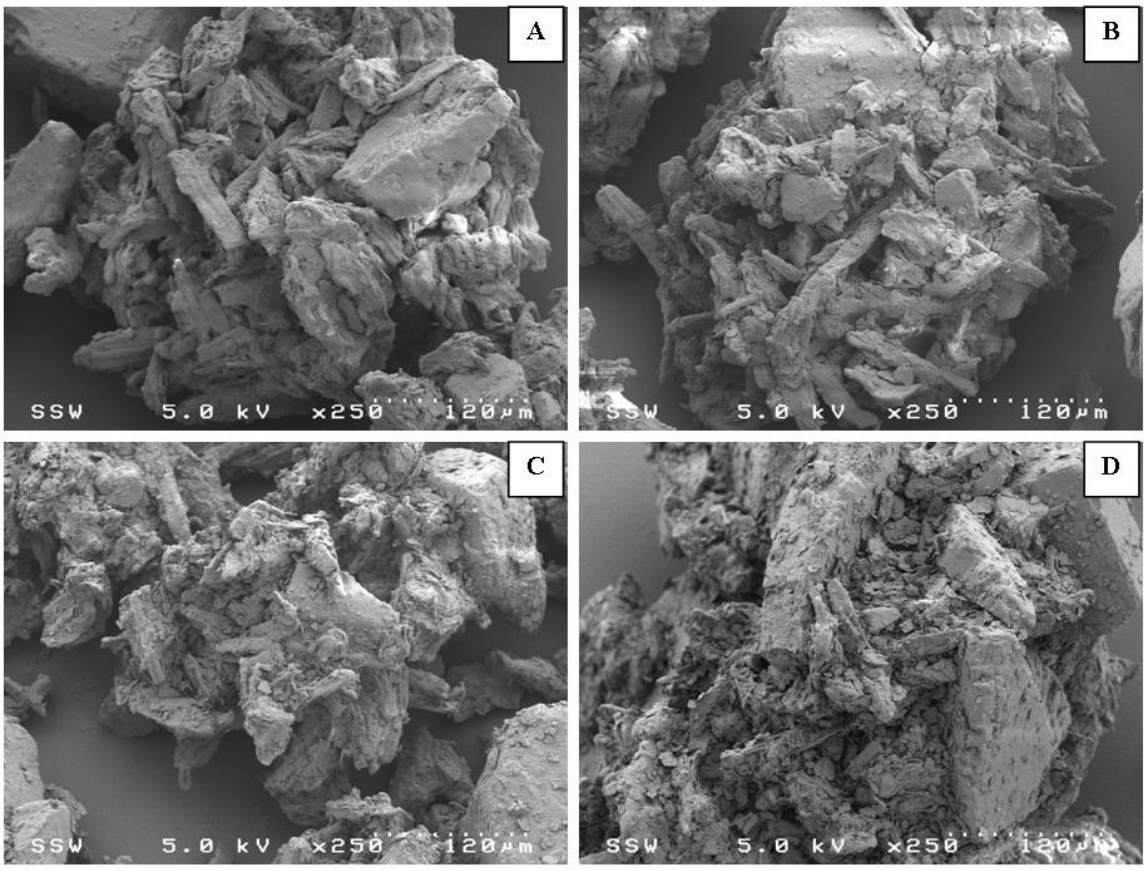

Figure 4.6: Scanning electron micrographs of fluidized bed granules mixed with magnesium stearate (A- 1%, B- 2%, C-3%, D-5%).

4.3.3. Flowability

4.3.3.1. Angle of repose

Figure 4.7 shows the measured static angle of repose for the various lubricant mixtures. Both the high shear and fluidized bed granules exhibited good flowability without the additions of lubricant, with static angles of repose of 32.1 and 32.7^{o}, respectively. The addition of lubricant lowered the static angle of repose for both granule types indicating an improvement in flowability. For the high shear granules, the addition in 1 wt% magnesium stearate resulted in the lowest static angle of repose of 30^{o}. For the fluidized bed granules, the static angle of repose continued to increase with magnesium stearate to a value of 30.4^{o} by 4 wt% addition.

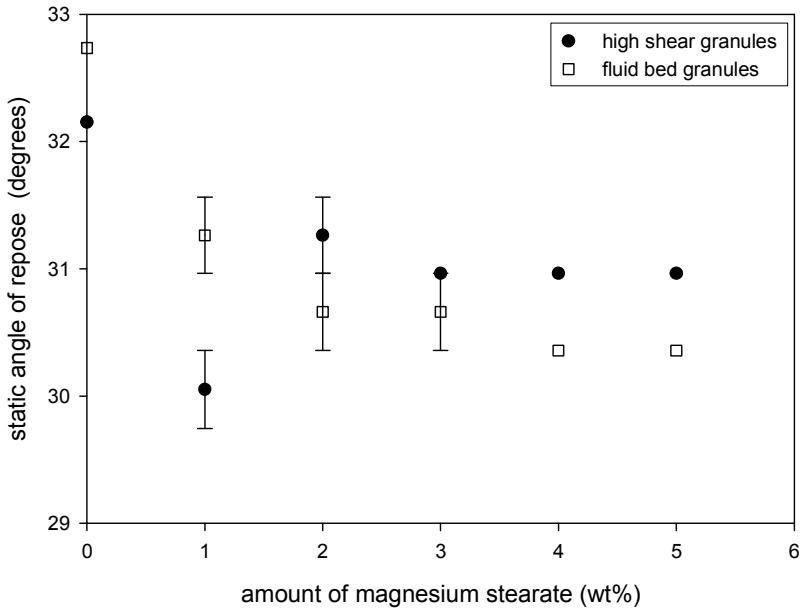

Figure 4.7: Static angles of repose for the lubricant mixtures.

4.3.3.2. Density measurements

The Hausner ratio is determined from the tapped and bulk densities. Figure 4.8 shows that the addition of magnesium stearate to improve the Hausner ratio for both fluidized bed and high shear granules, showing minimum ratios of 1.19 and 1.11, down from 1.24 and 1.19, respectively. Similar to the profiles obtained with the static angle of repose, continued addition of magnesium stearate to the fluidized bed granules showed flowability improvement until about 3-4 wt% addition. The addition magnesium stearate beyond 2 wt% to the high shear granules began to result in an increase in the Hausner ratio indicating a decrease in flowability.

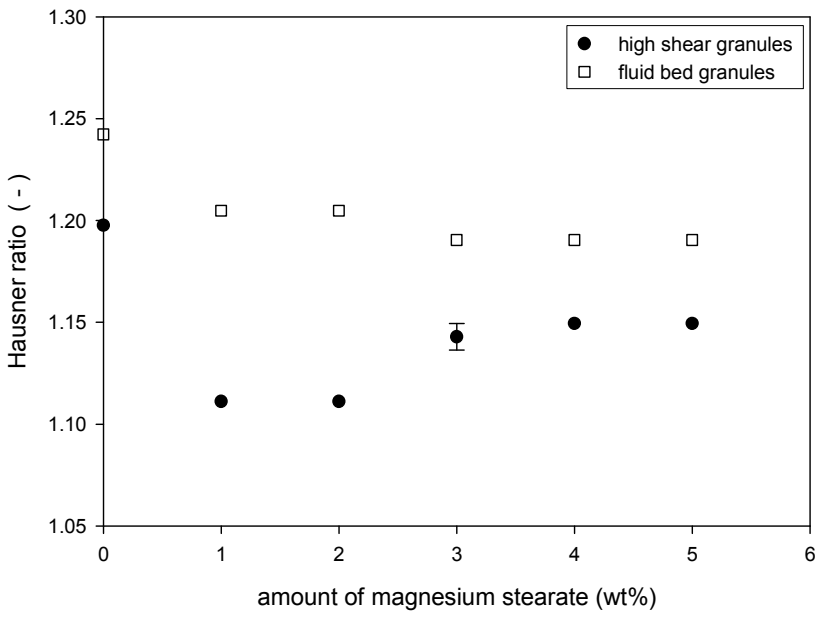

Figure 4.8: Hausner ratios of the lubricant mixtures.

The Carr index also uses the bulk and tapped densities to indicate flowability. A Carr index below 20-25% indicates good flowability (Carr, 1965). As shown in Figure 4.9, profiles of the lubricant and granule mixtures for the Carr index were similar to those of the Hausner ratio.

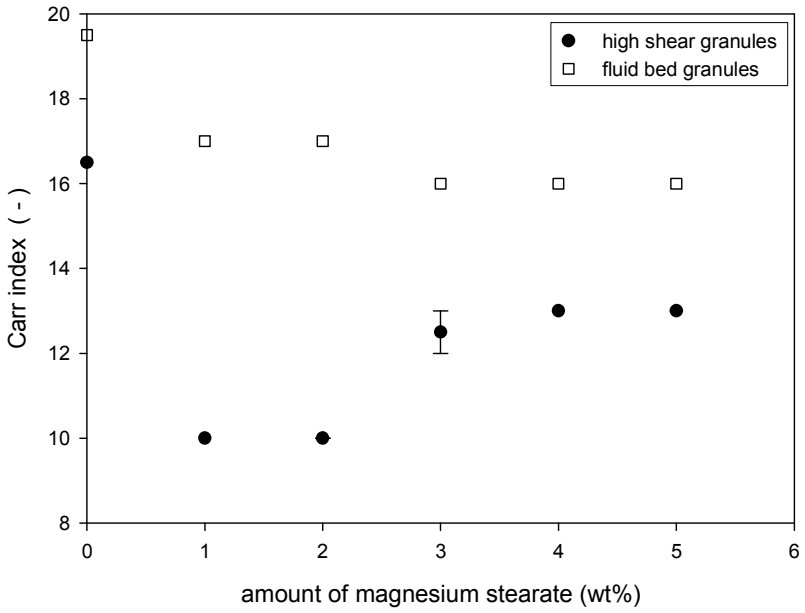

Figure 4.9: Carr indices of the lubricant mixtures.

4.3.3.3. Avalanche behaviour

The avalanche time is a flowability indicator measured by the Mercury Scientific revolution Powder Analyzer. Figure 4.10 shows the avalanche time decreased with the addition of magnesium stearate to both the high shear and fluidized bed granules. The addition of magnesium stearate had a more significant effect on the fluidized bed granules. As for the other flowability measurements, the addition of large amounts of

magnesium stearate decreased flow for the high shear granules while flowability continued to increase slightly for the fluidized bed granules.

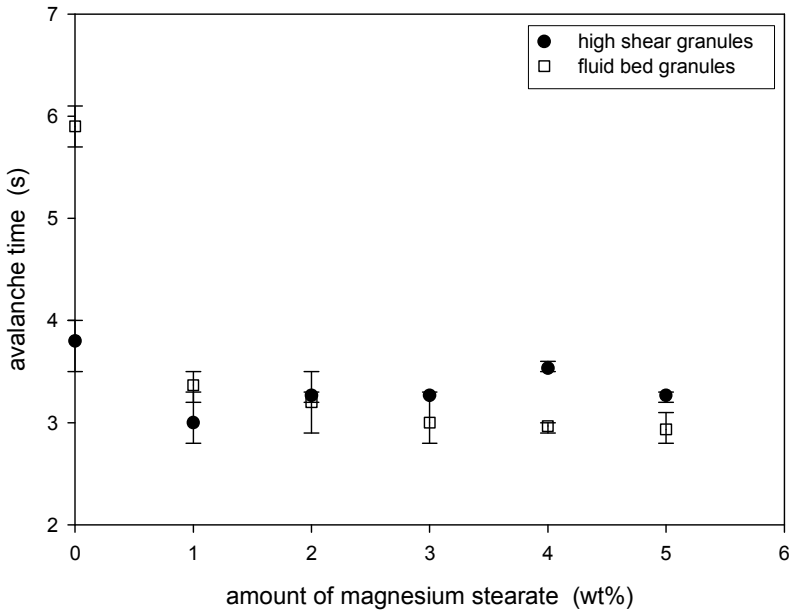

Figure 4.10: Avalanche times of the lubricant mixtures.

4.4. Discussion

The granules were made using the same formulation, dried in an oven tray dryer to less than 2 wt% moisture content and sieved to include only granules between 150 and 600 μm in size. The scanning electron images, however, showed that the method of granulation affected the granule shape, surface morphology and density or porosity. The fluidized bed granules were more irregular in shape and surface morphology than the semi-spherical high-shear granules. The large surface cavities of the fluidized bed granules indicated lower density granules with higher porosity than the high shear granules. The

shape, surface and density of the granules corresponded to differences in the flowability. For all the flowability measurements (static angle of repose in Figure 4.7, Hausner ratio in Figure 4.8, Carr index in Figure 4.9, and avalanche time in Figure 4.10), the high shear granules exhibited better flowability than the fluidized bed granules.

The scanning electron micrographs in Figure 4.4 and Figure 4.5 showed that the magnesium stearate flakes first filled the cavities of the granules. Once the cavities were partially filled, the magnesium stearate no longer adhered to the granules, but began to form self-agglomerates. As the high shear granules had fewer and shallower surface cavities than the fluidized bed granules, the transition in behaviour of the magnesium stearate occurred at a lower level at about 1–2 wt% instead of 3-4 wt%.

The magnesium stearate improved the flowability of the granules changing their surface morphology: the granules became more spherical with a smoother surface morphology which reduced the frictional forces by reducing contact points (Morin and Briens, 2012; Perrault et al., 2010; Roblot-Treupel and Puiseux, 1986). For the high shear granules, the surface cavities filled quickly and then self agglomerates of magnesium stearate began to form. The magnesium stearate agglomerates were small and irregularly shaped which then started to decrease flowability as the apparent composition of the powder shifted towards smaller and irregularly shaped particles. This transition from adhesion to the granules to self-agglomerate formation was observed at 1-2 wt% for all the flowability measurements of the lubricant additions to the high shear granules (Figure 4.7, Figure 4.8, Figure 4.9, and Figure 4.10). For the fluidized bed granules, the surface cavities

initially filled quickly with magnesium stearate up to 1 wt% addition with corresponding significant improvements in the flowability. Further addition of magnesium stearate up to 3-4wt% continued to fill the deep cavities with small improvements in flowability. Beyond 4 wt% addition, the magnesium stearate still appeared to fill in some deep surface cavities, but also began to form self-agglomerates. At this point, the flowability showed no further significant changes.

The Revolution Powder Analyzer measured the behaviour of the powders as they were tumbled at a rate of 0.3 rpm. The powder builds along the perimeter of the drum until it collapses in an avalanche. The average avalanche time is one of the parameters that indicate flowability. A large avalanche time indicates a cohesive and poorly flowing powder that builds significantly around the perimeter before collapsing. The avalanching measurements are dynamic and averaged over a large number of events (128 avalanches per trial with trials conducted in triplicate). The avalanche time is therefore considered very sensitive and valuable measurement for evaluating critical flowability of pharmaceutical powders into tablet dies. The avalanche times shown in Figure 4.10, indicated that the addition more than 2 wt% magnesium stearate could improve the flowability of fluidized bed granules beyond that exhibited by high shear granules.

The results indicated that the flowability of the fluidized bed granules could at least be as good as, if not better, than the flowability of high shear granules with the addition of more magnesium stearate. Other parameters must, however, also be considered to determine the best granules to form a tablet of specified properties. The large addition of

magnesium stearate to the high shear granules may lead to tablets with unacceptable dissolution rates and mechanical strength. However, the low density fluidized bed granules may provide excellent compressability properties. A detailed analysis of the entire process from granulation through to tableting is required to completely compare the granulation methods and the overall effect of magnesium stearate.

4.5. Conclusions

A lactose based placebo formulation was granulated using both high shear and fluidized bed methods. The granules were then mixed with varying amount of magnesium stearate. The results indicated that magnesium stearate affected the two granule types differently, due to differences in granule surface morphology. Magnesium stearate increased the flowability of both granule types by filling in the surface cavities thereby creating a smoother surface morphology. As the fluidized bed granules were more irregular, larger amounts of magnesium stearate were required to achieve the same level of flowability as the high shear granules. As flowability is critical for tablet formation, this study highlights the differences and importance of granulation methods and lubricant concentrations in optimizing a formulation and its manufacturing process.

4.6. Acknowledgements

The authors would like to acknowledge the support of the Natural Sciences and Engineering Research Council of Canada (NSERC) as well as the Ontario Graduate Scholarship (OGS) for their financial support. The University of Western Ontario

Graduate Thesis Research Award Fund (GTRAF) is also acknowledged for financial contribution.

4.7. References

Alderborn, G., 2002. Tablets and compaction. Aulton ME. Pharmaceutics The Science of Dosage Form Design.

Armstrong, N.A., 2007. Tablet manufacture. Encyclopedia of pharmaceutical technology 6, 3655.

Asker, A., Saied, K., Abdel-Khalek, M., 1975. Investigation of some materials as dry binders for direct compression in tablet manufacture. Part 5: Effects of lubricants and flow conditions. Die Pharmazie 30, 378.

Carr, R.L., 1965. Evaluating flow properties of solids. Chem Eng 72.

Faqih, A.M.N., Mehrotra, A., Hammond, S.V., Muzzio, F.J., 2007. Effect of moisture and magnesium stearate concentration on flow properties of cohesive granular materials. International journal of pharmaceutics 336, 338-345.

Fassihi, A., Kanfer, I., 1986. Effect of compressibility and powder flow properties on tablet weight variation. Drug development and industrial pharmacy 12, 1947-1966.

Jarosz, P.J., Parrott, E.L., 1984. Effect of lubricants on tensile strengths of tablets. Drug development and industrial pharmacy 10, 259-273.

Johansson, M., 1985a. Investigations of the mixing time dependence of the lubricating properties of granular and powdered magnesium stearate. Acta pharmaceutica suecica 22, 343.

Johansson, M., Astra Laekemedel, A., Soedertaelje, S., 1986. The effect of scaling-up of the mixing process on the lubricating effect of powdered and granular magnesium stearate. Acta Pharmaceutica Technologica 32, 39-42.

Johansson, M.E., 1985b. Influence of the granulation technique and starting material properties on the lubricating effect of granular magnesium stearate. Journal of pharmacy and pharmacology 37, 681-685.

Levy, G., Gumtow, R.H., 1963. Effect of certain tablet formulation factors on dissolution rate of the active ingredient III. Tablet lubricants. Journal of pharmaceutical sciences 52, 1139-1144.

Liu, L.X., Marziano, I., Bentham, A., Litster, J.D., White, E., Howes, T., 2008. Effect of particle properties on the flowability of ibuprofen powders. International journal of pharmaceutics 362, 109-117.

Logan, R., Briens, L., 2012. Investigation of the effect of impeller speed on granules formed using a PMA-1 high shear granulator. Drug development and industrial pharmacy, 1-11.

Mitrevej, A., Sinchaipanid, N., Faroongsarng, D., 1996. Spray-dried rice starch: comparative evaluation of direct compression fillers. Drug development and industrial pharmacy 22, 587-594.

Morin, G., Briens, L., 2012. The effects of lubricant on powder flowability for pharmaceutical application. *To be submitted to Powder technology*

Nalluri, V.R., Kuentz, M., 2010. Flowability characterisation of drug-excipient blends using a novel powder avalanching method. European Journal of Pharmaceutics and Biopharmaceutics 74, 388-396.

Niazi, S., 2004. Handbook of Pharmaceutical Manufacturing Formulations: Compressed solid products. CRC Press.

Perrault, M., Bertrand, F., Chaouki, J., 2010. An investigation of magnesium stearate mixing in a V-blender through gamma-ray detection. Powder technology 200, 234-245.

Pingali, K.C., Saranteas, K., Foroughi, R., Muzzio, F.J., 2009. Practical methods for improving flow properties of active pharmaceutical ingredients. Drug development and industrial pharmacy 35, 1460-1469.

Roblot-Treupel, L., Puisieux, F., 1986. Distribution of magnesium stearate on the surface of lubricated particles. International journal of pharmaceutics 31, 131-136.

Sandler, N., Wilson, D., 2010. Prediction of granule packing and flow behavior based on particle size and shape analysis. Journal of pharmaceutical sciences 99, 958-968.

Strickland Jr, W., Nelson, E., Busse, L., Higuchi, T., 1956. The physics of tablet compression IX. Fundamental aspects of tablet lubrication. Journal of the American Pharmaceutical Association 45, 51-55.

Tan, S., Newton, J., 1990. Powder flowability as an indication of capsule filling performance. International journal of pharmaceutics 61, 145-155.

Wang, J., Wen, H., Desai, D., 2010. Lubrication in tablet formulations. European Journal of Pharmaceutics and Biopharmaceutics 75, 1-15.

CHAPTER.5. GENERAL DISCUSSION AND CONCLUSIONS

Pharmaceutical tablets are created by compressing a formulation of powders into a desired shape. As tablets are the most widely used dosage form in medicine, the tablet manufacturing process is critical in pharmaceutics. Two major steps that most affect the tablet compression process and ultimately the final tablet properties are the granulation of the active and excipients and the addition of lubricant to the granule. A better understanding of these two processes would help process optimization, leading to improved tablet quality, reduced development time, reduced waste, and in due course, manufacturing cost.

The success of many of the manufacturing steps relies on the flowability of the powders. Poor powder flow results in tablets that are not uniform in content and weight and therefore must be discarded as inadequate, unsuitable and possibly unsafe for distribution to patients. Lubricants reduce the friction between the tablet and the die metal surface, which reduces the ejection force and helps to ensure that the tablet is completely ejected with no visible surface imperfections. Most lubricant-related research has focused on the effect of the lubricants on tablet properties. The objective of this research was to investigate the effect of the lubricants on powder flowability, as flowability is critical for tablet formation. Four frequently used lubricants (magnesium stearate, magnesium silicate, stearic acid and calcium stearate) were mixed, in varying amounts, with spray dried lactose, a common excipient used in the pharmaceutical industry. Traditional

measurements including angle of repose, Hausner ratio, and Carr index were used to determine static properties of the powder mixtures. In addition, a novel measurement based on dynamic avalanche powder behaviour was used to indicate flowability potential. The results indicated differences in the lubrication mechanism between lubricants, subsequently affecting powder flow. Both magnesium stearate and magnesium silicate preferentially filled the voids and cavities on the spray dried lactose before forming self agglomerates. Since the observed mechanism was similar, flowability trends were similar for both lubricants, with magnesium stearate being more effective at improving powder flow. Calcium stearate did not seem to preferentially fill surface voids, and thus showed a different flowability effect. After an initial improvement in flow, excess calcium stearate decreased overall flow, since the excess lubricant increased surface irregularities on the spray dried lactose. Stearic acid produced little effect on flowability, with only a minor improvement. As flowability is critical for tablet formation, the conclusions of this study highlight the importance of including flowability measurements in lubricant selection.

In order to understand the effects of lubricant on pharmaceutical granules produced by a placebo formulation, differences in granule properties needed to be taken into account. Although much research has been conducted to investigate individual wet granulation techniques, little comparison of the physical properties of the granules produced by different techniques has been published in literature. Granules were produced using the two most utilized wet granulation techniques, fluidized bed and high shear granulation. Granules were compared via granulation mechanism, flowability, particle size, and size distribution. At a lower moisture content (~20%), size distributions were similar for both granules, while at a higher moisture content (~30%), the fluidized bed granules how a

wider size distribution. However, the highest percentage of optimal granules was produced using a fluidized bed granulator. Overall, the high shear granules showed better flow properties, significantly improving flow over the un-agglomerated formulation. The granule nuclei showed different mechanisms of formation: the high shear granulation nuclei contained only microcrystalline cellulose, while the fluidized bed granulation nuclei consisted primarily of lactose monohydrate particles with a few attached microcrystalline cellulose fibres. Significant differences were observed in the properties of fluidized bed and high shear granules.

Once the difference properties between fluidized bed and high shear granules were known, experiments were conducted to investigate the effect of lubricants on powder flowability utilizing full placebo granules with different physical properties. Research conducted studying the effect of lubrication on powder flow typically utilizes a substitute powder to represent granules. Magnesium stearate, a commonly used lubricant, was mixed in varying amounts with granules produced by both high shear and fluidized bed processes. Traditional measurements including angle of repose, Hausner ratio, and Carr index were used to determine static properties of the powder mixtures. In addition, a novel measurement based on dynamic avalanche powder behaviour was used to indicate flowability potential. The results indicated that magnesium stearate affected the two granule types differently, due to differences in granule porosity. The addition of lubricant increased the flowability of both granule types, with the greatest improvement observed in the fluidized bed granules. Furthermore, excess addition of lubricant caused a decrease in flow for the high shear granules, since the excess lubricant increased surface irregularities on the granules. However, the same phenomenon was not witnessed in the

fluidized bed granules. As flowability is critical for tablet formation, the conclusions of this study highlight the importance of including granule type and lubricant concentration in formulation optimization.

5.1. Recommended Future Work

In order to continue the investigation into the effect of lubricants on pharmaceutical granules, tableting work ought to be completed. As the next step in the investigation, tableting the granule mixtures would allow a more in depth analysis of the effect of lubricants – not only with respect to granule flowability, but to the final tablet properties as well. Since excess lubricant addition can be detrimental to overall tablet quality, a balance must be stricken between increasing flow by lubricant addition and reducing other important tablet qualities, like disintegration and hardness.

Furthermore, in order to fully understand the difference between granules produced by high shear and fluidized bed processes, the granules should be compressed into tablet form; an analysis of the properties of tablets produced by both processes will provide a more in depth understanding of the effect of process choice on final granule and tablet properties.

Curriculum Vitae

Garett J. Morin

EDUCATION

2011-2012 **Master of Engineering Science, Biomedical Engineering**
The University of Western Ontario, London ON
MESc Thesis Title: *The effects of lubrication on pharmaceutical granules*

2007-2011 **Bachelor of Engineering Science, Chemical Engineering (with distinction)**
The University of Western Ontario, London ON

AWARDS & ACCOMPLISHMENTS

2011-2012 Ontario Graduate Scholarship
Biomedical Engineering Graduate Program,
The University of Western Ontario

Western Graduate Research Scholarship
Biomedical Engineering Graduate Program,
The University of Western Ontario

Graduate Thesis Research Award
Biomedical Engineering Graduate Program,
The University of Western Ontario

2007-2011 Dean's Honour List
Faculty of Engineering, The University of Western Ontario

2007-2011 Richard and Jean Ivey President's Entrance Scholarship ($34,000)
Faculty of Engineering, The University of Western Ontario

Milleniun Provincial Excellence Award ($14,000)
Faculty of Engineering, The University of Western Ontario

RELATED WORK EXPERIENCE

2009-2011 Graduate Research Assistant, Biomedical Engineering
Biomedical Engineering Graduate Program,
The University of Western Ontario

Teaching Assistant, Chemical and Biochemical Engineering
Biomedical Engineering Graduate Program,
The University of Western Ontario

Teaching Assistant, Business Management
The Richard Ivey School of Business,
The University of Western Ontario